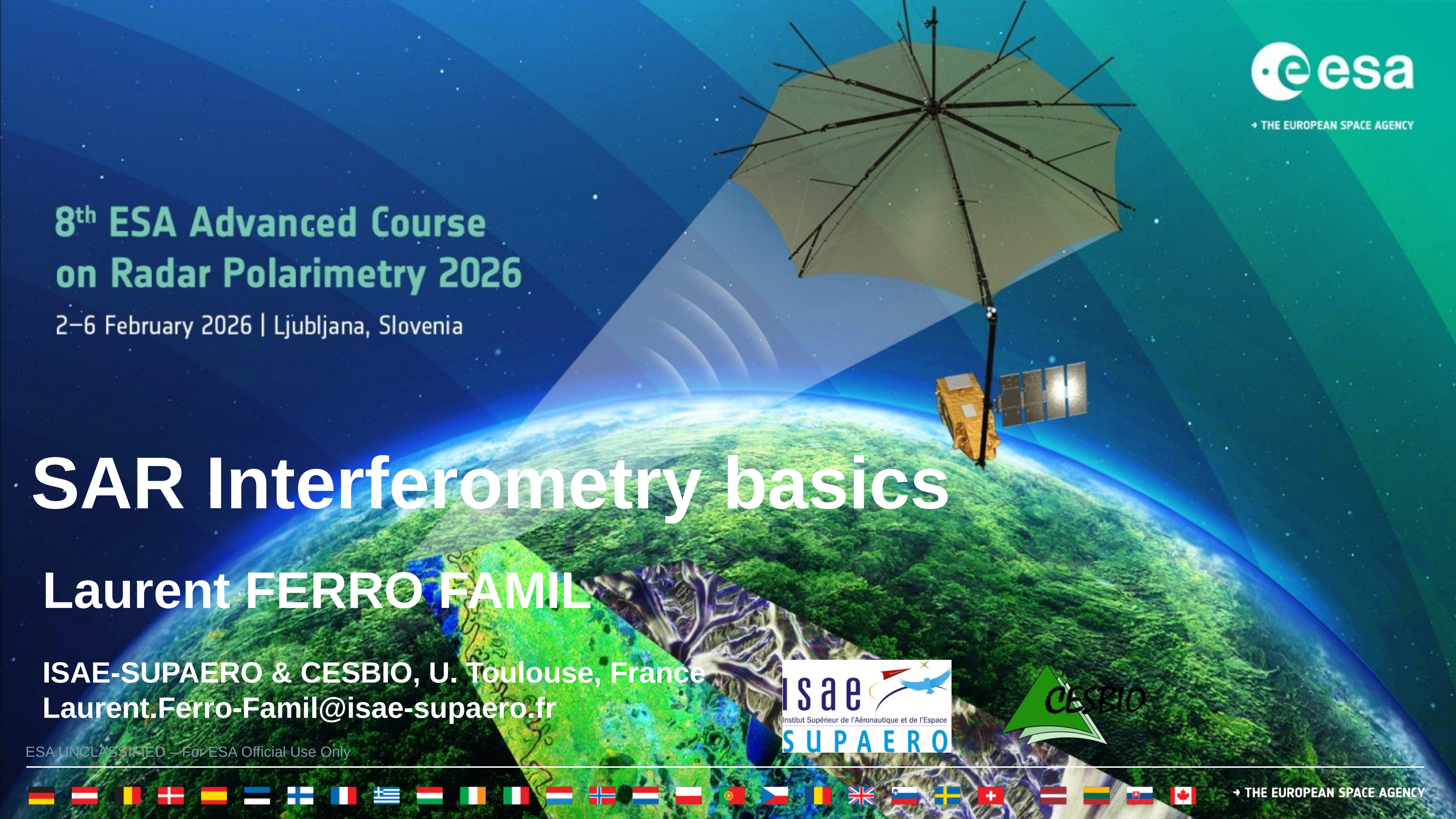

8th ESA Advanced Course on Radar Polarimetry 2026

2–6 February 2026 | Ljubljana, Slovenia

SAR Interferometry basics

Laurent FERRO FAMIL

ISAE-SUPAERO & CESBIO, U. Toulouse, France
Laurent.Ferro-Famil@isae-supaero.fr

SAR Interferometry basics

A geometrical approach

SAR acquisition geometry

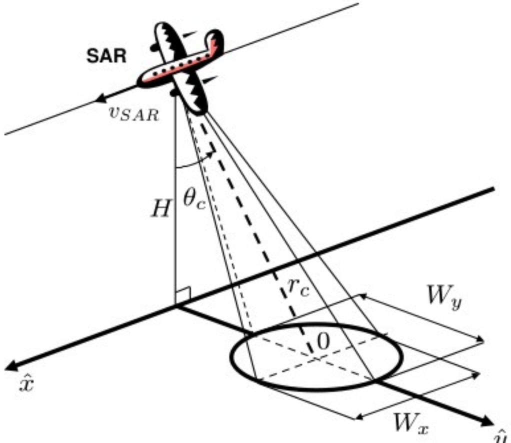

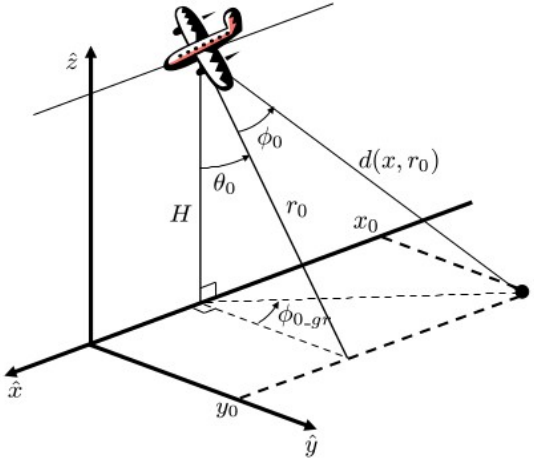

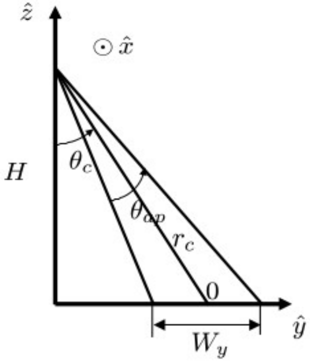

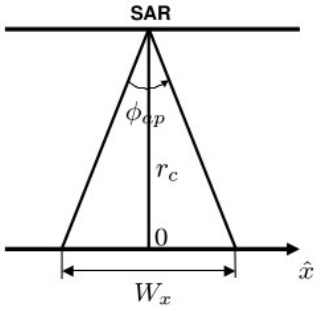

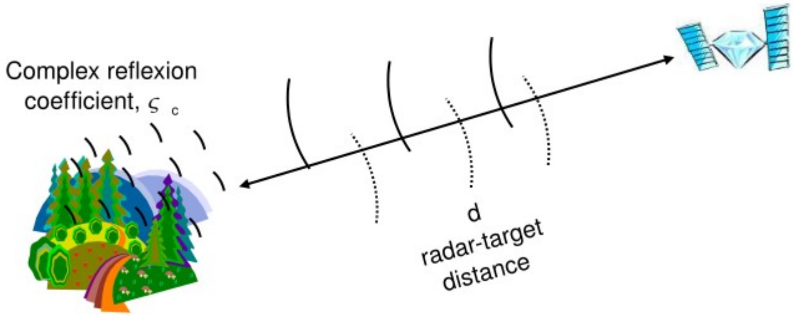

2D SAR focusing

SAR raw signal for a single scatterer

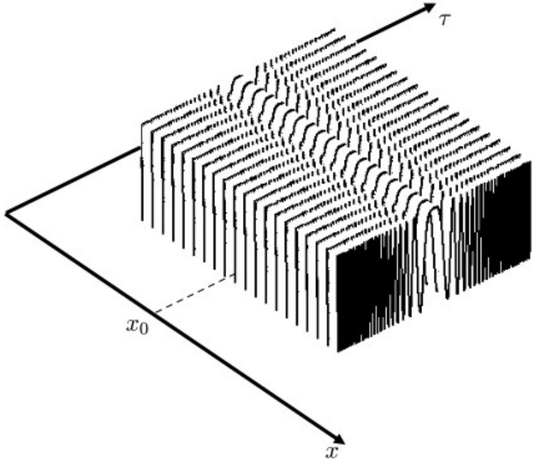

$$
\begin{aligned}
s_r(x,\tau) = & a_c \\
& p(\tau - \tau_0(x)) \longleftarrow \text{delayed pulse} \\
& \exp(-j2\pi f_c \tau_0(x)) \longleftarrow \text{phase delay} \\
& \mathrm{rect}\left(\frac{x - x_0}{W_x}\right)
\end{aligned}
$$

- Scatterer's location: (x_0, r_0)
- Reflection coefficient: a_c
- Baseband pulsed waveform: $p(\tau)$
- Migrations are neglected

azimuth-varying delay

$$\tau_0(x) = \frac{2}{c} d_0(x) = \frac{2}{c}\sqrt{r_0^2 + (x - x_0)^2}$$

2D SAR focusing

Range-focused SAR signal for a single scatterer

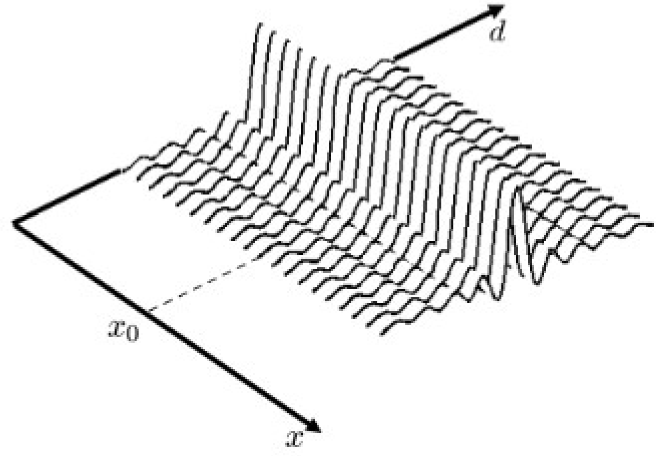

$$s_{rf}(x,d) = a_c$$

$$h_r(d - d_0(x)) \longleftarrow$$ range impulse response

$$\exp(-jk_c d_0(x))$$

$$\mathrm{rect}\left(\frac{x - x_0}{W_x}\right)$$

radar-scatterer distance

$$\mathrm{d}_0(x) = \sqrt{r_0^2 + (x - x_0)^2}$$

- Scatterer's location: (x_0, r_0)
- Reflection coefficient: a_c
- Migrations are neglected

2D SAR focusing

2D SAR image of a single scatterer

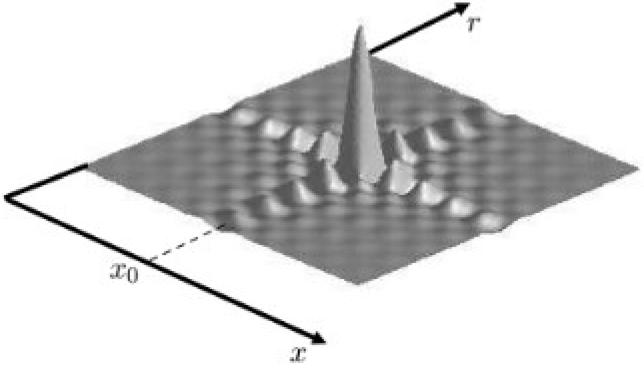

$$s_{rf}(x,r) = a_c$$

$$h_r(r - r_0) \longleftarrow$$ range impulse response

$$h_a(x - x_0) \longleftarrow$$ azimuth impulse response

$$\exp(-jk_c r_0) \longleftarrow$$ phase delay

r_0 can be measured using :

- $|s_{rf}(x,r)|$: precision $\approx \delta r$

- using $\arg(\exp(j k_r r_0))$: precision $\approx \lambda_c / 2$

- Scatterer's location: (x_0,r_0)
- Reflection coefficient: a_c

Phase sensitivity to motion in range

Differential interferogram of the "Hector Mine" earthquake (California), 16. October 1999

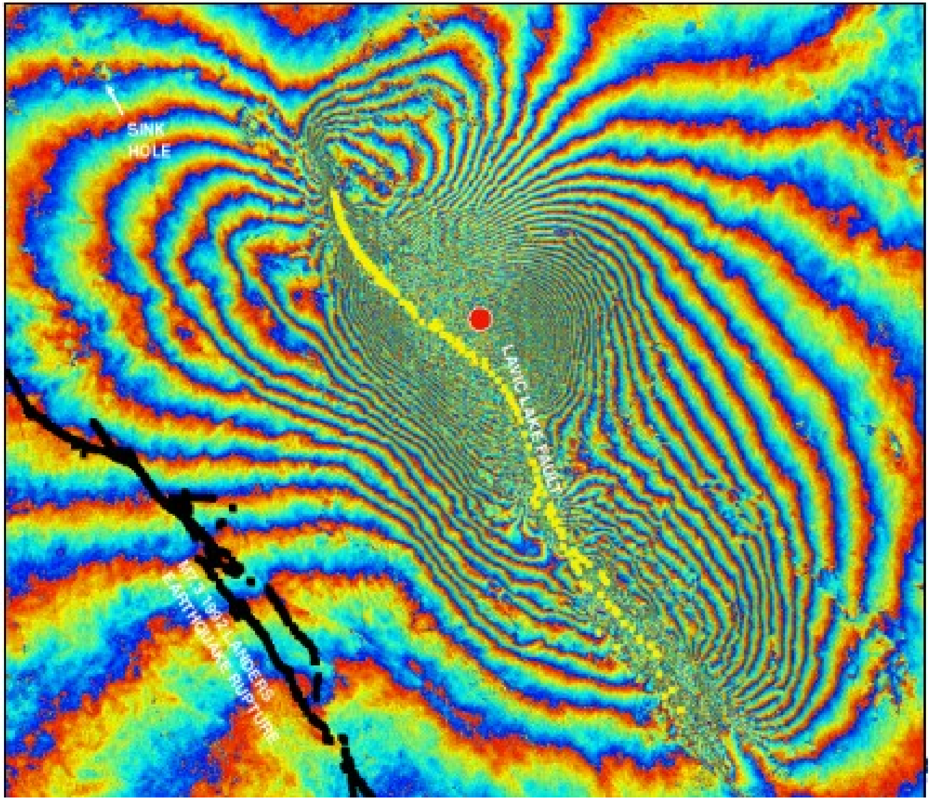

Each colour cycle represents a deformation of 2.8 cm.
temporal baseline = 35 days

Phase sensitivity to motion in range

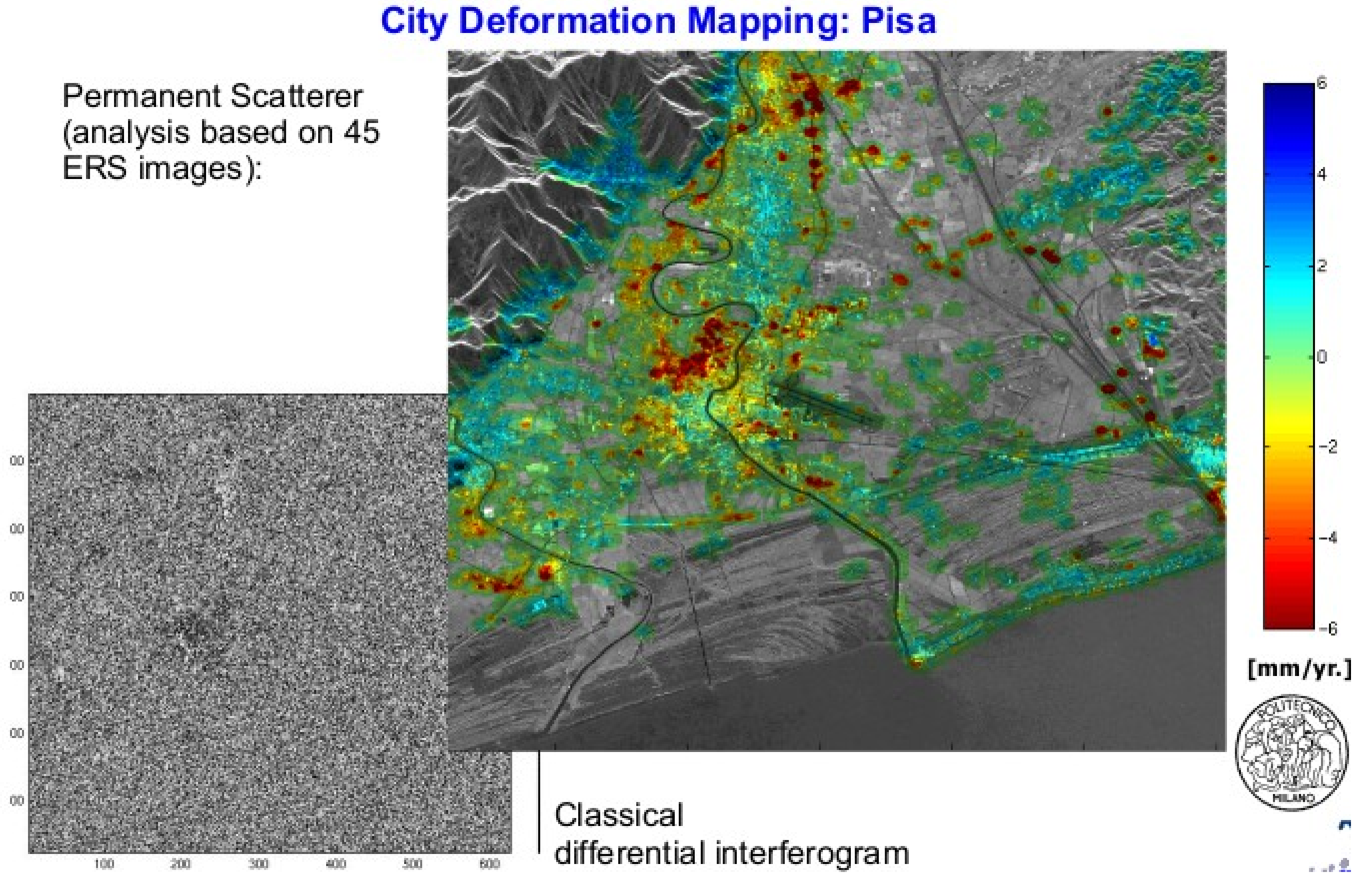

City Deformation Mapping: Pisa

Permanent Scatterer (analysis based on 45 ERS images):

Classical differential interferogram

3D mapping using SAR

Cylindrical ambiguity of 2D SAR imaging

3-D reflectivity		2-D raw data		2-D image
$\gamma(x, y, z)$	$\Rightarrow$	$s_r(x, \tau)$	$\Rightarrow$	$s(x, r)$

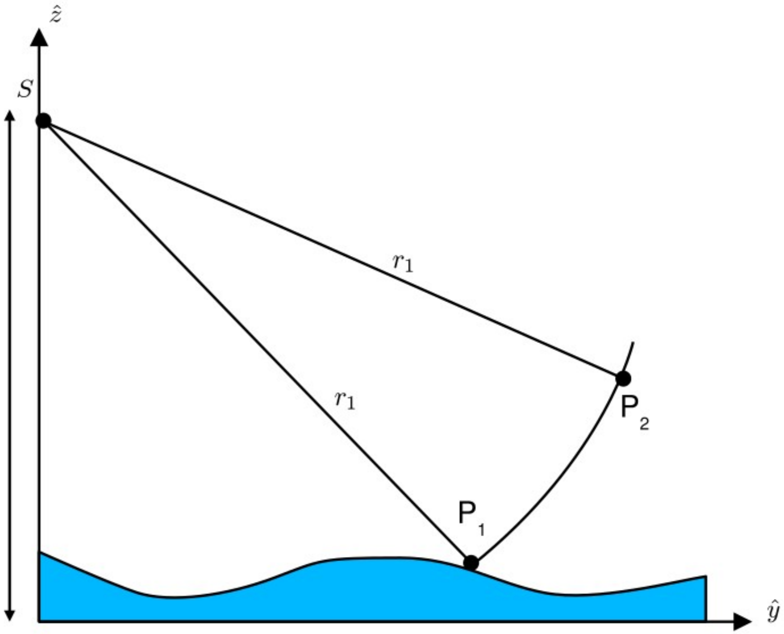

Mapping of $\gamma(x_0, y_0, z_0)$

- good localization in azimuth, x_0 (accuracy : δ_{az})
- circular ambiguity in the $(\hat{y}, \hat{z})$ plane

$$y_i^2 + (H - z_i)^2 = r_0^2$$

$\Rightarrow$ multiple solutions (y_i, z_i)

3D mapping using SAR

A solution: use of space diversity

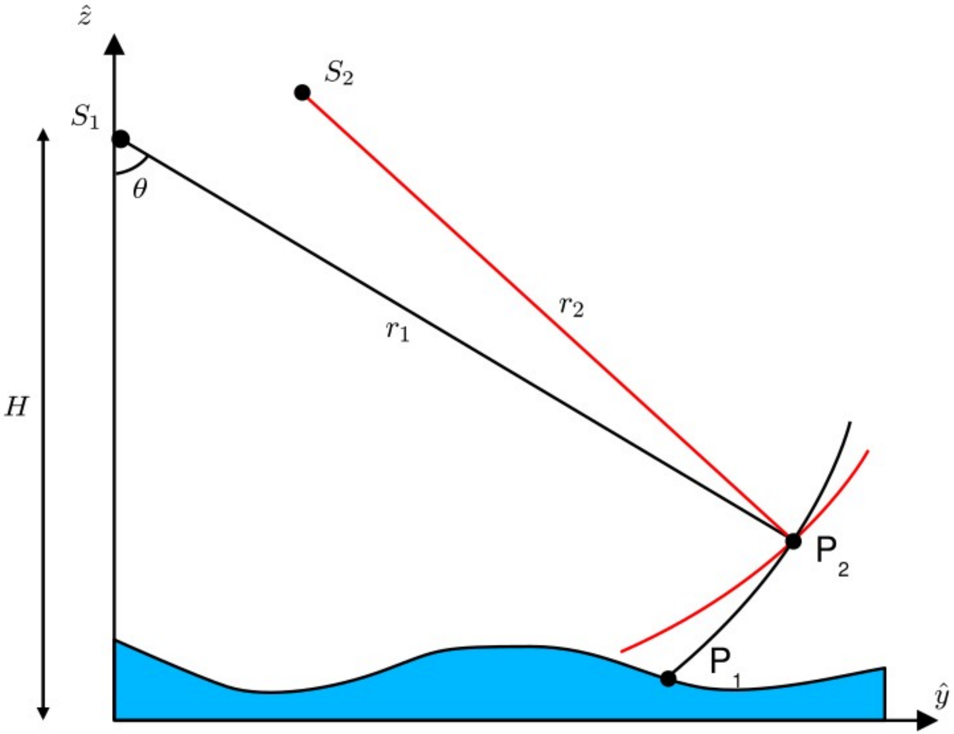

3-step unambiguous estimation

- Slant range distance from S_1

$$r_1 = ||\overrightarrow{S_1 P_2}|| = ||\overrightarrow{S_1 P_1}||$$

- Slant range distance from S_2

$$r_2 = ||\overrightarrow{S_2 P_2}||$$

- h_2 from r_1, r_2 and the geometrical configuration

3D mapping using SAR

Acquisition geometry

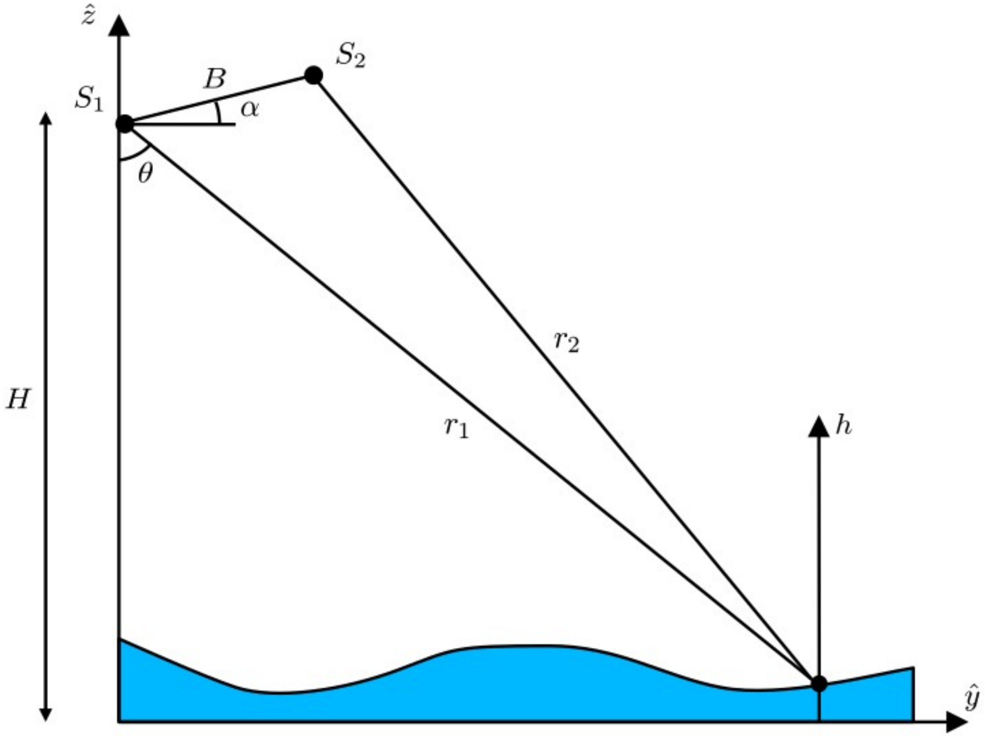

Acquisition geometry descriptors

- $S_{1,2}$: sensor positions
- B : baseline
- α : baseline inclination
- $r_{1,2}$: slant range distances
- h : elevation position
- H : altitude above reference
- θ : off-nadir incidence angle
- y : ground range position

3D mapping using SAR

Baseline conventions

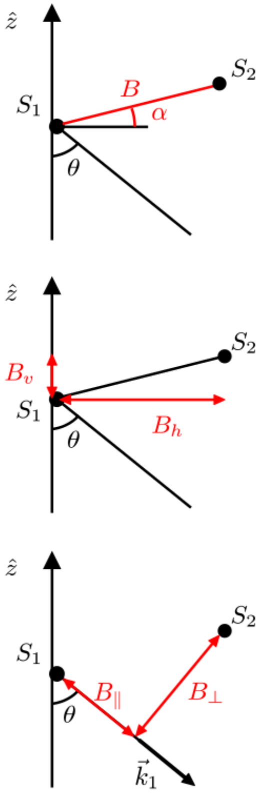

Polar convention

- B : baseline length
- α : baseline inclination

Cartesian convention

- $B_h = B \cos \alpha$: horizontal baseline
- $B_v = B \sin \alpha$: vertical baseline

Wave convention

- $B_{||} = B \sin(\theta - \alpha)$: baseline parallel to $\vec{k}_1$
- $B_\perp = B \cos(\theta - \alpha)$: baseline perpendicular to $\vec{k}_1$

Spatial diversity modes

Coregistration of a pair of images

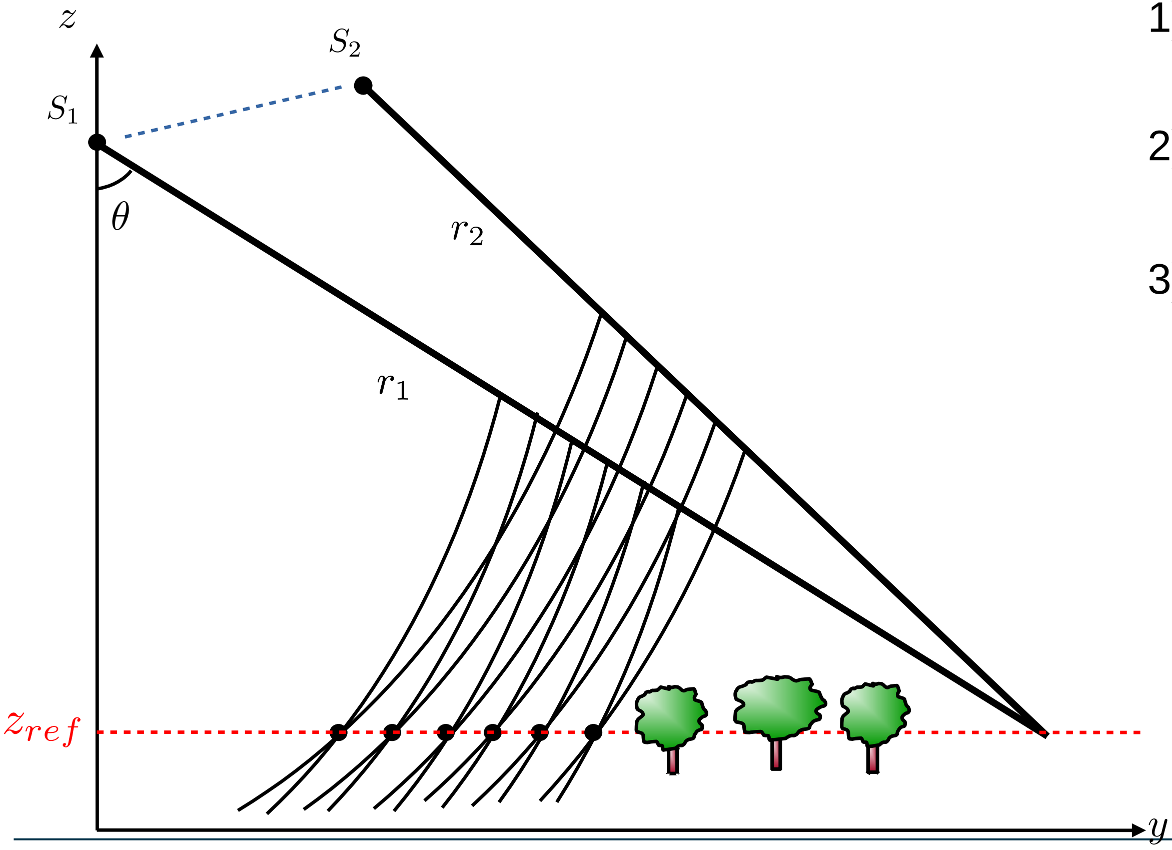

1) Set a reference common geometry

   $\{y_{ref}, z_{ref}\}$ plane, DTM...

2) Compute reference range coordinates

   $\{y_{ref}, z_{ref}\} \rightarrow \{r_{1ref}, r_{2ref}\}$

3) Co-register (resample) images to the reference geometry

$$
\begin{aligned}
s_i(x, r_{i_{ref}}) = a_c \\
h_r(r_{i_{ref}} - r_{i_0}) \\
h_a(x - x_0) \\
\exp(-jk_c r_{i_0})
\end{aligned}
$$

Spatial diversity modes

Retrieving topography from co-registered images

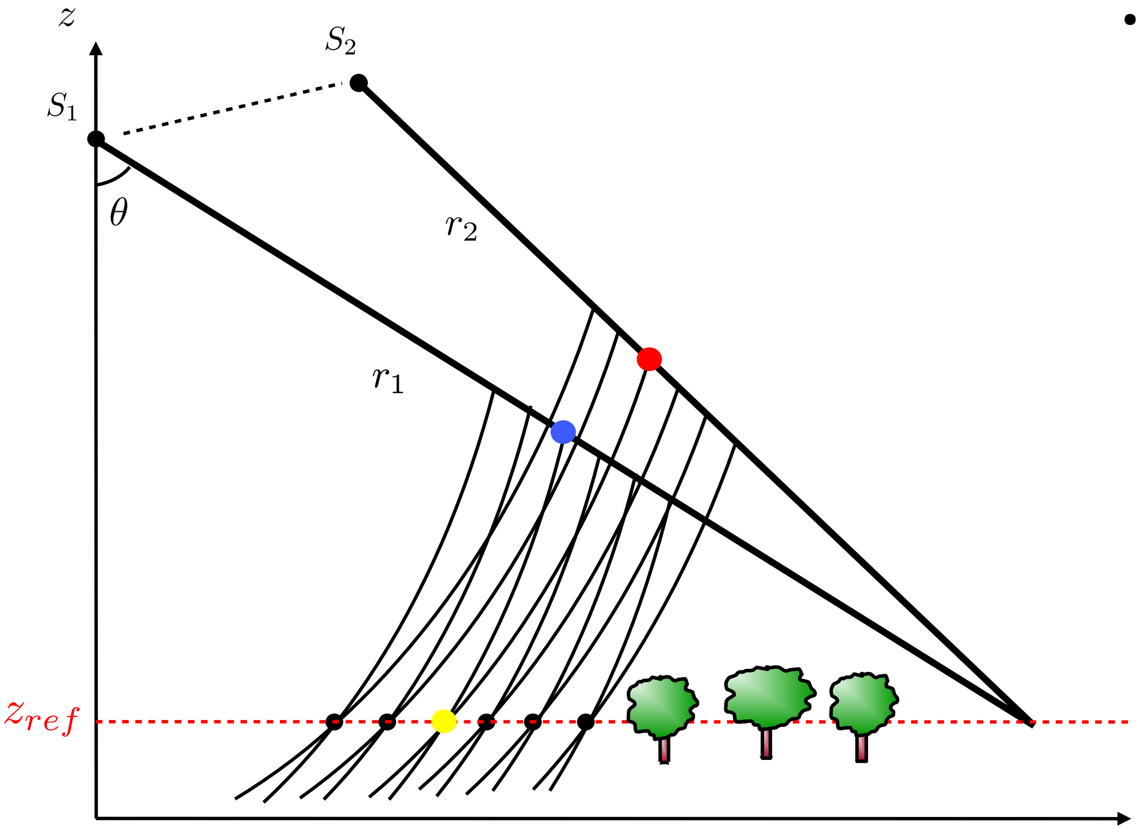

- Case 1:
  - the scatterer lies on the reference geometry
  - same coordinates in the co-registered images

$$r_{1ref} = r_1 \Rightarrow r_{2ref} = r_2$$

Spatial diversity modes

Retrieving topography from co-registered images

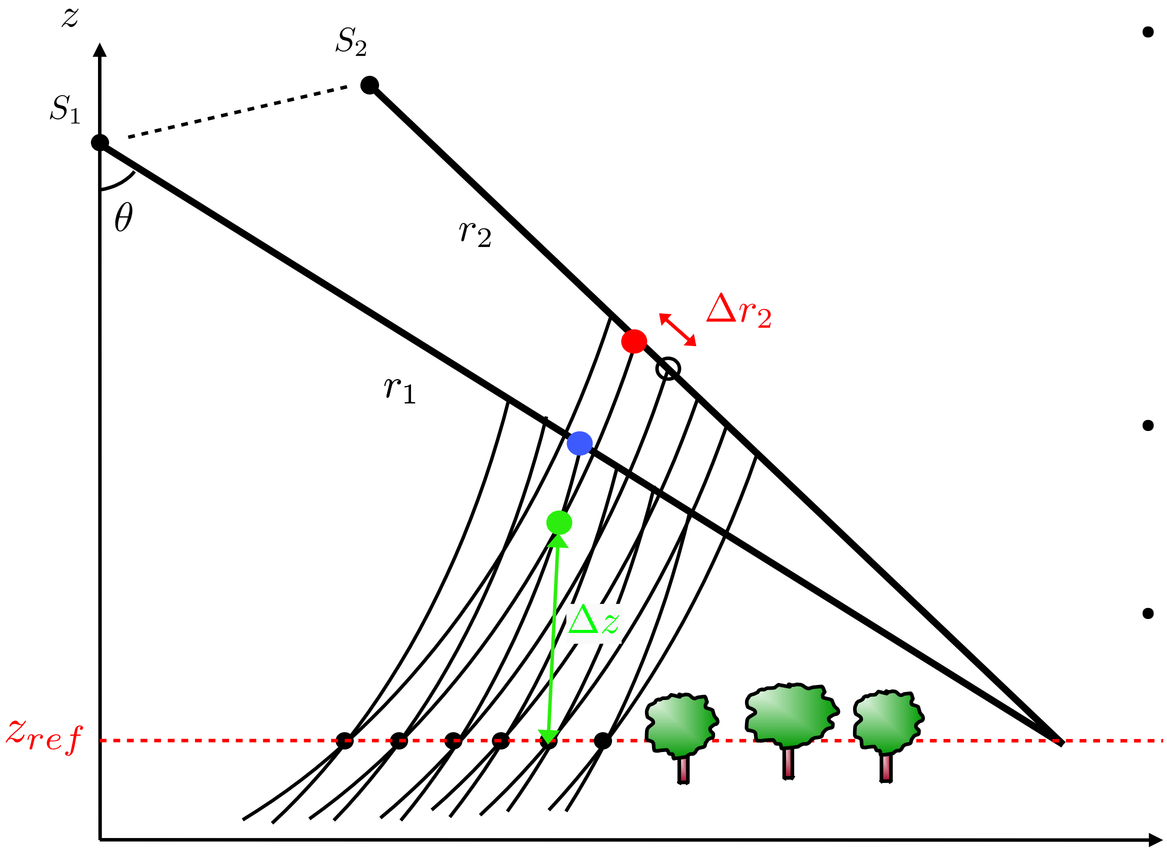

- Case 2
  - very large vertical offset Δz

$$r_{1ref} = r_1 \nRightarrow \quad r_{2ref} = r_2$$

  - range shift

$$\Delta r_2 = r_2 - r_{2ref} = f(r_1, \Delta z)$$

- Topography estimation

  stereo radar grammetry (deformation mapping)

- Heavy processing, low-resolution & robust estimation

Stereo radar-grammetry

DEM of Venus measured by the Magellan probe

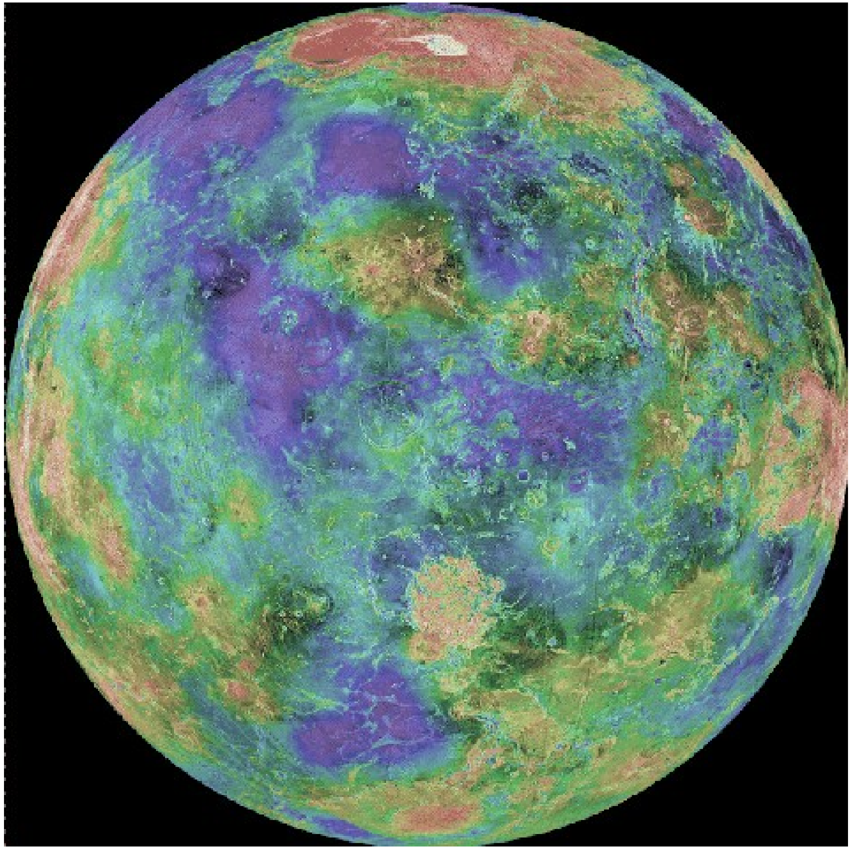

SAR interferometry

Retrieving topography from co-registered images

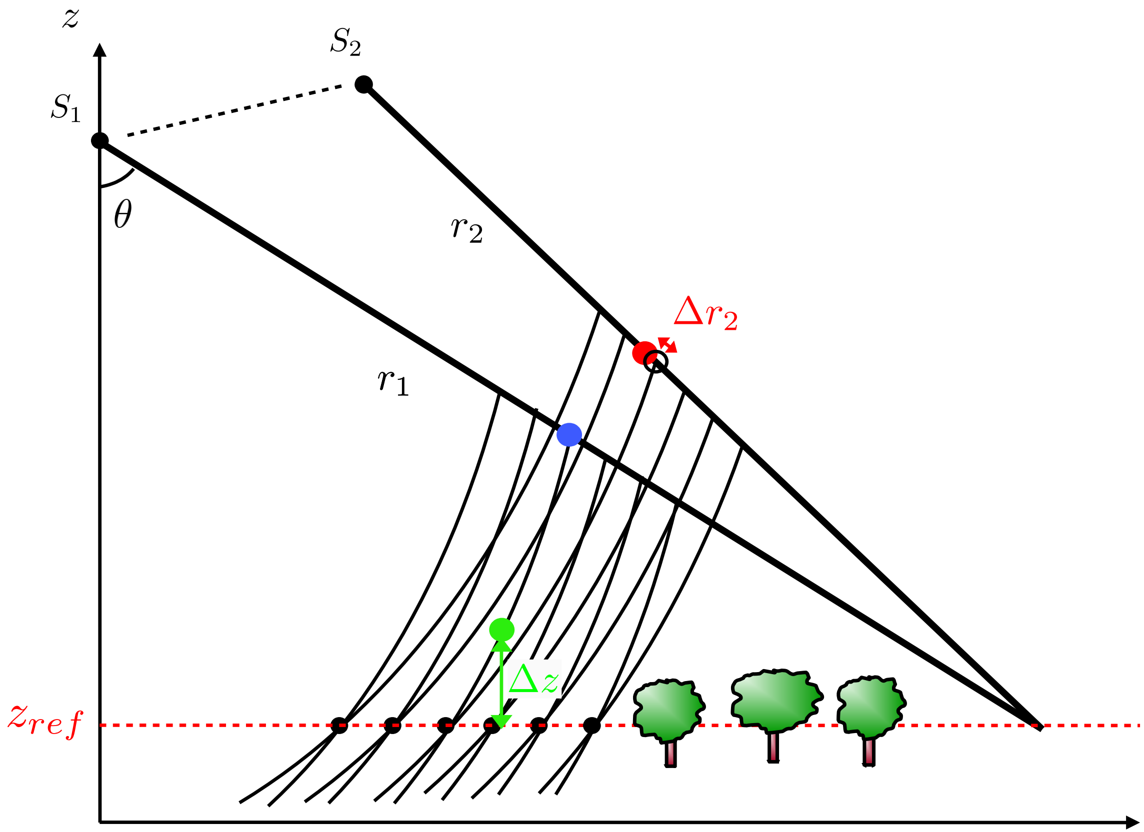

- Case 3
  - small Δz → no range shift

$$|\Delta r_2| \ll \delta r$$

  - topography estimation by interferometry

$$s_i(x, r_{i_{ref}}) \approx a_c \exp(-jk_c r_i)$$

$$\begin{aligned}\Delta\phi = \arg(s_1 s_2^*) &= k_c(r_2 - r_1)\\ &= f(r_1, \Delta z)\end{aligned}$$

- High-resolution estimation

$$|\Delta\phi| < \pi \Rightarrow |\Delta r| < \frac{\lambda}{4}$$

- Validity requirement $|\Delta r_2| < \alpha\, \delta r$

SAR interferometry

Interferometric phase components

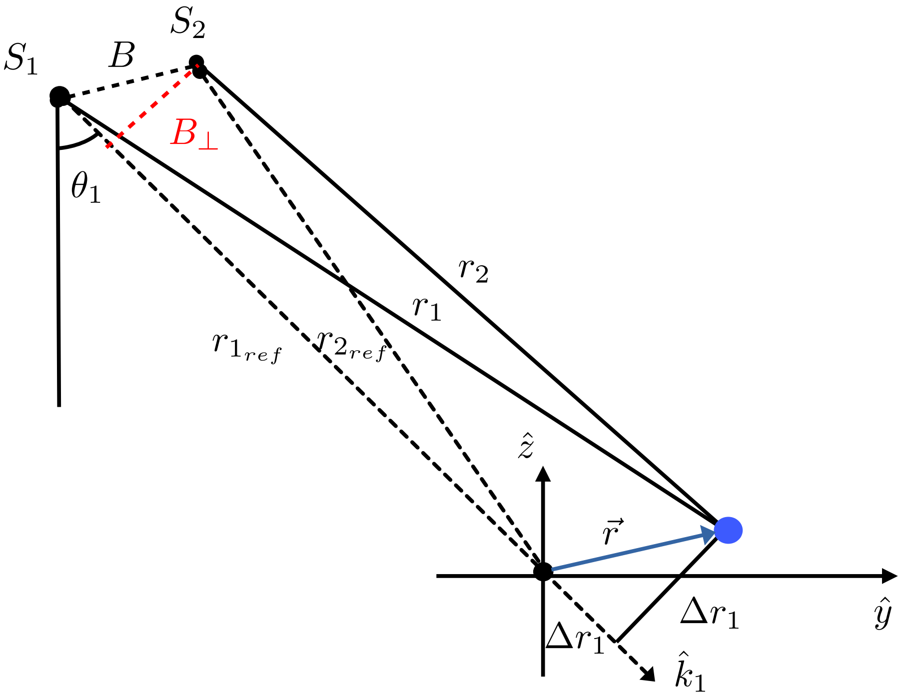

- Local plane wave approximation

$$\mathrm{r}_i \approx r_{i_{ref}} + \Delta r_i, \quad \Delta r_i = \vec{r} \cdot \hat{k}_i, \quad \Delta\theta = \frac{B_\perp}{r_{1_{ref}}}$$

- Compound interferometric phase

$$\Delta\phi = k_c(r_2 - r_1) = \Delta\phi_{ref} + \Delta\phi_{topo}, \quad k_c = \frac{4\pi}{\lambda}$$

- Reference (or flat-earth) phase component

$$\Delta\phi_{ref} = k_c(r_{2_{ref}} - r_{1_{ref}})$$

- Topographic phase component

$$\Delta\phi_{topo} = -k_c\Delta\theta\nu$$

$$= k_z\Delta z, \quad k_z = -\frac{4\pi}{\lambda}\frac{B_\perp}{r_{1_{ref}} \sin\theta_1}$$

SAR interferometry

Interferometric phase flattening

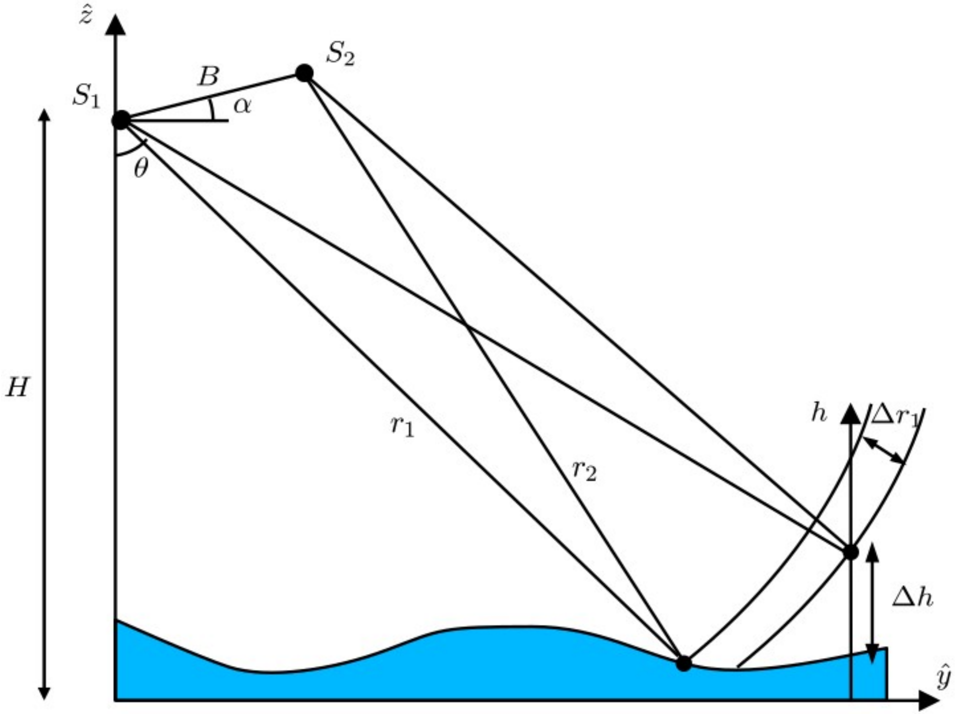

Compound interferometric phase

$$\Delta\phi = \Delta\phi_{ref} + \Delta\phi_{topo}$$

1) Compute reference phase (from acqu. Geometry)

$$\Delta\phi_{ref} = k_c(r_{2_{ref}} - r_{1_{ref}})$$

2) Flatten interferogram

$$\Delta\phi_{topo} = \arg(\exp(j(\Delta\phi - \Delta\phi_{ref}))$$

SAR interferometry

Topographic InSAR phase retrieval

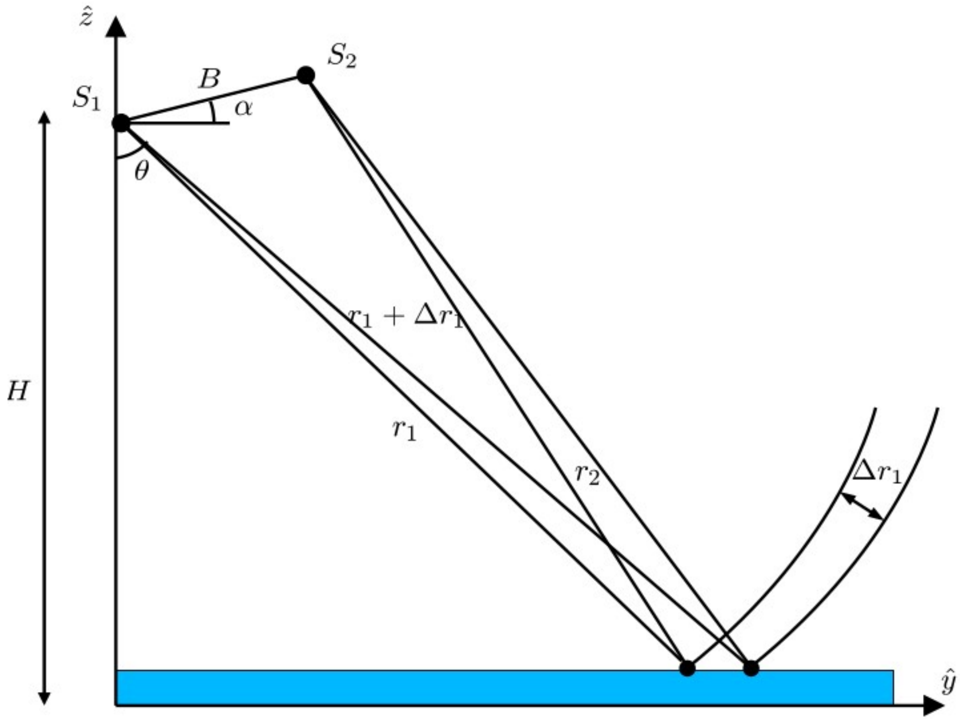

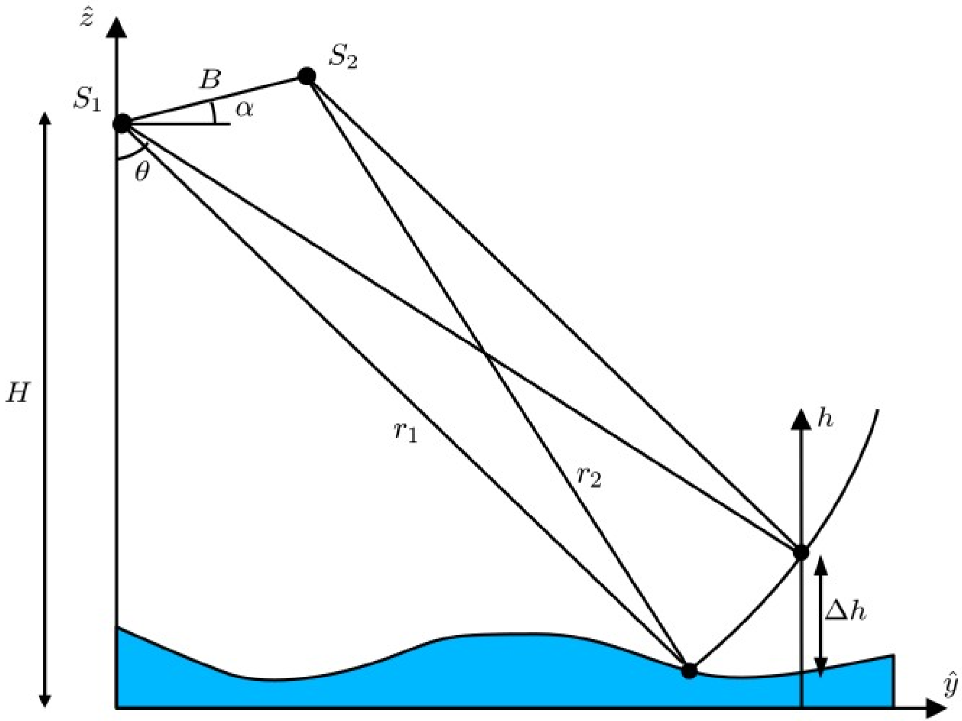

Sensitivity and ambiguity

- Sensitivity to:
  - baseline
  - Frequency (wavelength)
  - Off-nadir angle

$$\Delta\phi_{topo} = k_z \Delta z, \quad k_z = -\frac{4\pi}{\lambda}\frac{B_\perp}{r_{1_{ref}} \sin\theta_1}$$

- Ambiguous height h_{amb}

$$\mathrm{k}_z(\Delta z + h_{amb}) - k_z \Delta z = 2\pi \quad \Rightarrow \quad \boxed{h_{amb} = \frac{2\pi}{k_z}}$$

InSAR phase wrapping

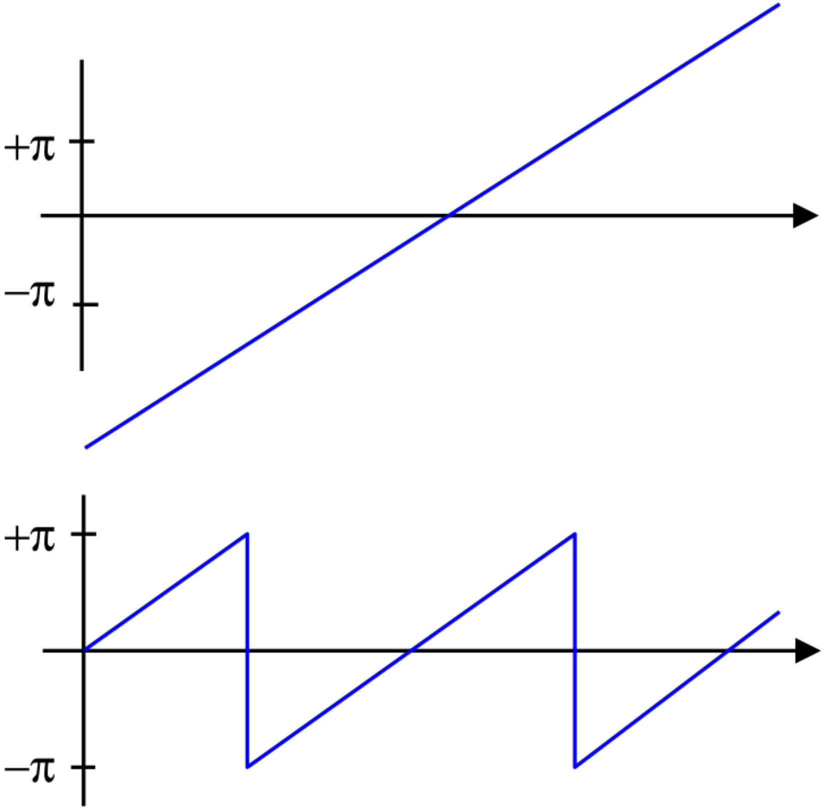

Interferometric phase computation

- $\Delta\phi_{12} = \arg(s_{12})$, with $s_{12} = s_1 s_2^*$
- Four-quadrant arc-tangent operator

$$\Delta\phi_{12\_est} = \arctan(\Im(S_{12}), \Re(S_{12}))$$

Interferometric phase computation

- $\Delta\phi_{12\_est} \in]-\pi, \pi]$
- $\Delta\phi_{12\_est} = \Delta\phi_{12} + k2\pi,\ k \in \mathbb{Z}$
- Phase wrapping effect : “fringes”

3D mapping using InSAR

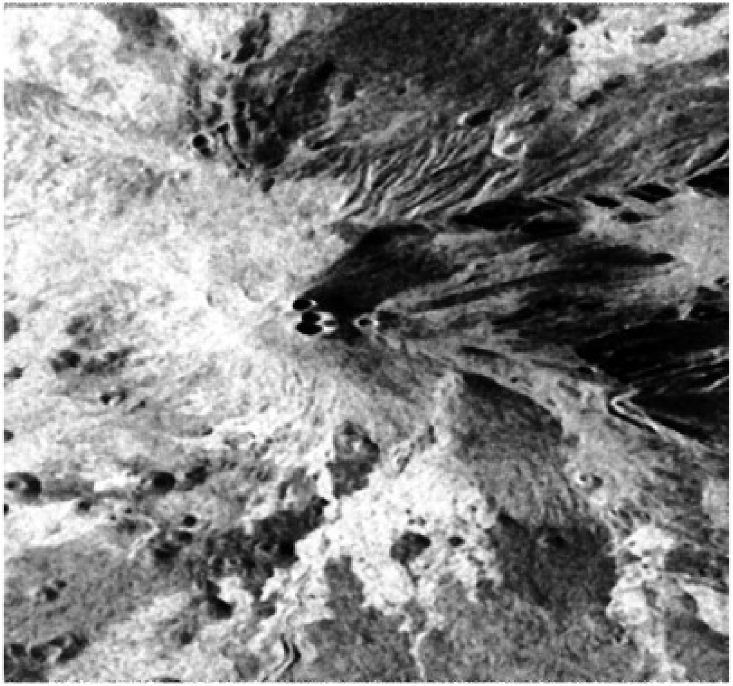

Amplitude image

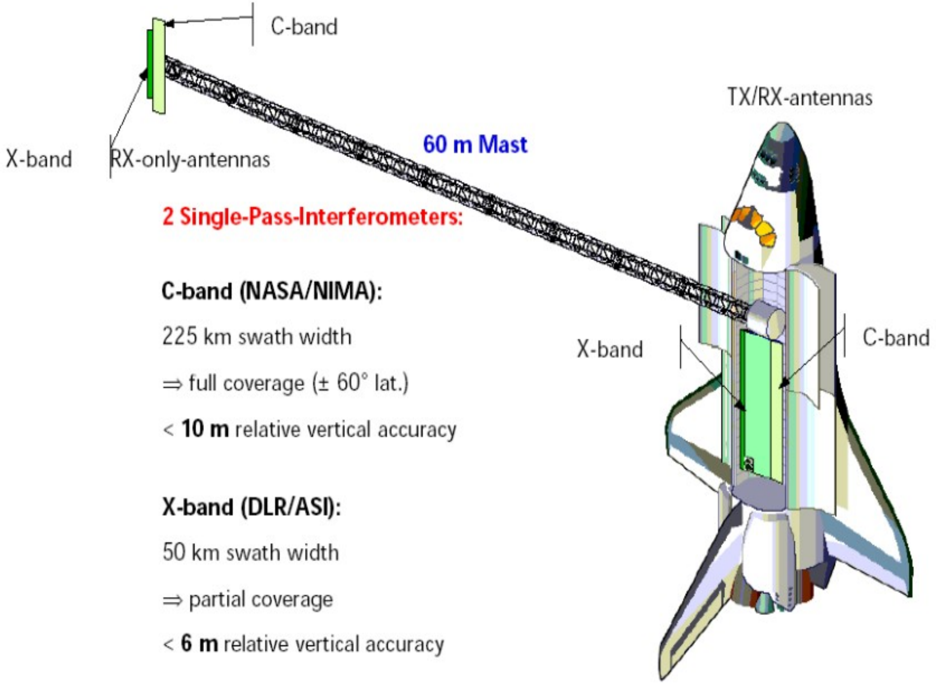

2 Single-Pass-Interferometers:

C-band (NASA/NIMA):

225 km swath width

⇒ full coverage (± 60° lat.)

< **10 m** relative vertical accuracy

X-band (DLR/ASI):

50 km swath width

⇒ partial coverage

< **6 m** relative vertical accuracy

Absolute phase image

SIR-C, X-band, Mount Etna, Italy

3D mapping using InSAR

InSAR phase flattening

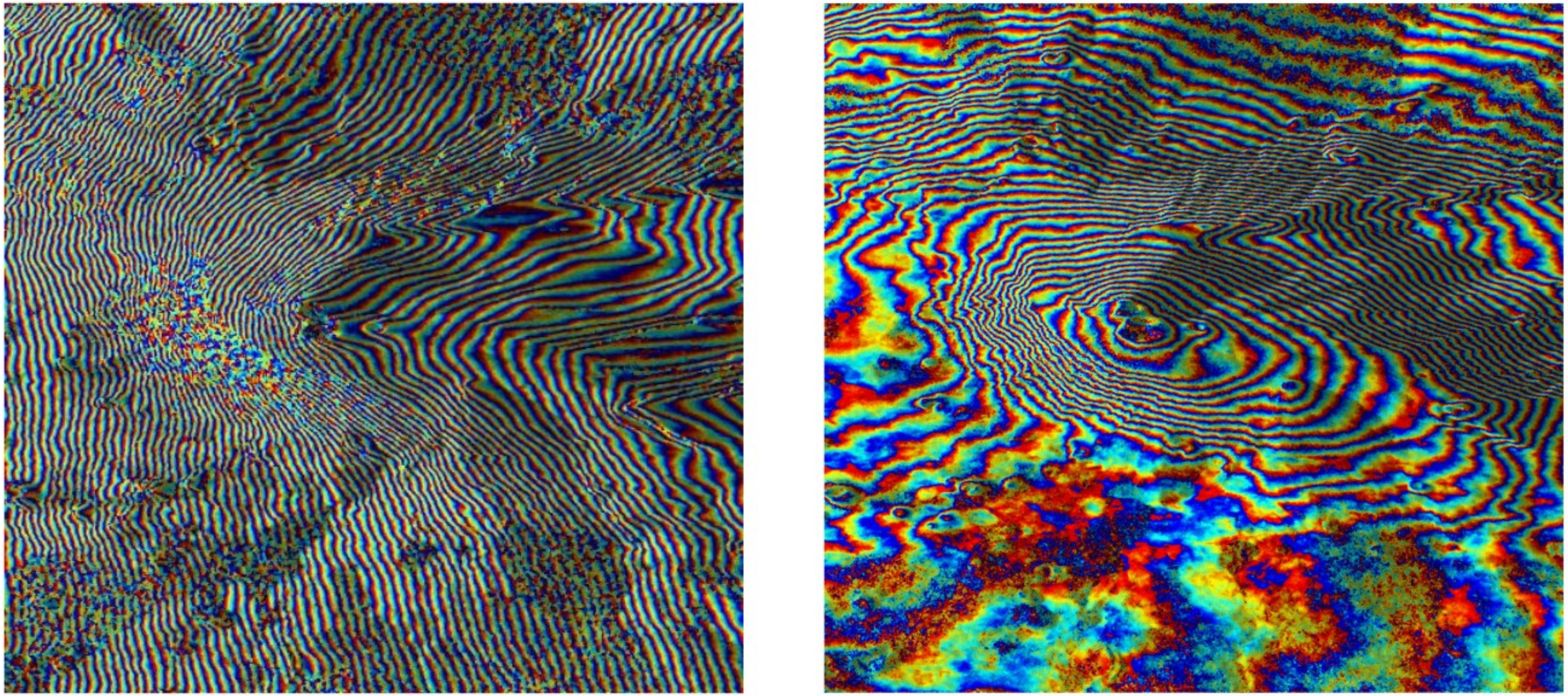

$\Delta\phi$

$\Delta\phi_{topo}$

Radar look direction ?

3D mapping using InSAR

Sensitivity to baseline

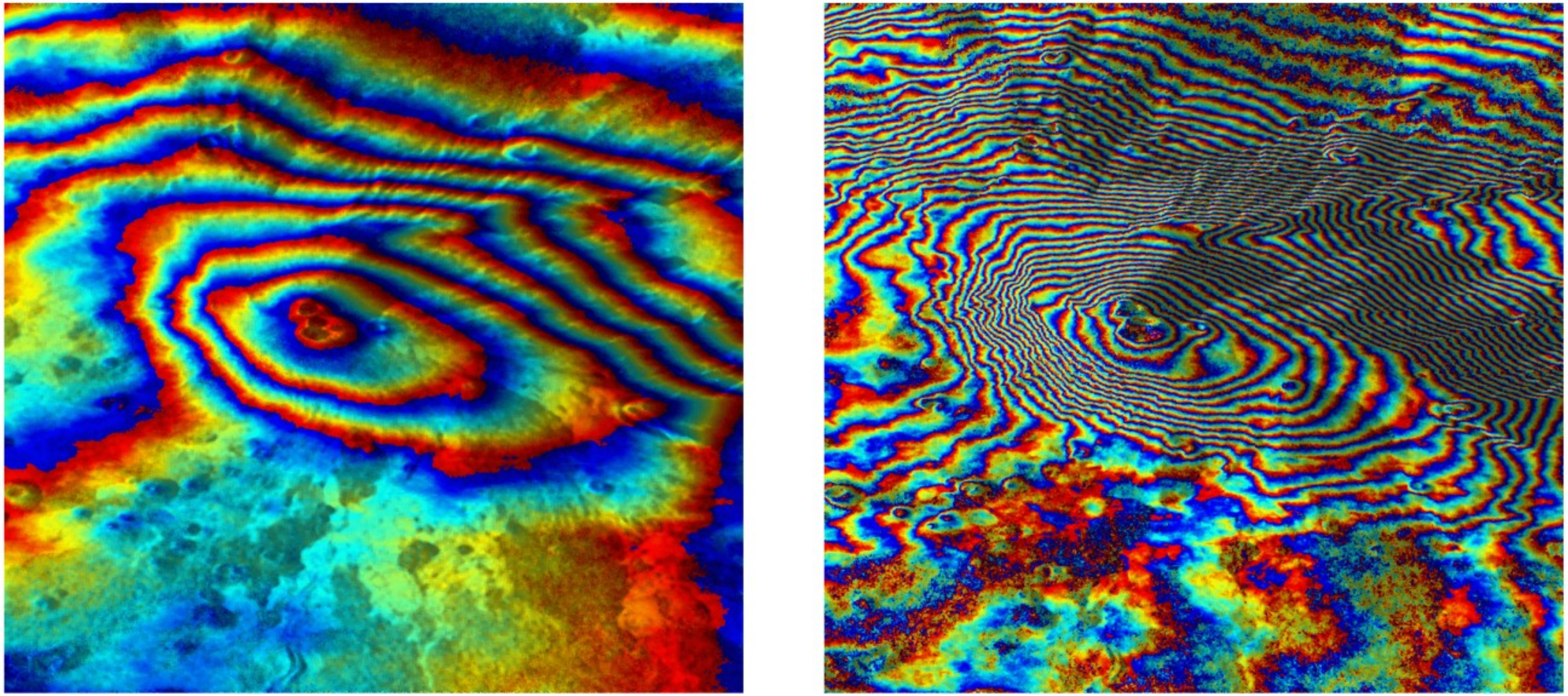

12m baseline

60m baseline

$$\Delta\phi_{topo} = -k_c \frac{B_\perp}{r_{1_{ref}} \sin\theta_1}$$

Sensitivity to frequency: reflectivity

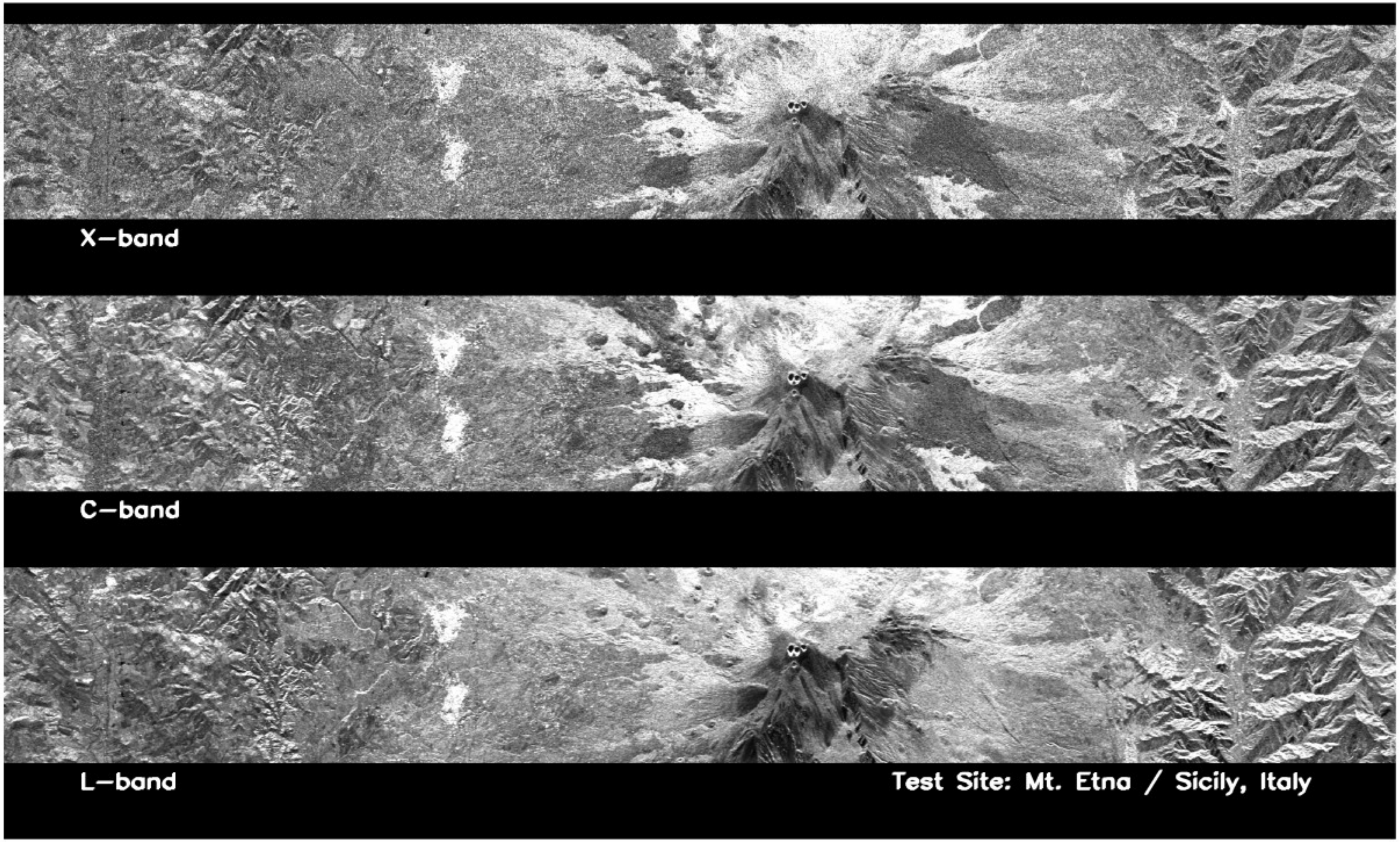

Sensitivity to frequency: raw phase

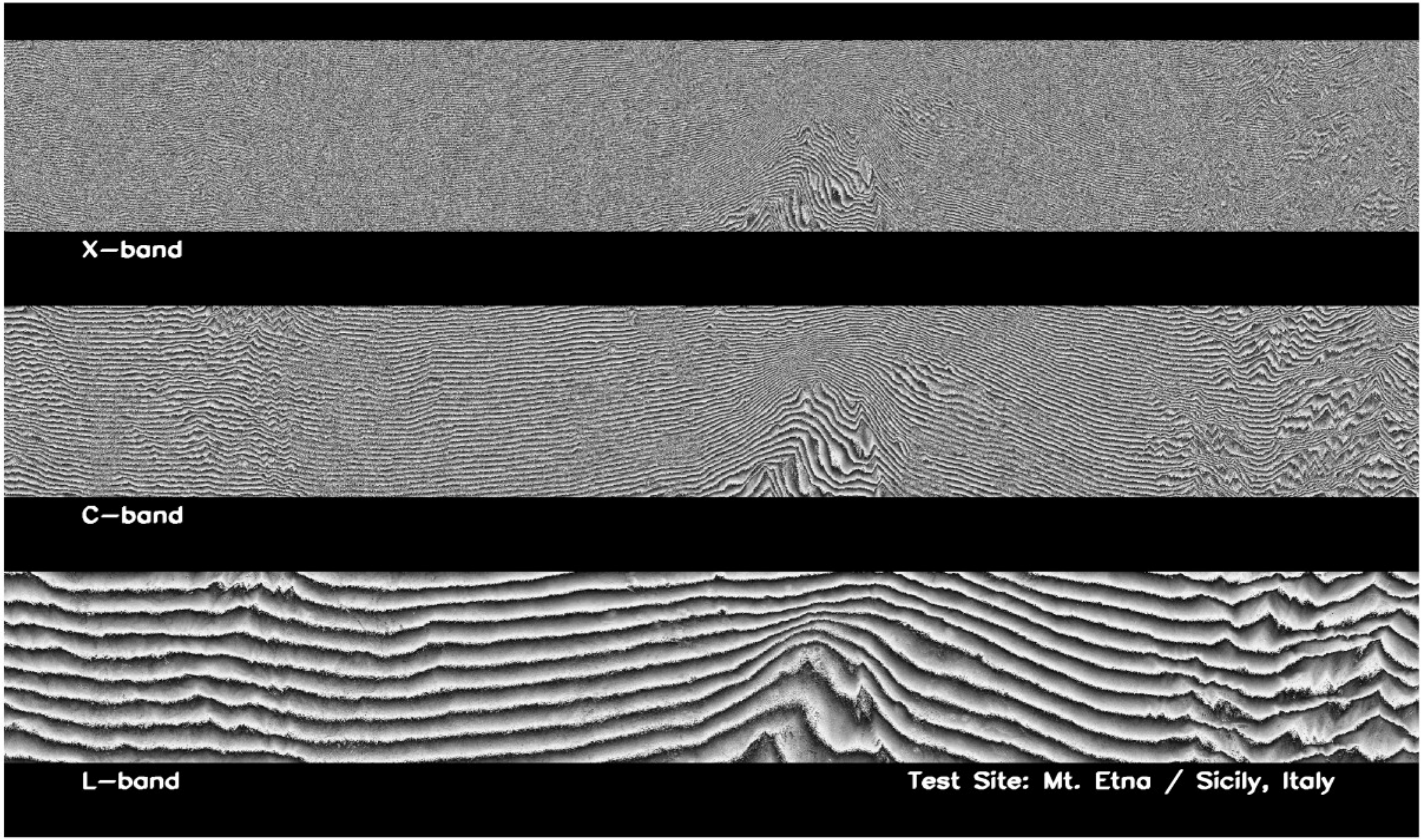

Sensitivity to frequency: flattened phase

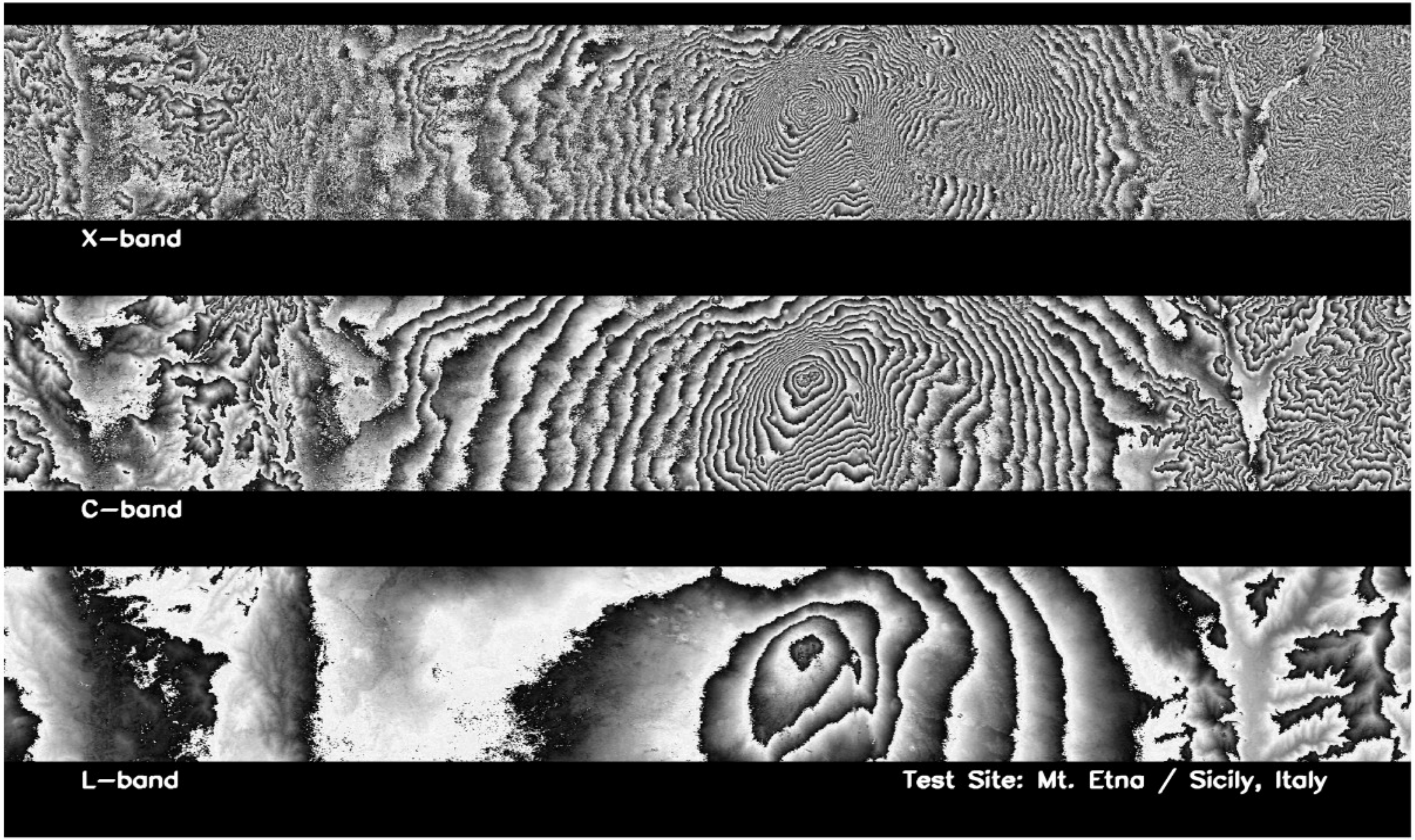

Phase unwrapping

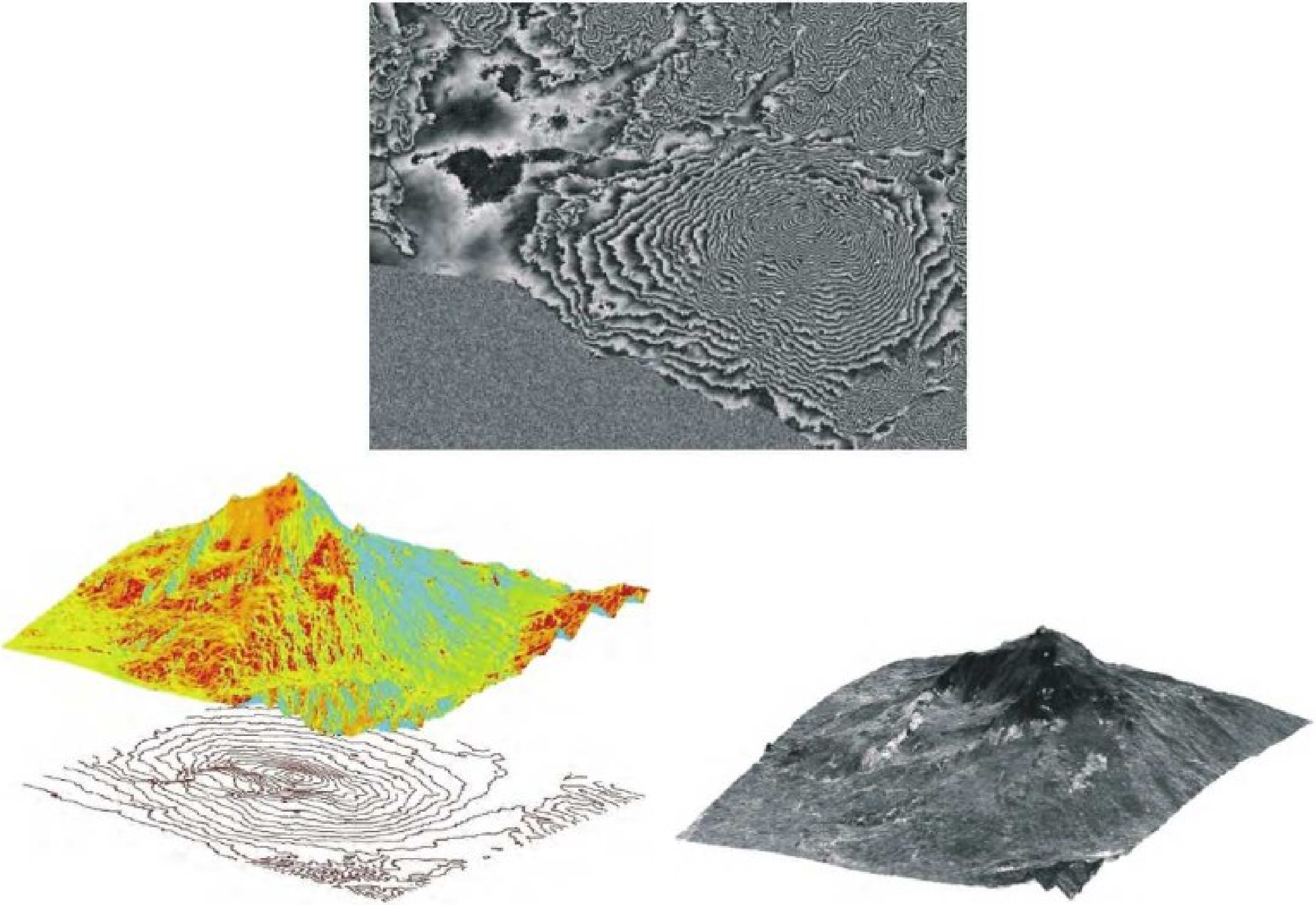

Need for phase unwrapping

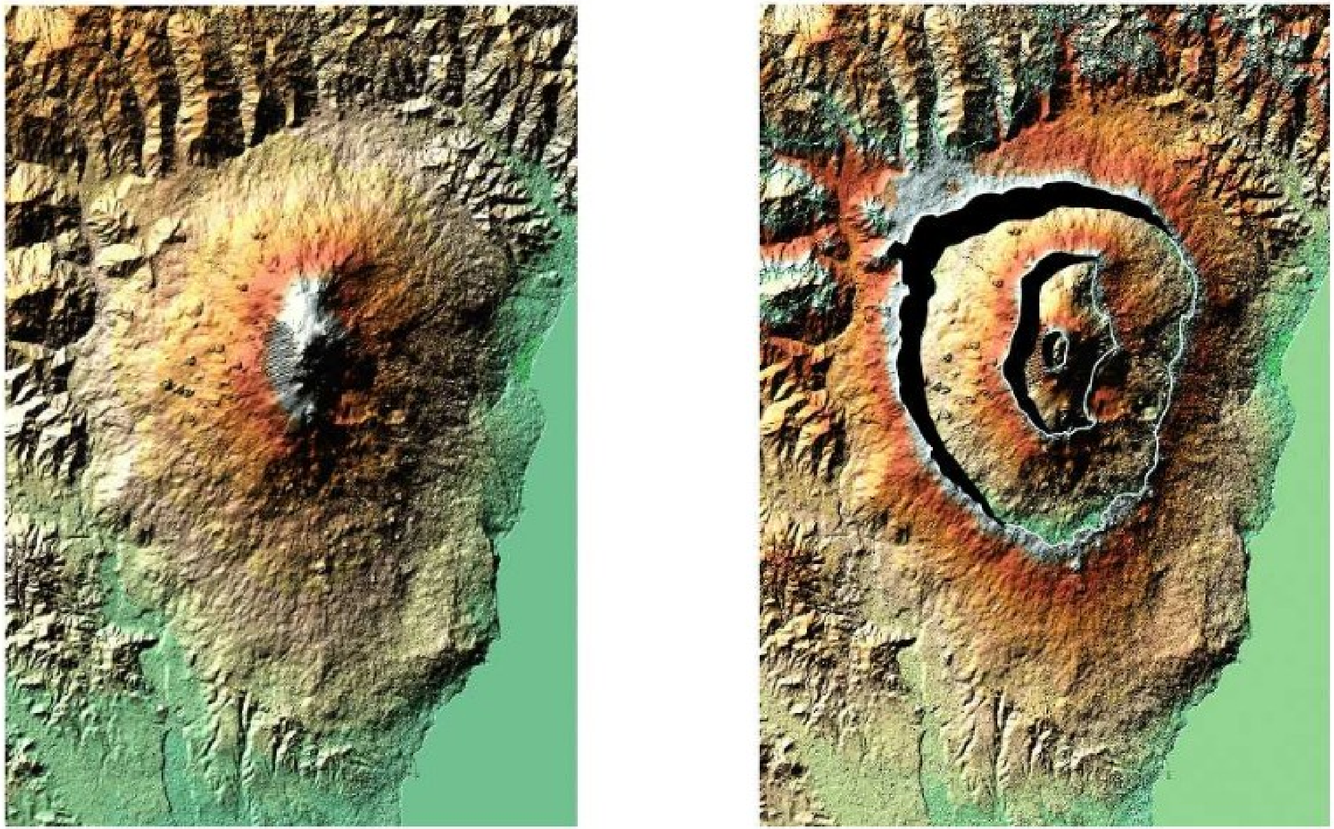

Phase unwrapping principle in 1D

Itoh's method

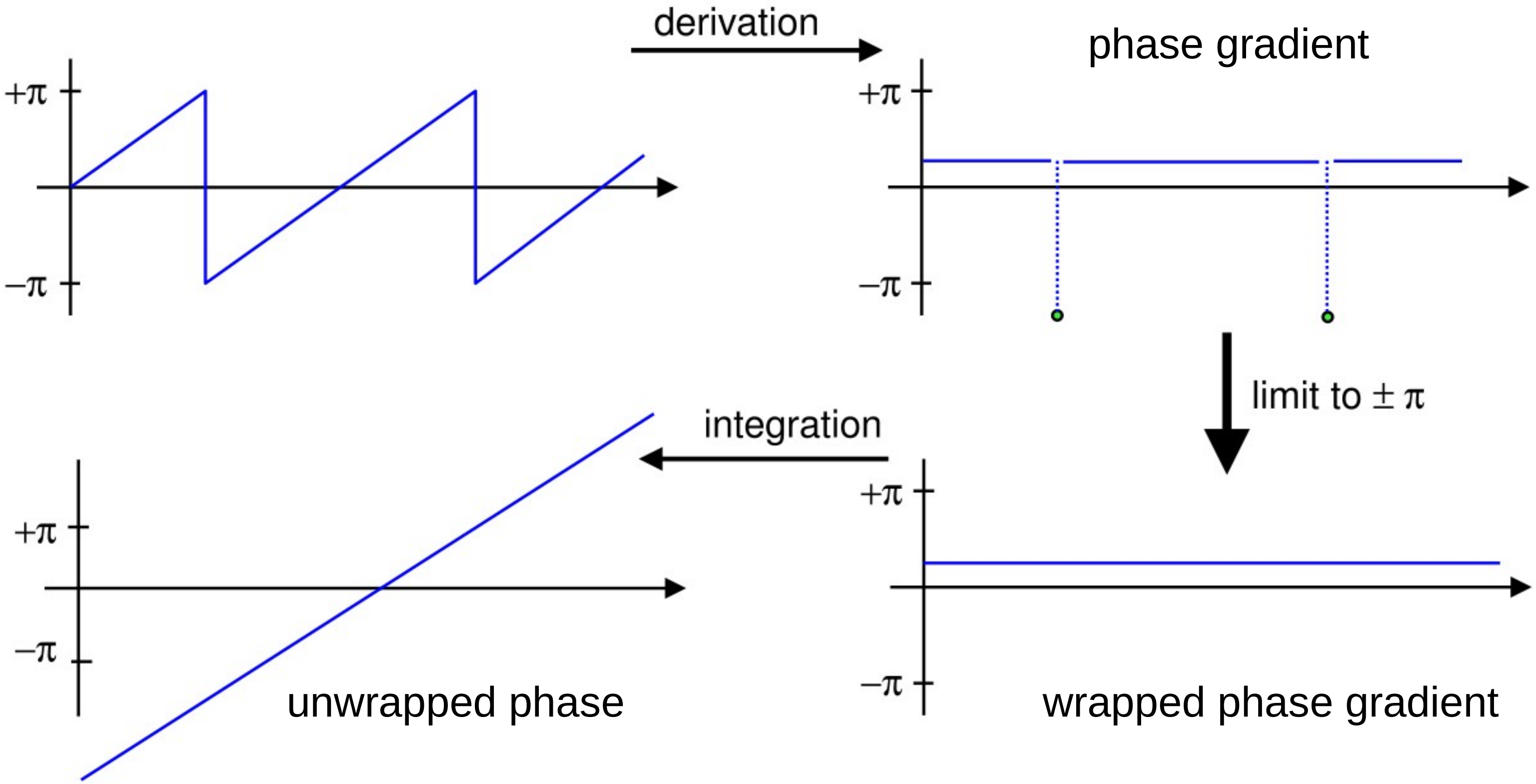

Aliasing-free phase unwrapping

Aliasing-free condition

$$\boxed{|\Delta\phi| < \pi}$$

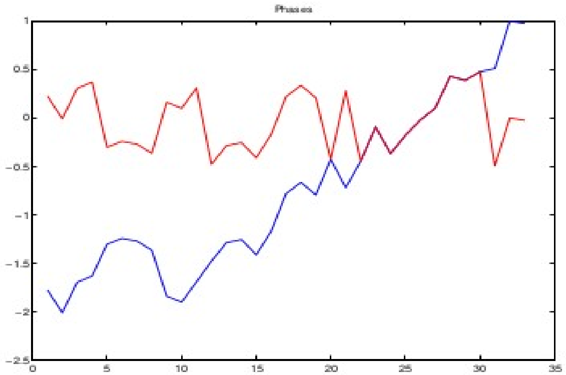

(a) $\phi/(2\pi), \psi/(2\pi)$

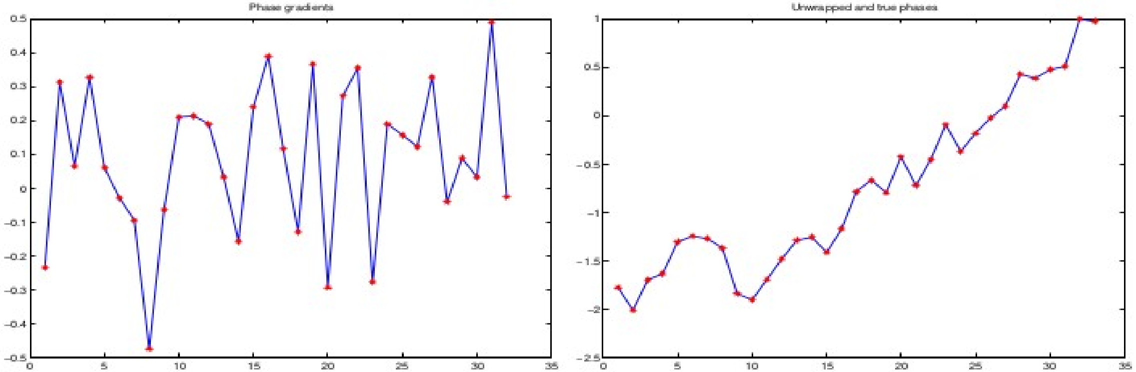

(b) $\Delta\phi/(2\pi), \mathcal{W}(\Delta\psi)/(2\pi)$

(c) $\phi/(2\pi), \hat{\phi}/(2\pi)$

Aliasing-free phase unwrapping

Possible alias if

$$\boxed{\exists|\Delta\phi| > \pi}$$

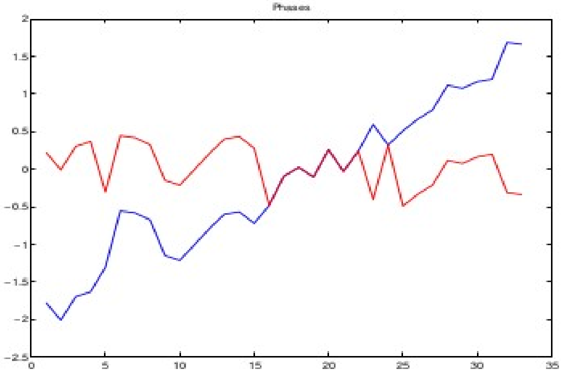

(a) $\phi/(2\pi), \psi/(2\pi)$

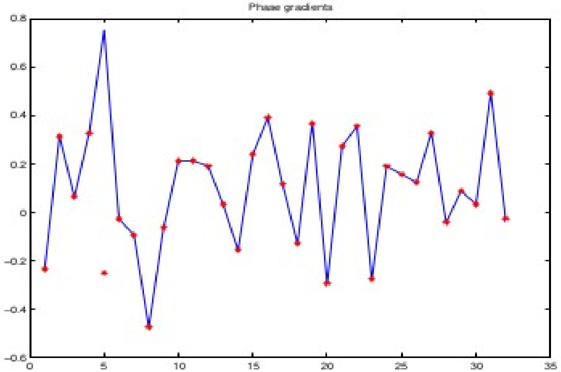

(b) $\Delta\phi/(2\pi), \mathcal{W}(\Delta\psi)/(2\pi)$

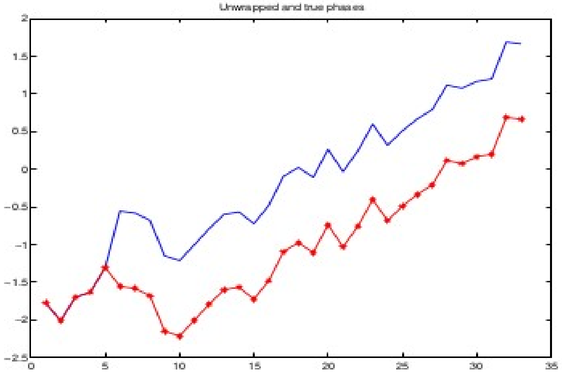

(c) $\phi/(2\pi), \hat{\phi}/(2\pi)$

2D phase unwrapping

Better conditioning through 2D integration path diversity

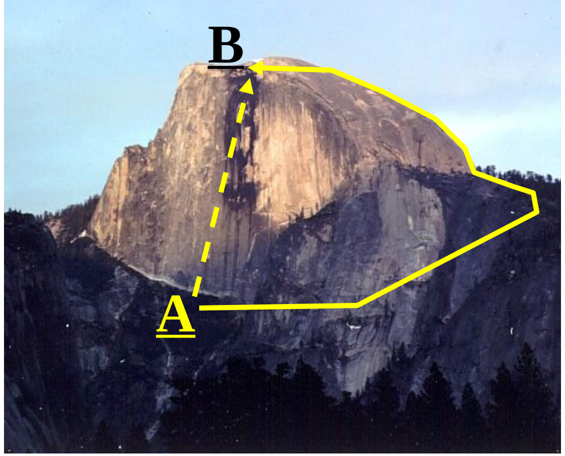

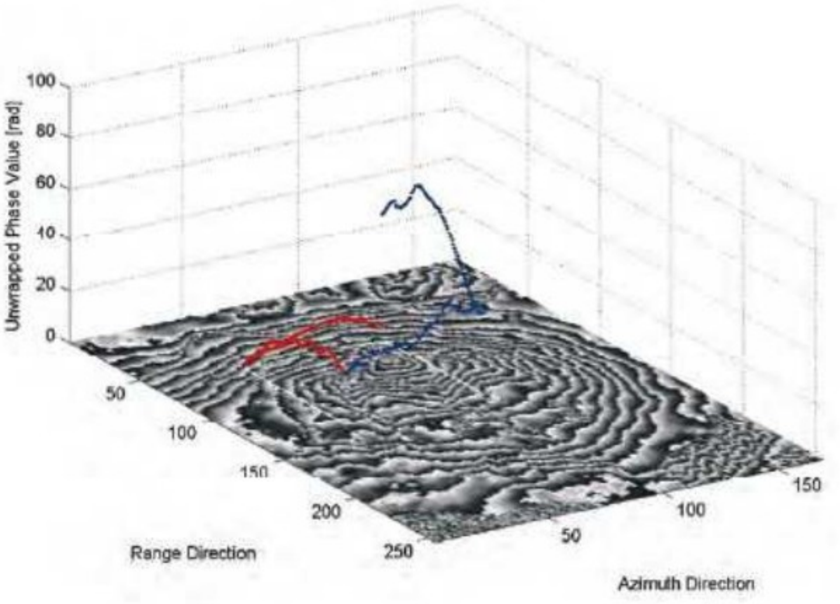

2D phase unwrapping

wrapped phase

residues

branches

2D phase unwrapping

2D phase unwrapping formalism

- Wrapped phase: $\psi(x,r) \rightarrow \boldsymbol{\psi} \in \mathbb{R}^{N_x N_r}$
- Gradient operator: $\boldsymbol{\Delta}(\boldsymbol{\psi}) = \begin{bmatrix} \boldsymbol{\Delta}_x(\boldsymbol{\psi}) \\ \boldsymbol{\Delta}_r(\boldsymbol{\psi}) \end{bmatrix}$
- Unwrapped phase: $\boldsymbol{\phi}$
- L^p norm: $\|\mathbf{x}\|_p = \left(\frac{1}{N} \sum_i |x_i|^p \right)^{1/p}$
- Wrapping operator $\mathcal{W}(\phi) = \arg e^{j\phi}$

$$\boxed{\hat{\boldsymbol{\phi}} = \arg\min_{\boldsymbol{\phi}} \|\boldsymbol{\Delta}\boldsymbol{\phi} - \mathcal{W}(\boldsymbol{\Delta}\boldsymbol{\psi})\|_p}$$

- L^2 solution:
  - very fast
  - Inaccurate (smooth)
- L^1 solution
  - slower
  - very robust
  - better performance

Interferometric SAR processing chain

Acquired images

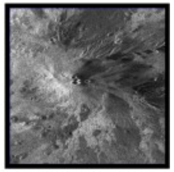

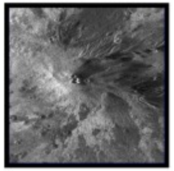

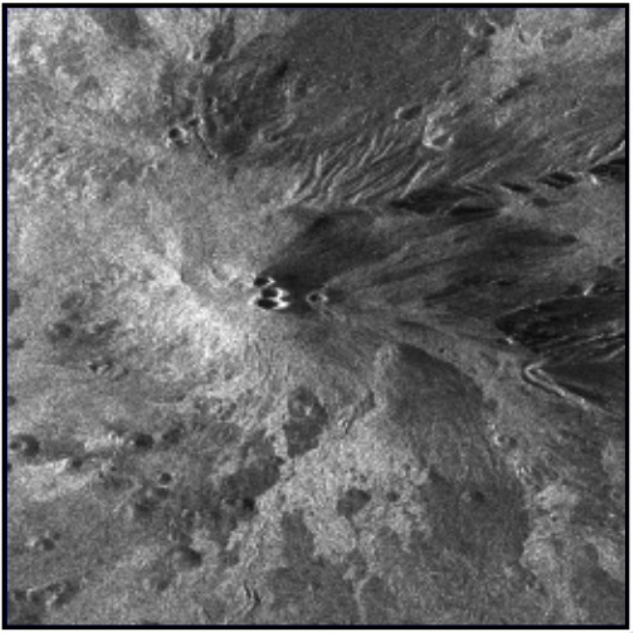

Interferometric SAR processing chain

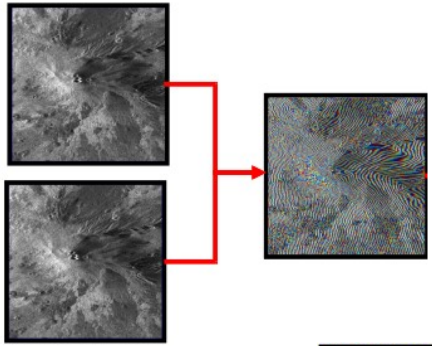

Raw interferogram

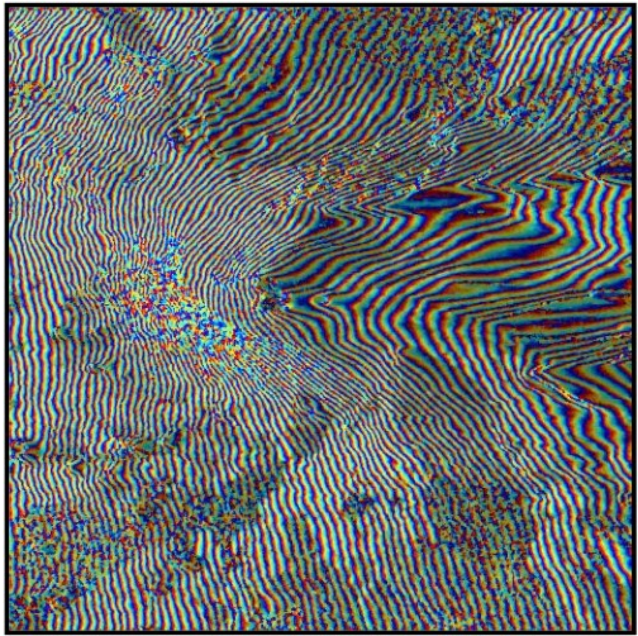

Interferometric SAR processing chain

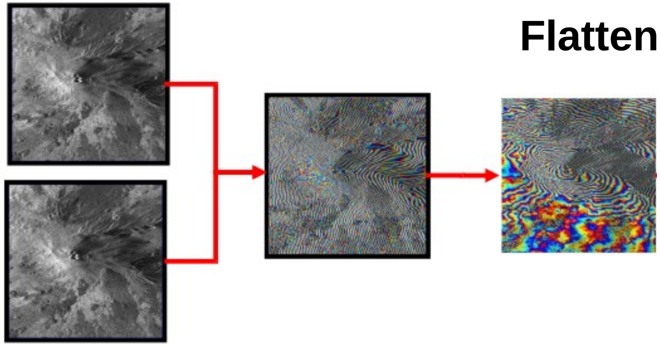

Flattened interferogram

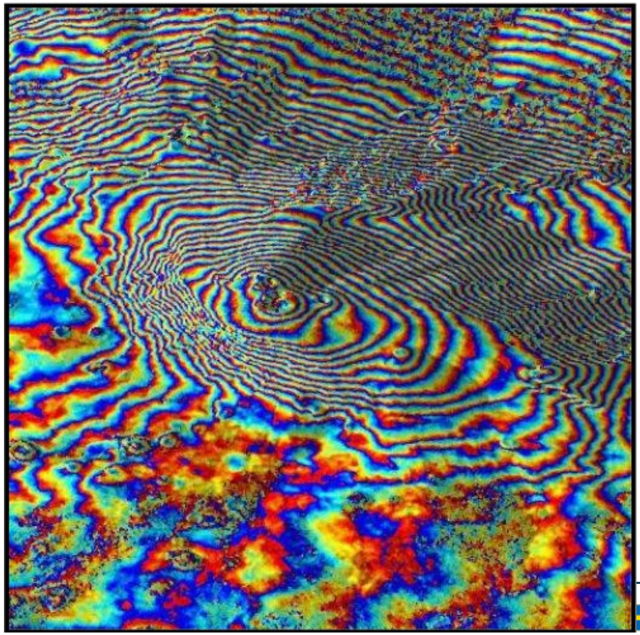

Interferometric SAR processing chain

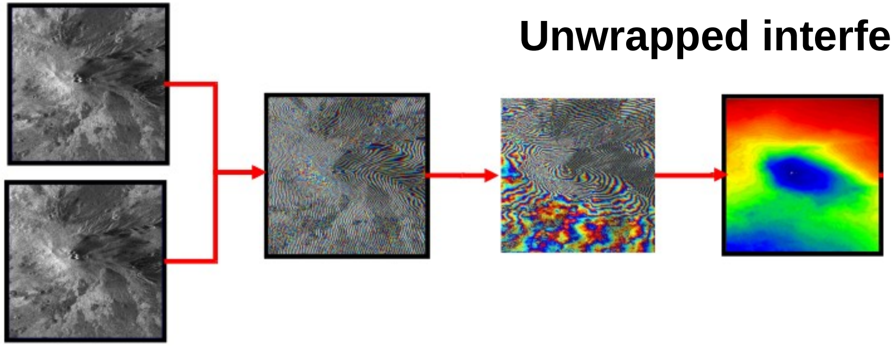

Unwrapped interferogram

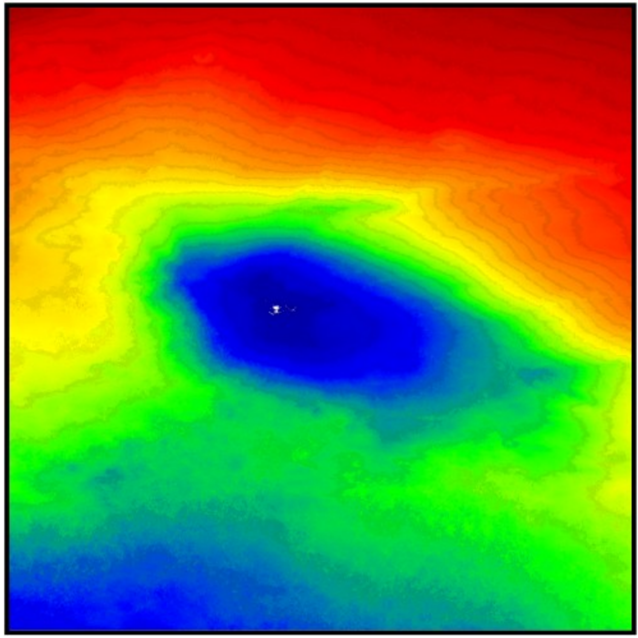

Interferometric SAR processing chain

Geocoded DEM

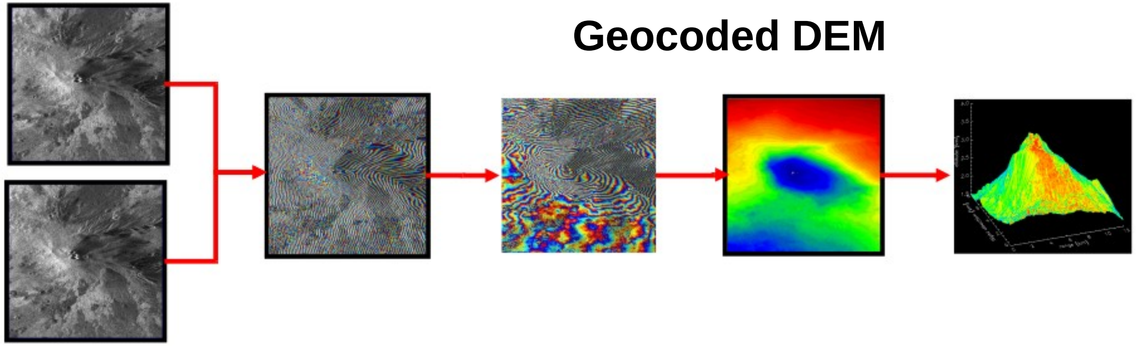

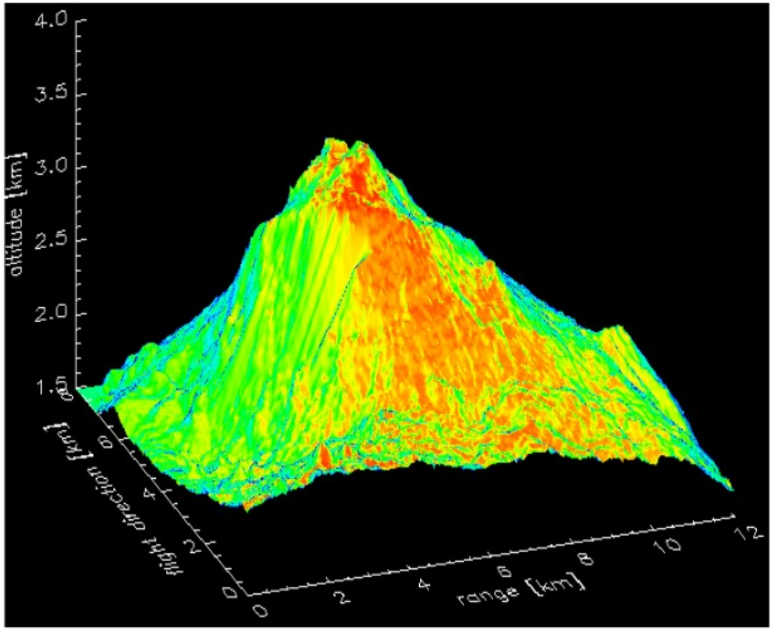

SRTM/X-SAR DEM, Mount Kotopaxi, Ecuador

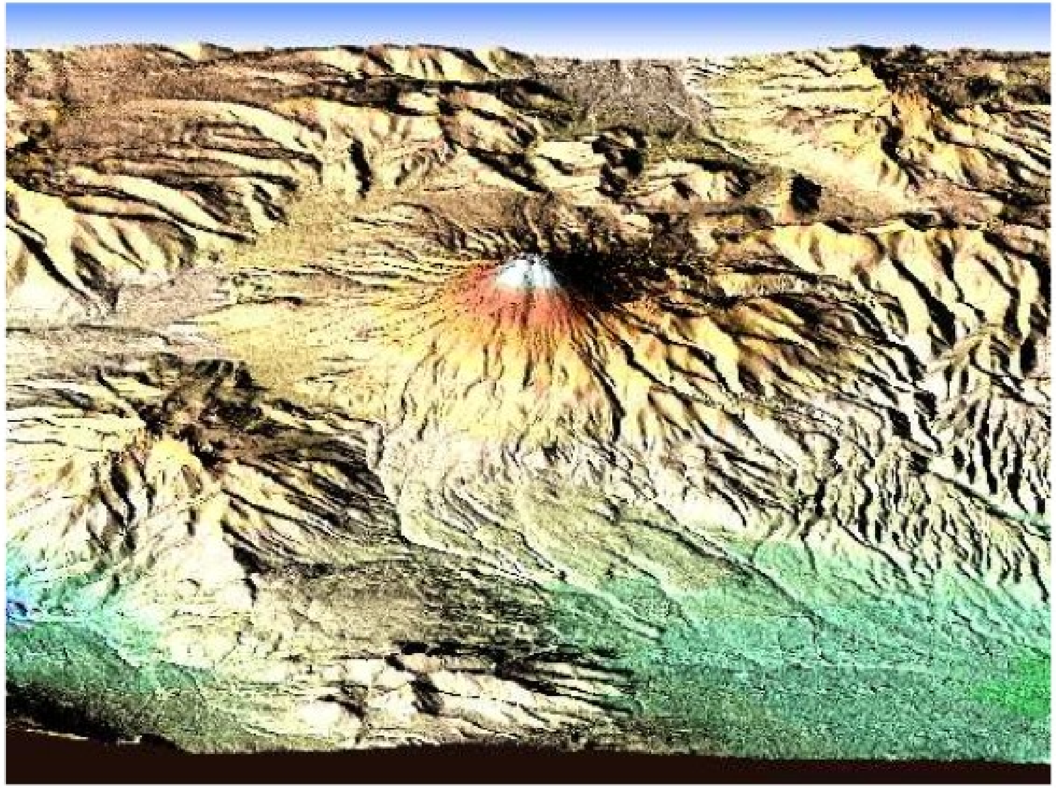

High resolution elevation mapping worldwide

GTOP-030

Spatial Resolution: 30 Arc Sec = 1km
Height Accuracy : 100 m – 500 m

February 2000
Single Pol Channel

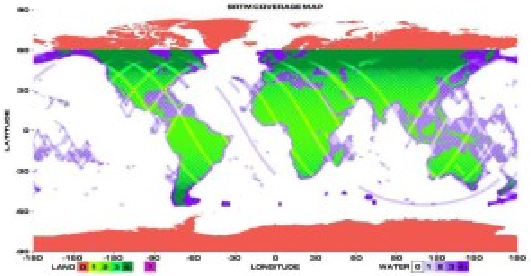

SRTM: X-SAR

Spatial Resolution: 1 Arc Sec = 30m
Height Accuracy : 6-10 m

Hydrological water flow simulation

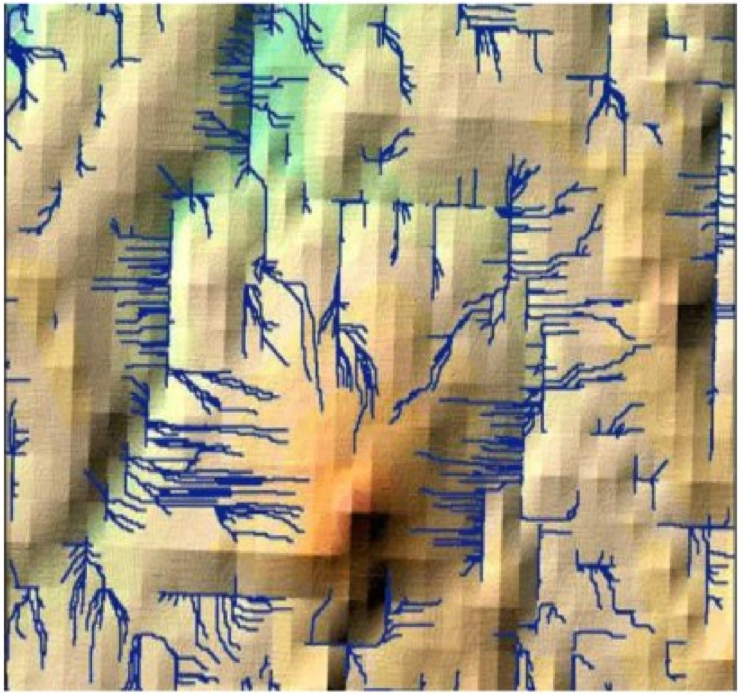

Globe-30 DEM

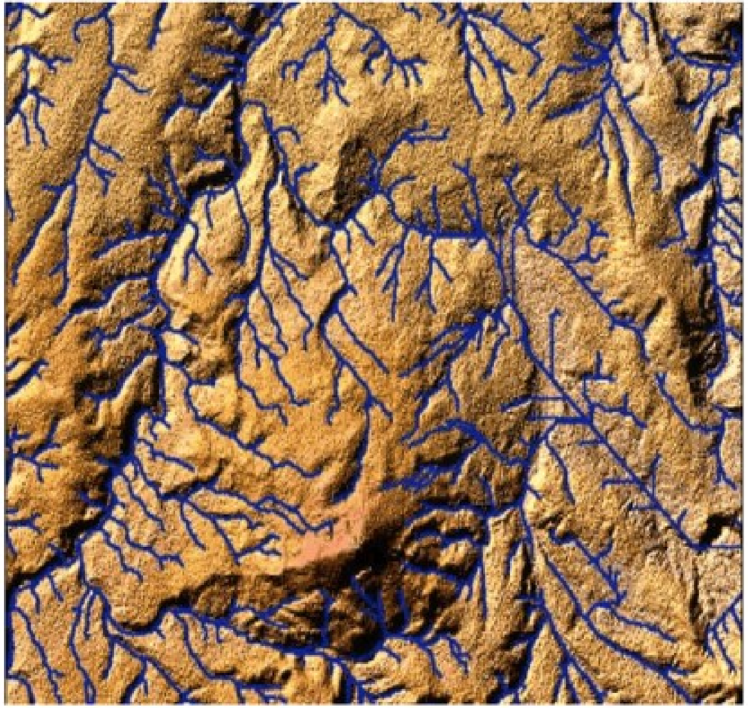

SRTM DEM

SAR Interferometry basics

A signal processing approach

Single SAR image statistics

S : Single Look Complex (SLC) image

Array of coherent coefficients $S_{(x,r)} = \rho_{(x,r)} \mathrm{e}^{j\phi_{(x,r)}}$

Reflexion coefficient amplitude image

$$\rho_{(x,r)} \propto |A_c(x,r)|$$

Composite phase image

$$\phi_{(x,r)} = \phi_r + \phi_{obj} = kr + \phi_{obj}$$

ϕ_r deterministic component

ϕ_{obj} may be random

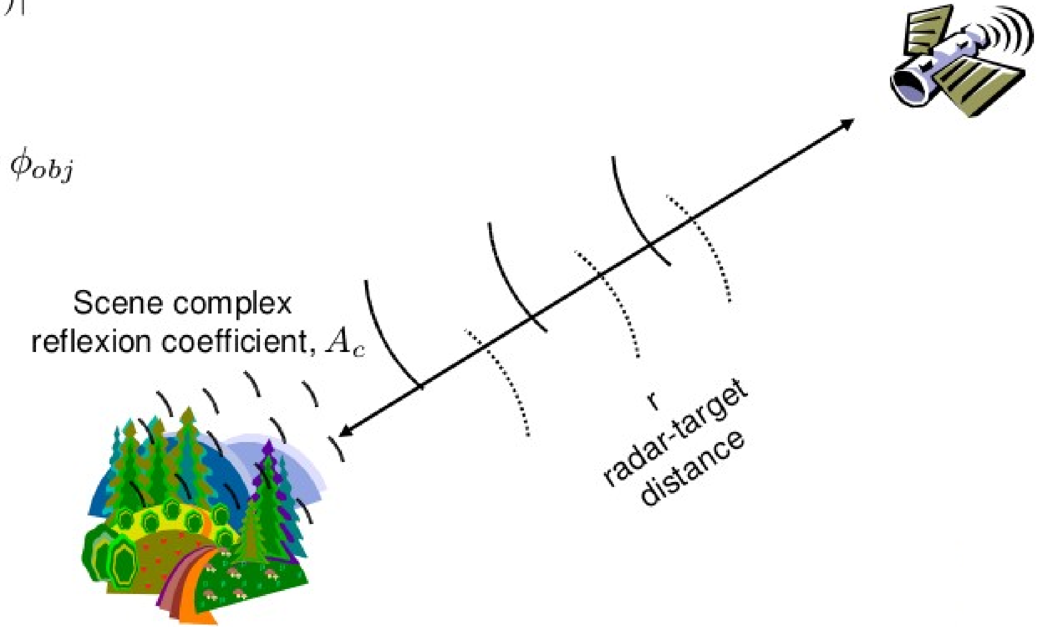

Speckle effect

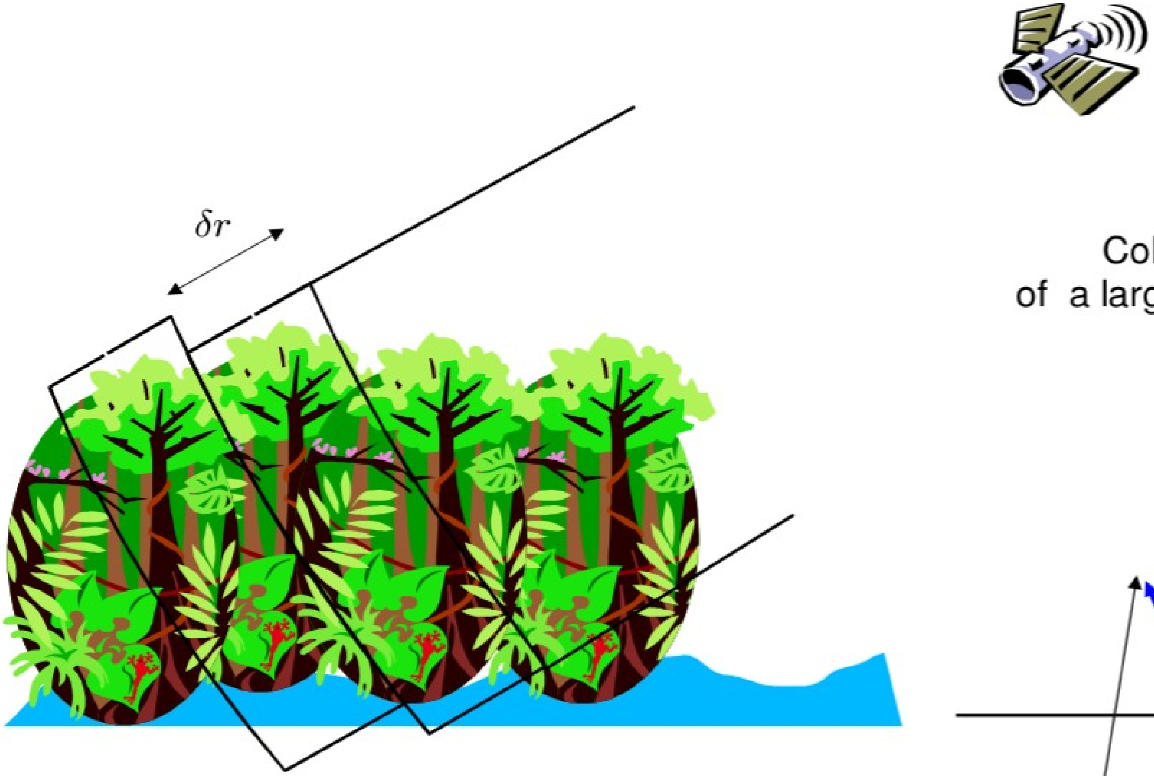

Coherent superposition
of a large number of contributions

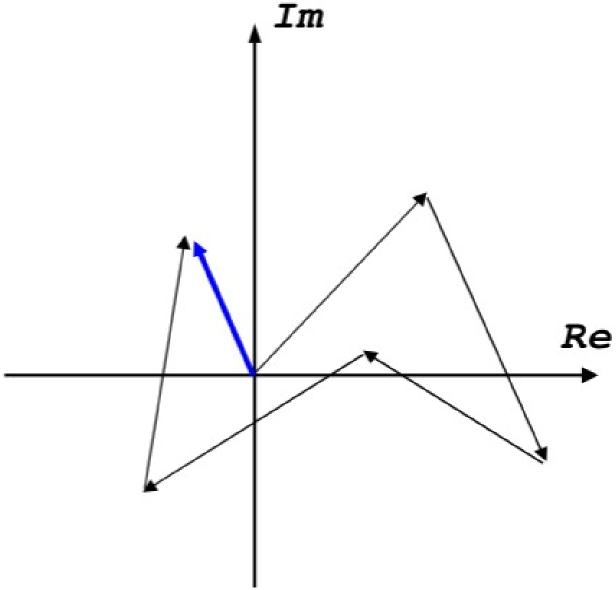

ϕ_{obj} is usually random

Deterministic vs random scattering

Point-like strong scatterers

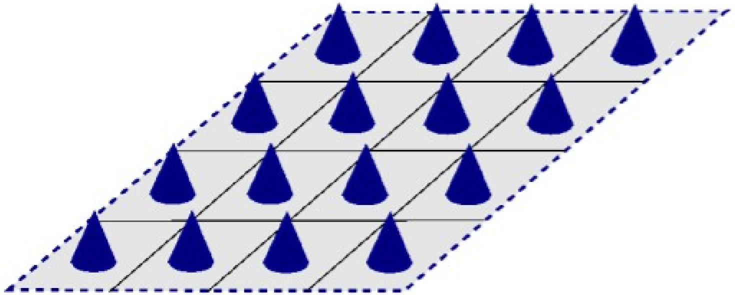

⇧
A single dominant response
within a resolution cell

Sum of a large number of contributions
with random position, amplitude and phase ⇨
within a resolution cell

Natural surfaces

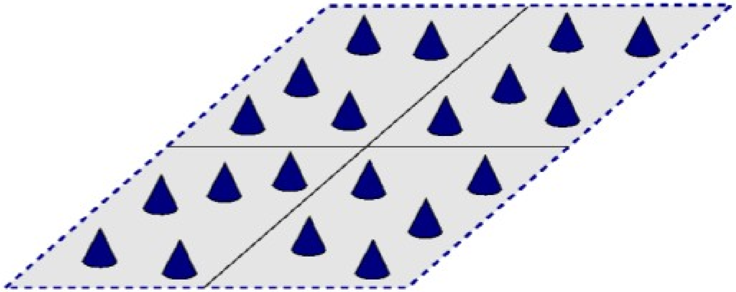

Volumetric media

Deterministic scattering

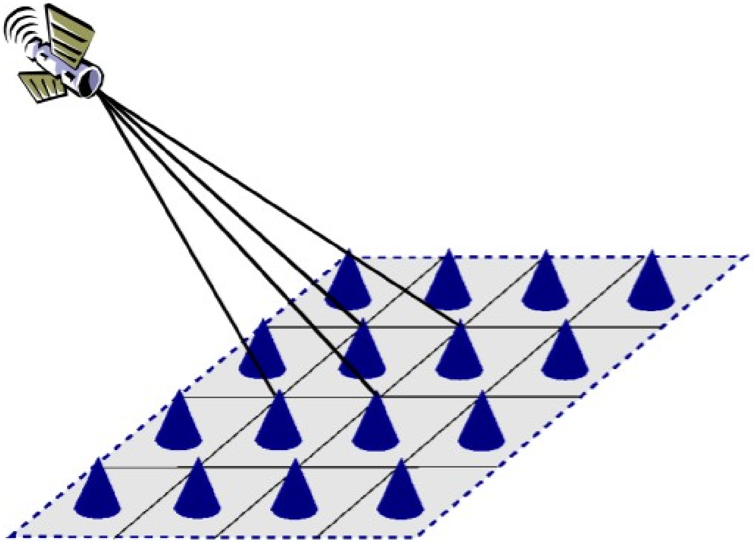

A single dominant response within a resolution cell

SAR signal for a given resolution cell

$$s(x,r) = \int a_c(r')\,\mathrm{e}^{-jkr'}\,h(x-x',r-r')dv'$$

For a point-like scatterer

$$a_c(r) = A\,\mathrm{e}^{j\phi_0}\,\delta(r-r_0) + \epsilon \approx A\,\mathrm{e}^{j\phi_0}\,\delta(r-r_0)$$

$$s(x,r) = A\,\mathrm{e}^{j\phi_0}\,\mathrm{e}^{-jkr_0}\,h(x-x_0,r-r_0)$$

Deterministic signal components

$$s(x,r) = \sqrt{I}\mathrm{e}^{j\phi}$$

- intensity: $I = |s(x,r)|^2$

phase: $\phi = \phi_0 - kr_0 = \arg s(x,r)$

Random scattering

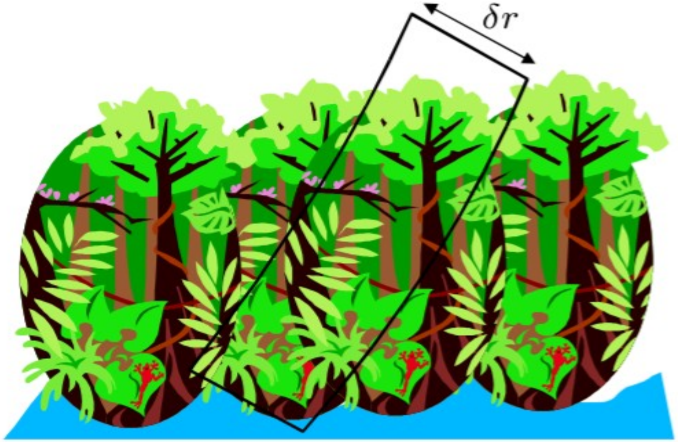

⇧

Distributed medium
with numerous random contributions
within a resolution cell

SAR signal for a given resolution cell

$$s(x,r) = \int a_c(r')\, \mathrm{e}^{-jkr'}\, h(x-x', r-r')dv'$$

For a set of random scatterers

Complex amplitude density $a_c(r) = a_c(r)\mathrm{e}^{j\phi_0(r)}$

Coherent integration

⇨ random behavior : « speckle effect »

Speckle product model

$$s(x,r) = \sqrt{I}\mathrm{e}^{j\phi} = \sqrt{I_{eq}}\mathrm{e}^{j\phi_{eq}}\, n_c$$

- random intensity: $I = |s(x,r)|^2$

random phase: $\phi = \arg(s(x,r))$

speckle component: n_c

Deterministic scattering

- One realization

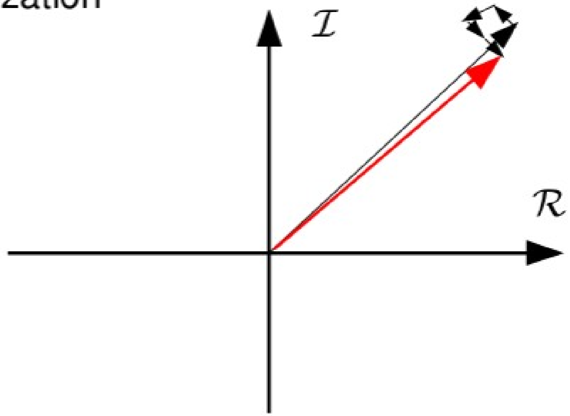

- Another one

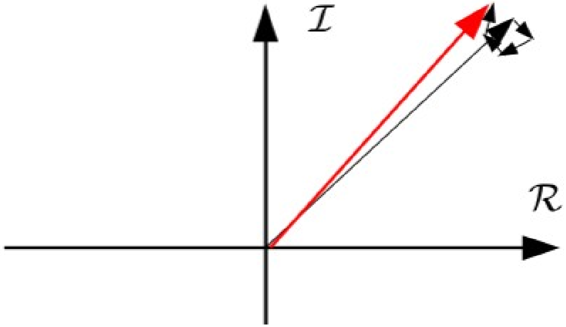

Random scattering

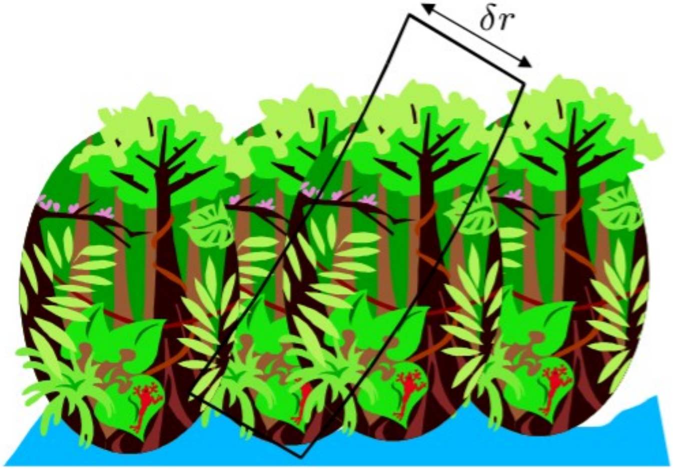

⇧
Distributed medium
with numerous random contributions
within a resolution cell

- One realization

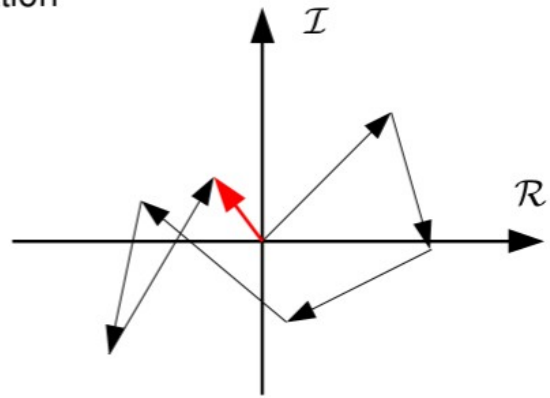

- Another one

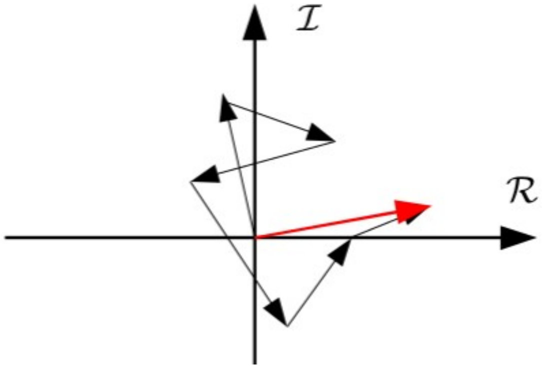

Fully developed speckle statistics

Central limit theorem

Assumptions :
- no dominant scatterer
- uniformely distributed object phase
- uncorrelated scatters
- large number of scatterers

→

s follows a complex normal distribution

$E(s) = 0$ uniform phase argument

$\mathrm{var}(s) = \mathrm{E}(I) = \bar{I}$ « true » reflectivity

Complex signal distribution $s = \sqrt{\bar{I}} e^{j\bar{\phi}} n_c$

Multiplicative speckle component with circular Gaussian distribution

$$n_c = \mathcal{R}(n_c) + j\mathcal{I}(n_c) \sim \mathcal{N}_c(0,1)$$

Fully developed speckle statistics

Single-look complex (SLC) data

Complex circular normal distribution $s = \sqrt{\bar{I}} e^{j\bar{\phi}} n \sim \mathcal{N}_C(0, \bar{I})$

Intensity

Exponential distribution $\hat{I} = |s|^2 \sim \mathcal{E}(\bar{I})$

Unbiased reflectivity estimate $\mathrm{E}(\hat{I}) = \bar{I} = \mathrm{var}(s)$

Extremely high dispersion $\mathrm{var}(\hat{I}) = \bar{I}^2$

Phase

Uniform distribution → mean value cannot be retrieved

Multi-looked data statistics

Single-look intensity

Exponential distribution $\hat{I} = |s|^2 \sim \mathcal{E}(\bar{I})$

Unbiased reflectivity estimate $\mathrm{E}(\hat{I}) = \bar{I} = \mathrm{var}(s)$

Extremely high dispersion $\mathrm{var}(\hat{I}) = \bar{I}^2$

Multi-look intensity

L independent realizations (or looks) $\{I(l) = |s(l)|^2\}_{l=1}^{L}$

Multi-look intensity estimate

$$\boxed{\hat{I} = \frac{1}{L}\sum_{l} I(l)}$$

Bias, variance $\mathrm{E}(\hat{I}) = \bar{I} = \mathrm{var}(s)$ $\boxed{\mathrm{var}(\hat{I}) = \frac{\bar{I}^2}{L}}$

Multilooking

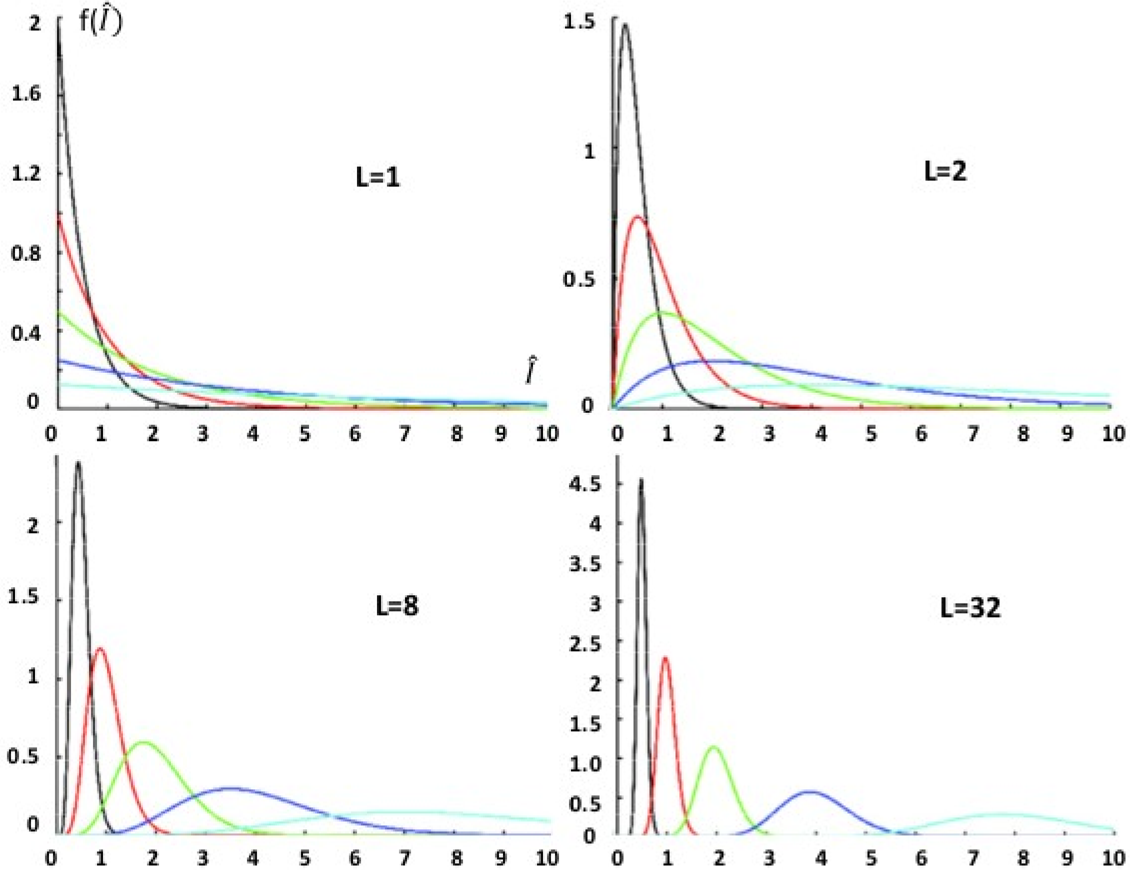

$$\bar{I} = 0.5, 1, 2, 4, 8$$

Single Look Complex (SLC) SAR image

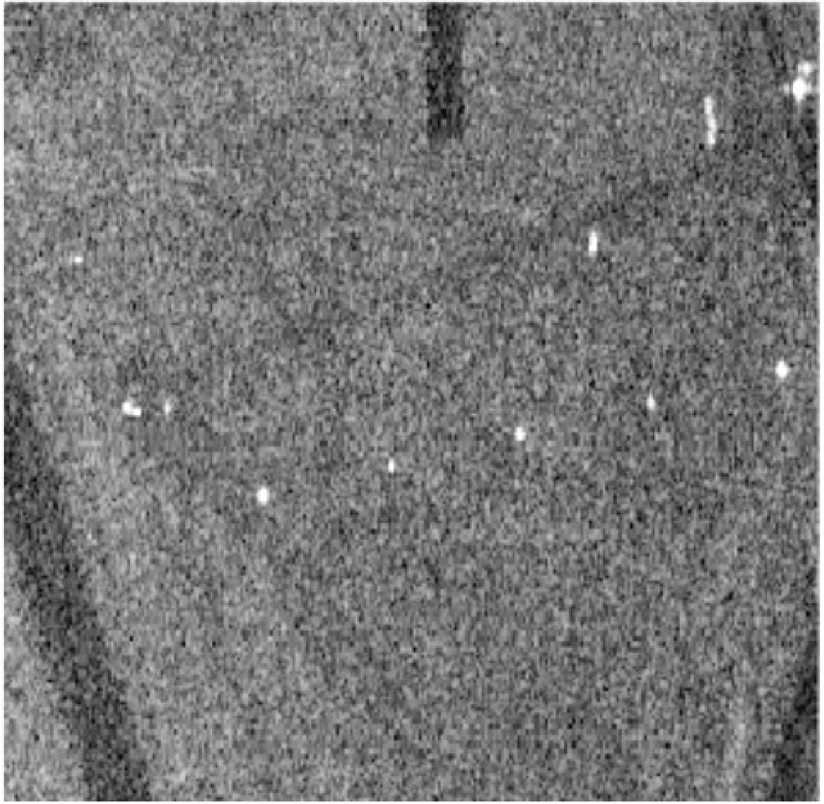

Intensity image

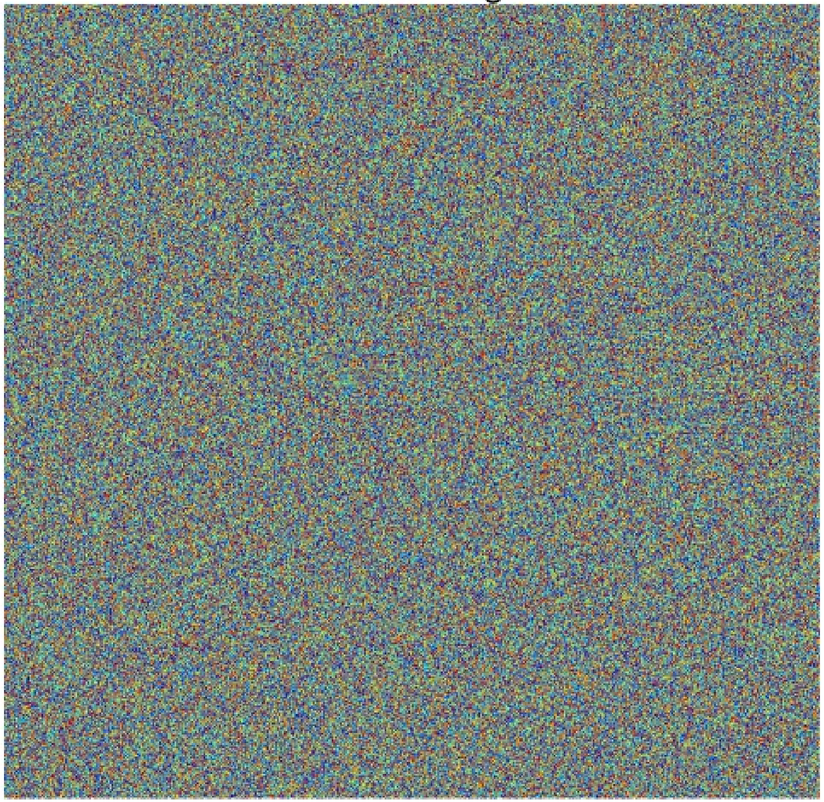

Phase image

Single Look Complex (SLC) SAR image

$$\hat{I} = \frac{1}{L}\sum_{L} I_i$$

Single look image

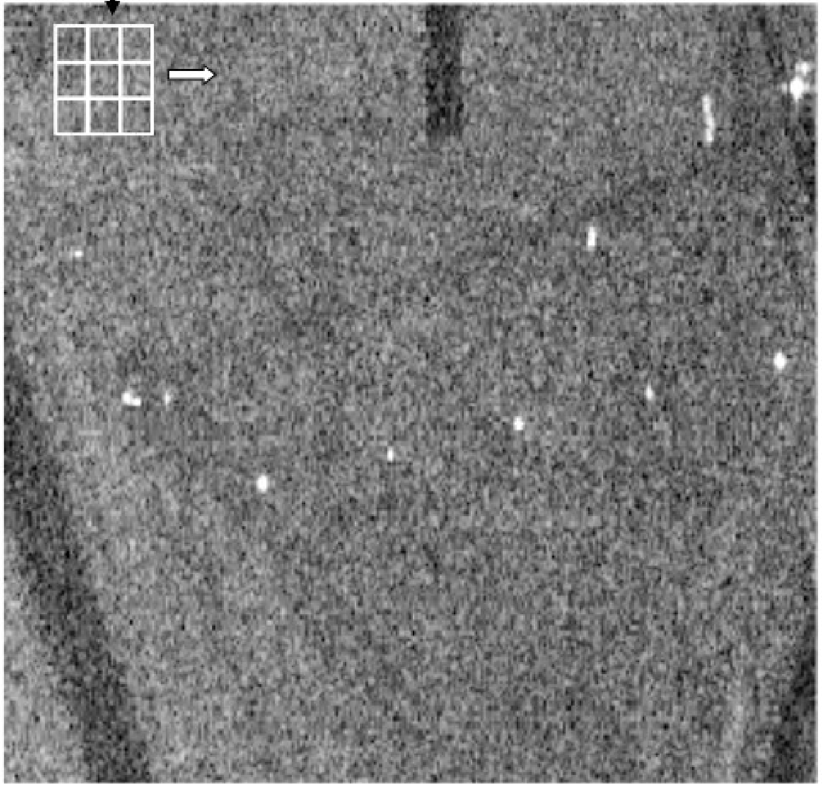

After spatial filtering (N*N boxcar)

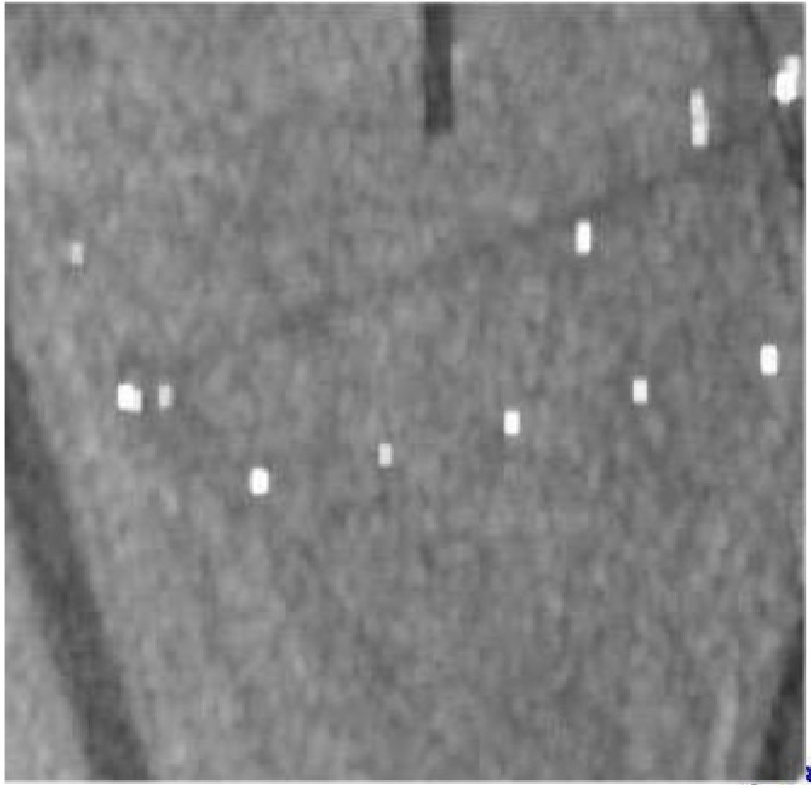

Speckle filtering

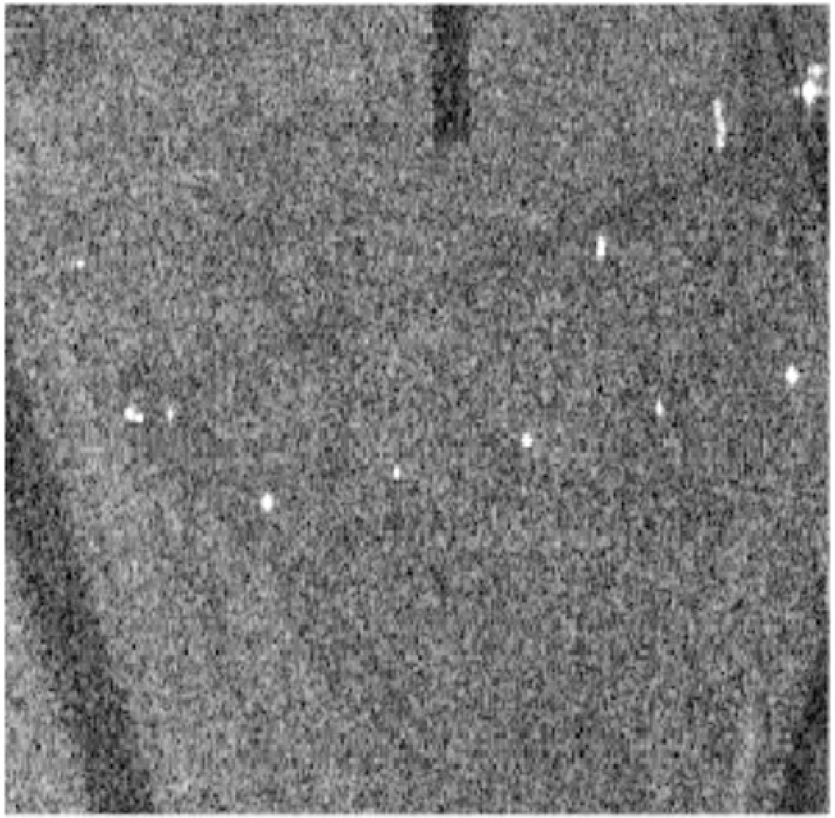

Single look image

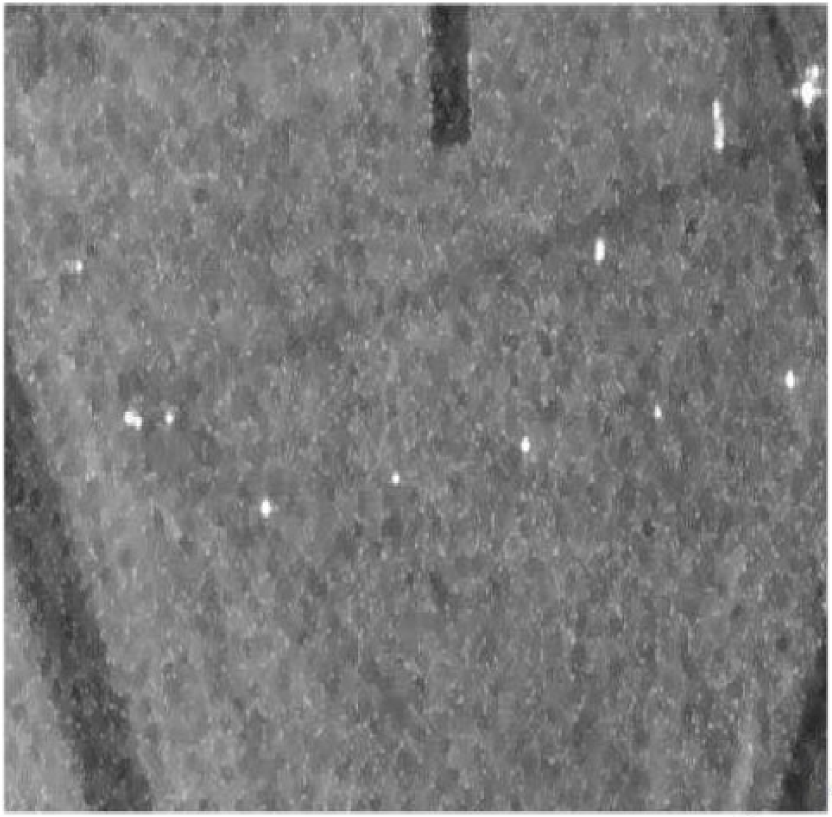

After spatial filtering (N*N Lee filter)

Single Look Complex (SLC) SAR image

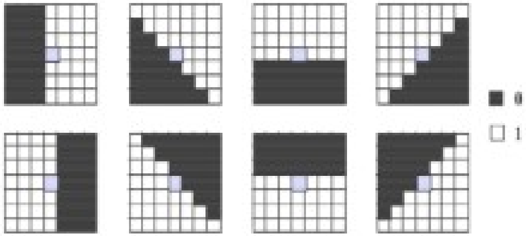

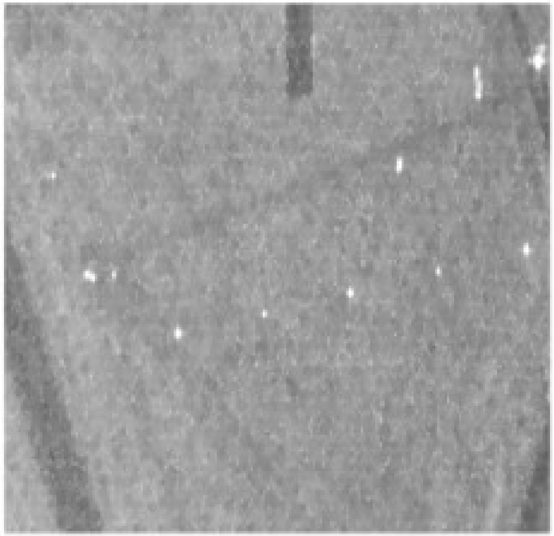

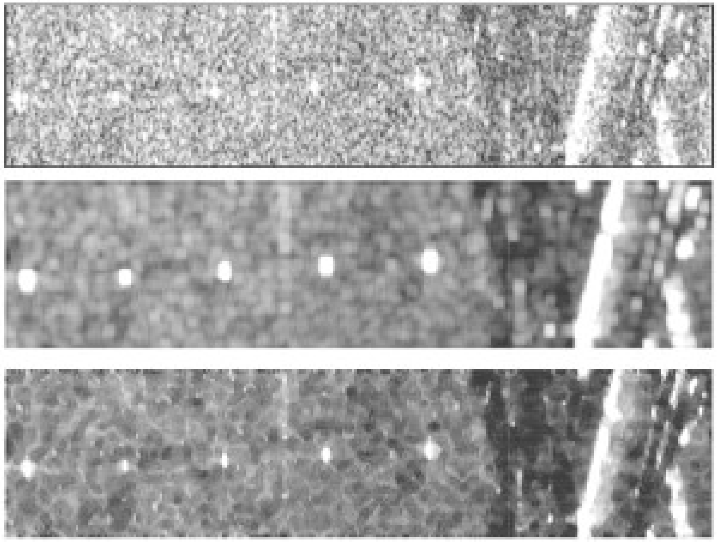

Interferometric SAR image statistics

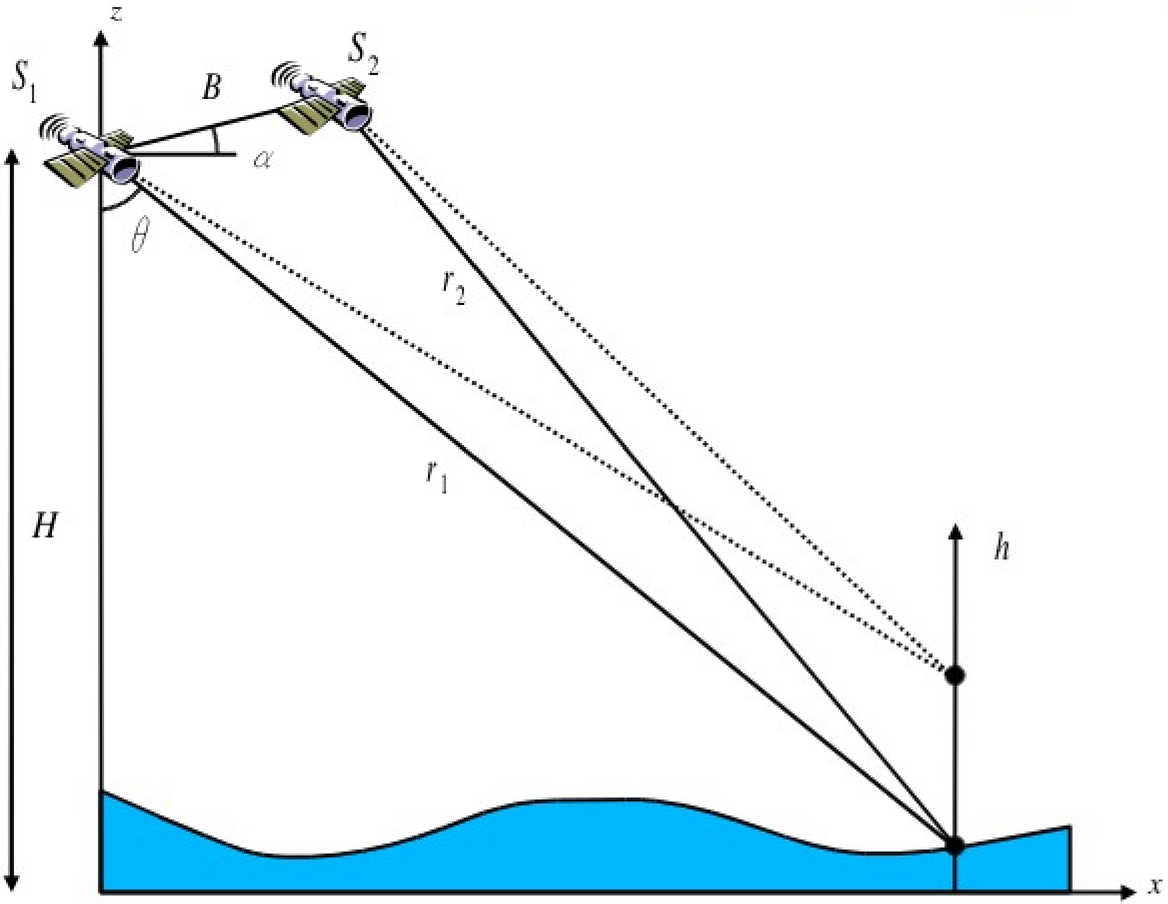

Coherent SAR image pair

$$s_1 = \sqrt{I_1}\, e^{j\phi_1} = \sqrt{I_1}\, e^{j(-kr_1 + \phi_{obj1})}$$

$$s_2 = \sqrt{I_2}\, e^{j\phi_2} = \sqrt{I_2}\, e^{j(-kr_2 + \phi_{obj2})}$$

Assumptions

$$I_1 \approx I_2 \quad \text{and} \quad \phi_{obj1} \approx \phi_{obj2}$$

Interferometric phase difference

$$\Delta\phi_{12} = \arg(s_1 s_2^*)$$

Interferometric SAR image statistics

Joint interferometric representation

$$\mathbf{k} = \begin{bmatrix} s_1 \\ s_2 \end{bmatrix} \sim \mathcal{N}_c(\mathbf{0}, \mathbf{C})$$

with $\mathbf{C} = \mathrm{E}(\mathbf{k}\mathbf{k}^\dagger) = \begin{bmatrix} \mathrm{E}(s_1 s_1^*) & \mathrm{E}(s_1 s_2^*) \\ \mathrm{E}(s_1^* s_2) & \mathrm{E}(s_2 s_2^*) \end{bmatrix} = \begin{bmatrix} \overline{I_1} & \gamma\sqrt{\overline{I_1}\,\overline{I_2}} \\ \gamma^*\sqrt{\overline{I_1}\,\overline{I_2}} & \overline{I_2} \end{bmatrix}$

Interferometric coherence : normalized correlation coefficient

$$\gamma = \frac{\mathrm{E}(s_1 s_2^*)}{\sqrt{\overline{I_1}\,\overline{I_2}}} = |\gamma|\,\mathrm{e}^{j\phi}$$

$|\gamma| \leq 1$ Cauchy-Schwarz inequality

$|\gamma| = 1 \Rightarrow \phi = \Delta\phi_{12}$ interferometric assumptions are fulfilled

$|\gamma| = 1 \Rightarrow \phi = ?$ interferometric images are totally uncorrelated

$|\gamma|$ is an indicator of the interferometric information (and phase) quality

Multi-looked InSAR data statistics

Multi-look covariance matrix

L independent realizations (or looks) $\{\mathbf{k}(l)\}_{l=1}^{L}$

Multi-look covariance estimate

$$\boxed{\widehat{\mathbf{C}} = \frac{1}{L}\sum_{l}\mathbf{k}(l)\mathbf{k}^{*t}(l)}$$

Unbiased $\mathrm{E}(\widehat{\mathbf{C}}) = \mathbf{C}$

Multi-look coherence estimate

$$\boxed{\hat{\gamma} = \frac{\sum_l s_1(l)s_2^*(l)}{\sqrt{(\sum_l |s_1(l)|^2)(\sum_l |s_2(l)|^2)}}}$$

Multilook InSAR coherence statistics

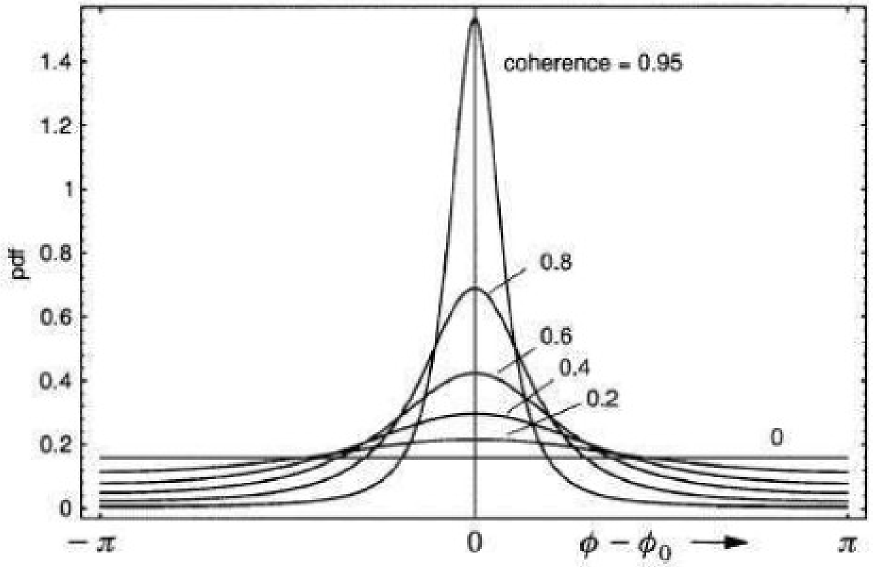

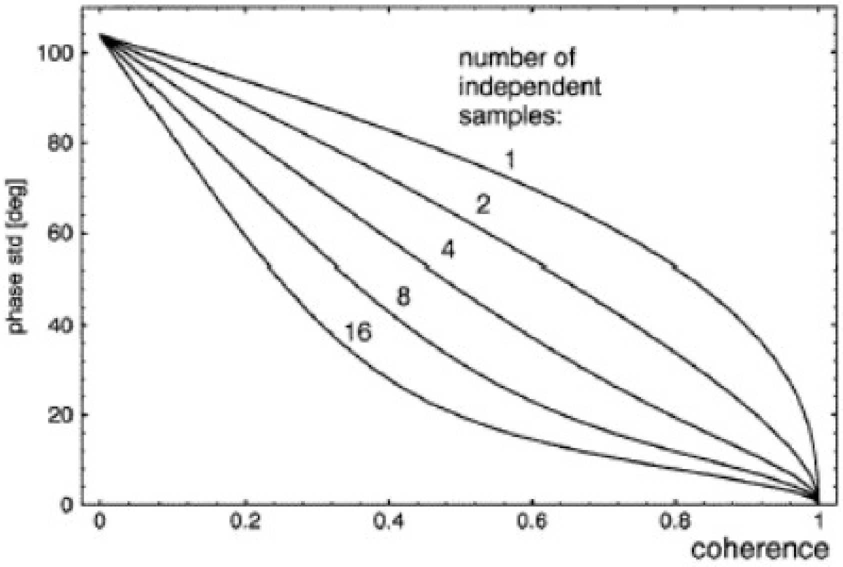

$$\boxed{\hat{\phi} = \arg \hat{\gamma}}$$

$$\boxed{\mathrm{E}(\hat{\phi}) = \phi}$$

$$\boxed{\mathrm{var}(\phi) = f(L, |\gamma|)}$$

Multilook InSAR coherence statistics

$$\boxed{\hat{\rho} = |\hat{\gamma}|}$$

$$\boxed{\mathrm{E}(\hat{\rho}) \neq |\gamma|}$$

$$\boxed{\lim_{L \to +\infty} \hat{\rho} = |\gamma|}$$

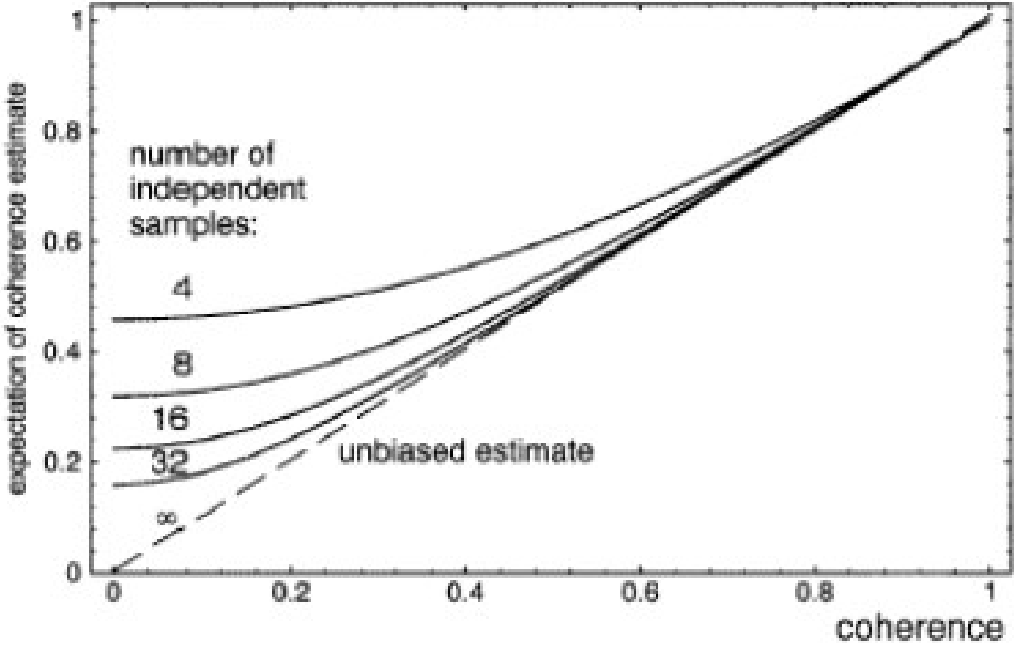

Multilook InSAR coherence

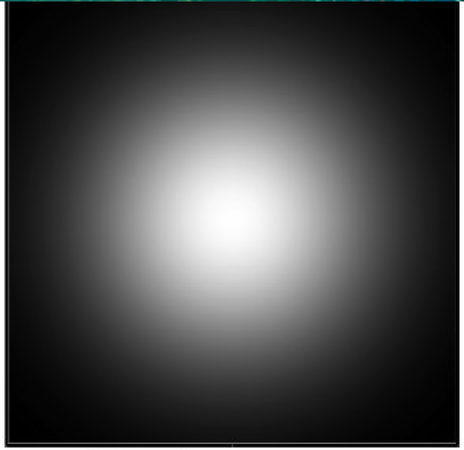

Absolute «True »
Phase

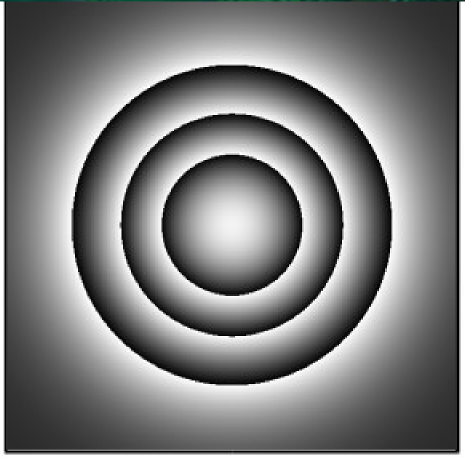

Coherence=1.0 L=1

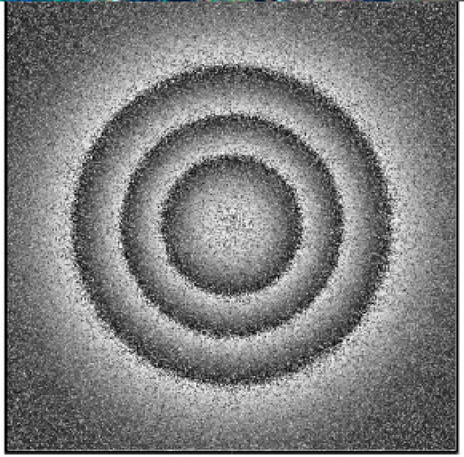

Coherence=0.8 L=1

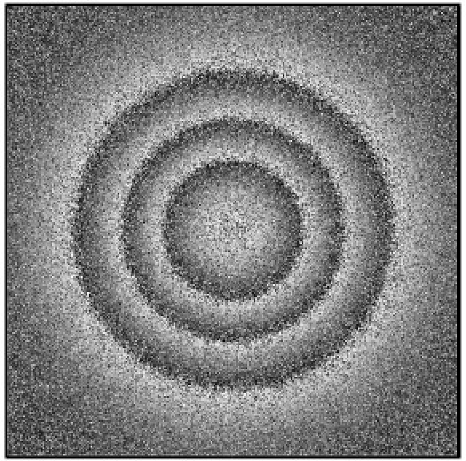

Coherence=0.6 L=1

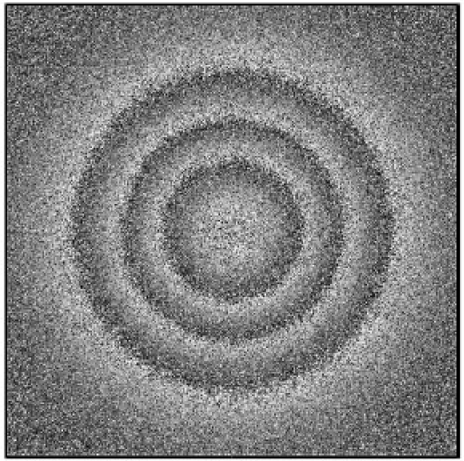

Coherence=0.4 L=1

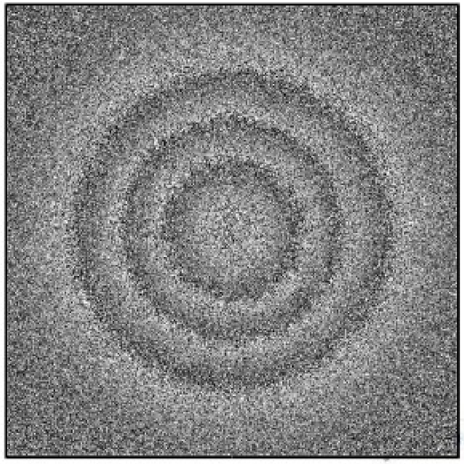

Coherence=0.2 L=1

Multilook InSAR coherence

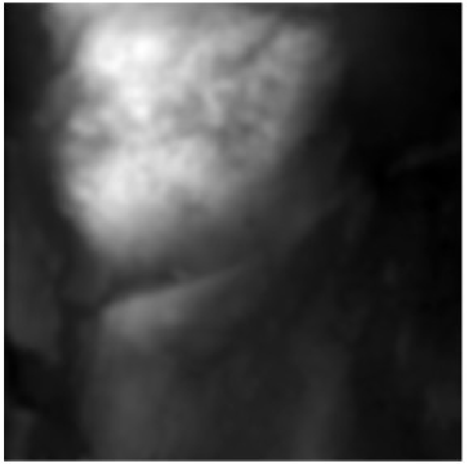

Absolute «True » Phase

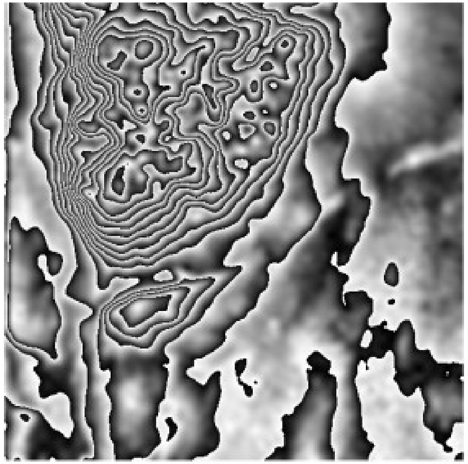

Coherence=1.0 L=1

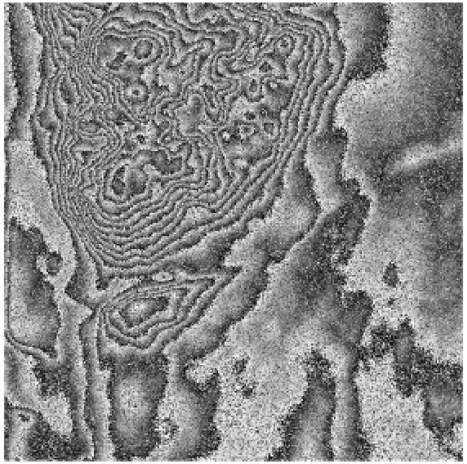

Coherence=0.8 L=1

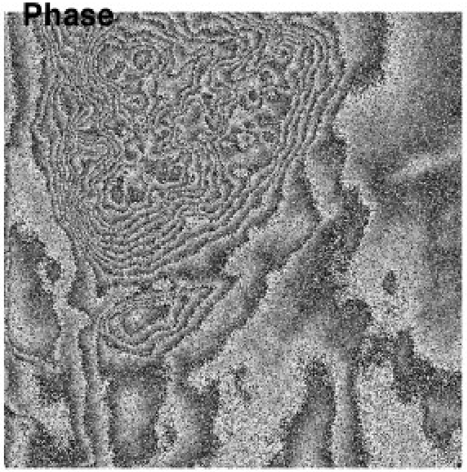

Coherence=0.6 L=1

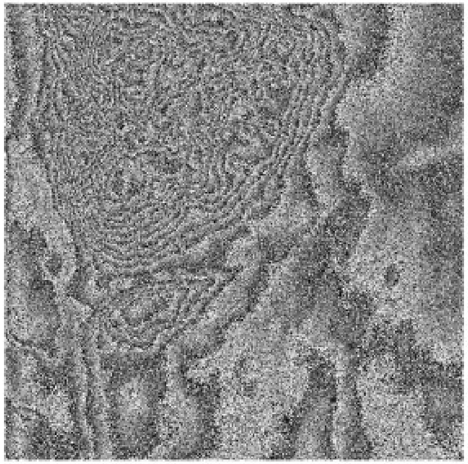

Coherence=0.4 L=1

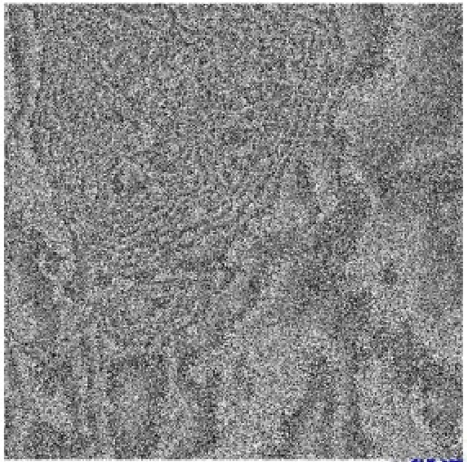

Coherence=0.2 L=1

Multilook InSAR coherence

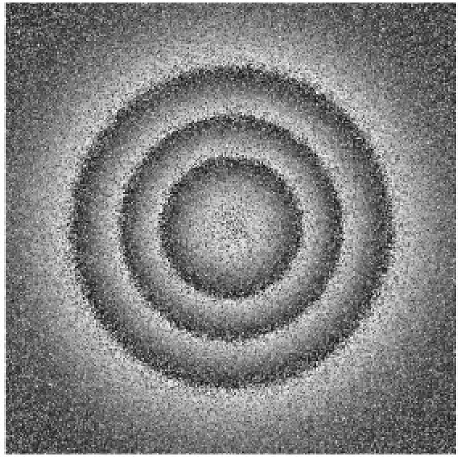

Coherence = 0.7 L=1

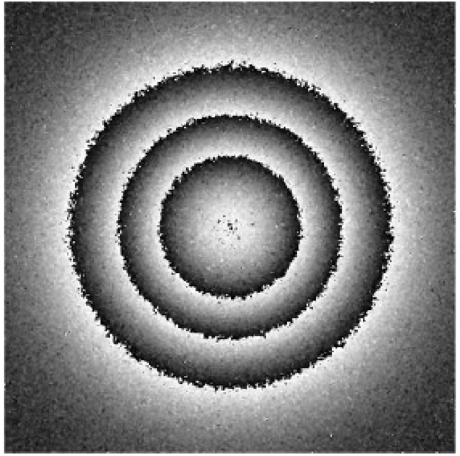

Coherence = 0.7 L=8

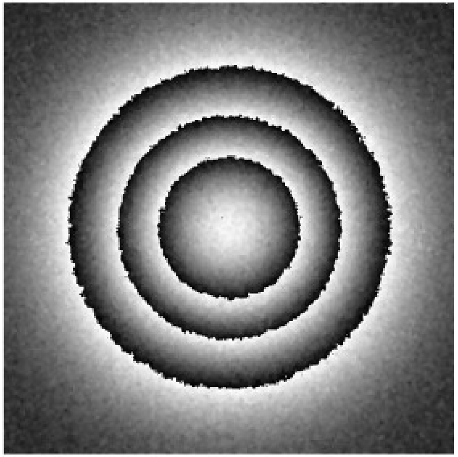

Coherence = 0.7 L=16

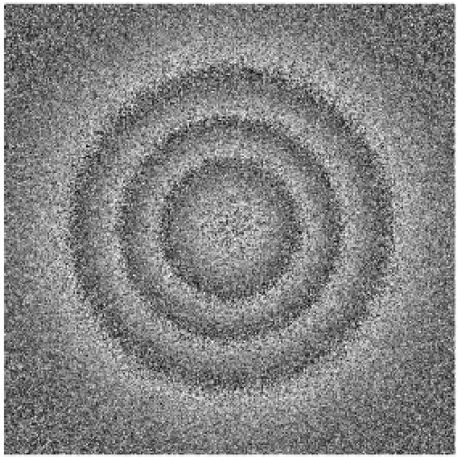

Coherence = 0.3 L=1

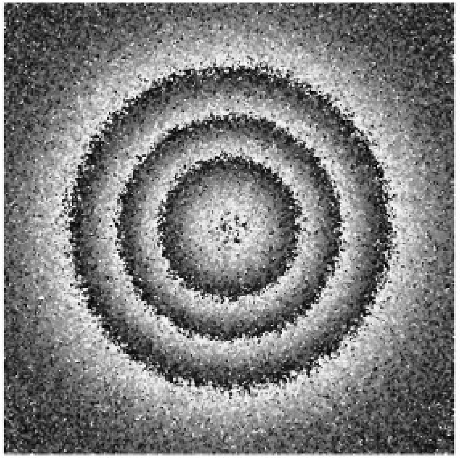

Coherence = 0.3 L=8

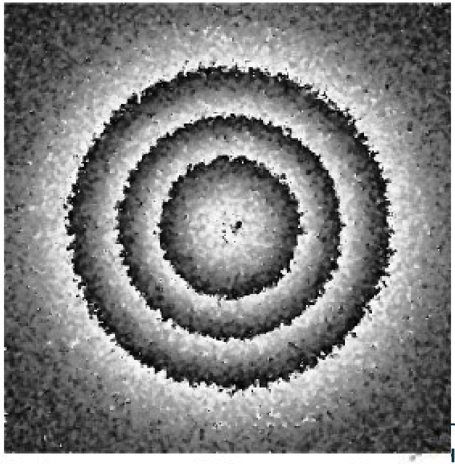

Coherence = 0.3 L=16

Multilook InSAR coherence

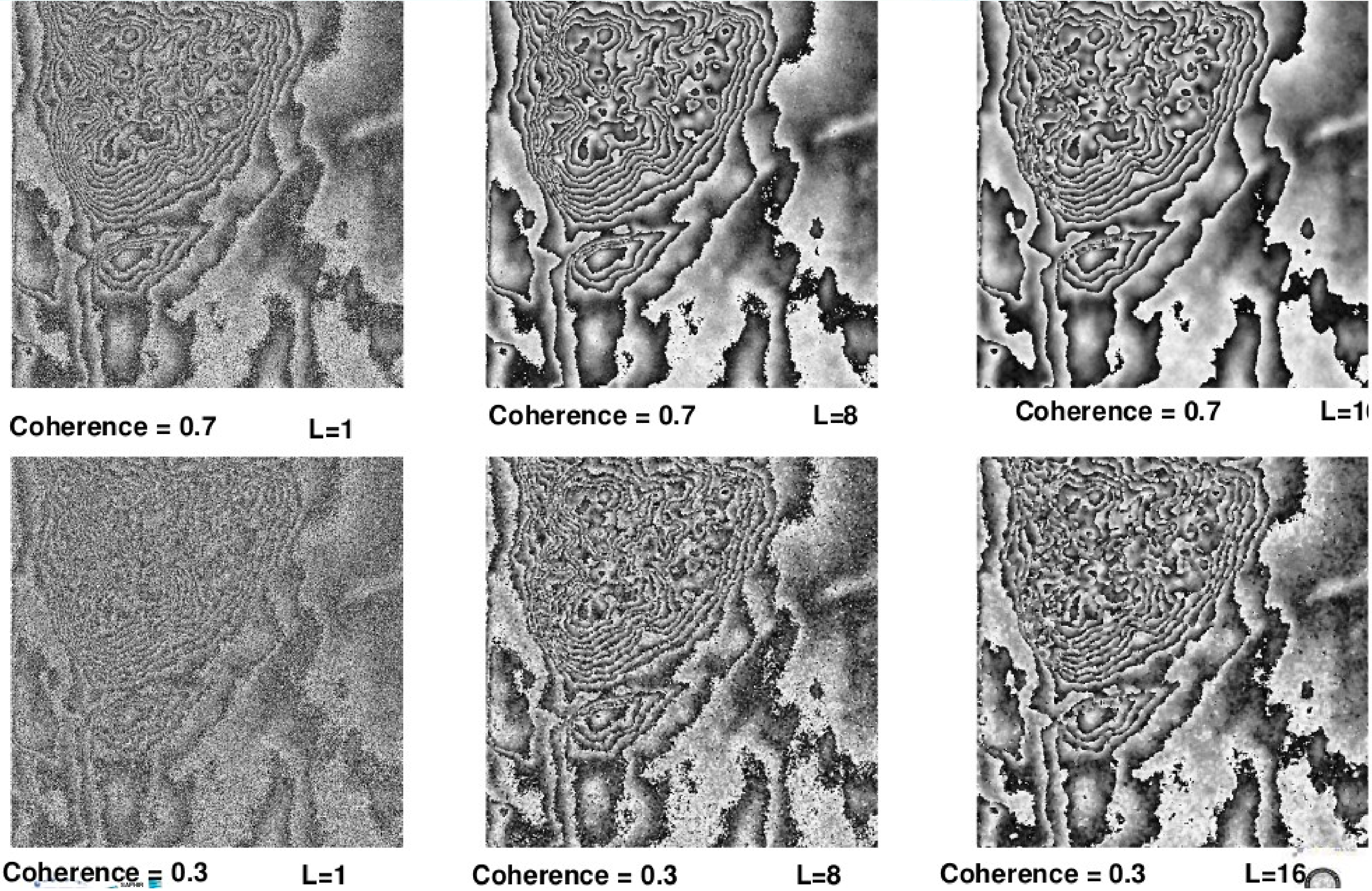
Coherence = 0.7 L=1

Coherence = 0.7 L=8

Coherence = 0.7 L=1

Coherence = 0.3 L=1

Coherence = 0.3 L=8

Coherence = 0.3 L=16

Sources of InSAR decorrelation

The true value of the coherence, γ , is fixed by a set of external sources :

Thermal or system noise : SAR amplifiers, ADC, antennas …

Geometric decorrelation : Baseline, squint …

Volume decorrelation : Volumetric media e.g. forest …

Temporal variations : wind, flowing or plowing, building …

Processing errors : coregistration, interpolation …

$$\gamma = \gamma_{th} \cdot \gamma_{geom} \cdot \gamma_{vol} \cdot \gamma_{temp} \cdot \gamma_{proc}$$

Thermal (SNR) decorrelation

- Signal plus system noise

Synthesized noisy signal $s_{th_i} = s_i + n_i$

Uncorrelated additive white noise terms

$$\mathrm{E}(n_i) = 0, \mathrm{var}(n_i) = \sigma^2_{N_e} \qquad \mathrm{E}(n_1 n_2^*) = 0, \mathrm{E}(n_i s_j) = 0$$

- Multiplicative coherence decomposition

$$\gamma = \frac{\mathrm{E}(s_{th_1} s^*_{th_2})}{\sqrt{\mathrm{E}(|s_{th_1}|^2)|\,\mathrm{E}(s_{th_2}|^2)}} = \frac{1}{1 + \frac{\sigma^2_{N_e}}{\mathrm{E}(|s_{th_i}|^2)}} \frac{\mathrm{E}(s_1 s_2^*)}{\sqrt{\mathrm{E}(|s_1|^2)|\,\mathrm{E}(s_2|^2)}}$$

$$= \gamma_{th} \gamma_{rem}$$ **(rem : remaining)**

$$\gamma_{th} = \frac{1}{1 + SNR^{-1}} \quad \text{with} \quad SNR = \frac{\mathrm{E}(|s_i|^2)}{\mathrm{E}(|n_i|^2}$$

Thermal (SNR) decorrelation

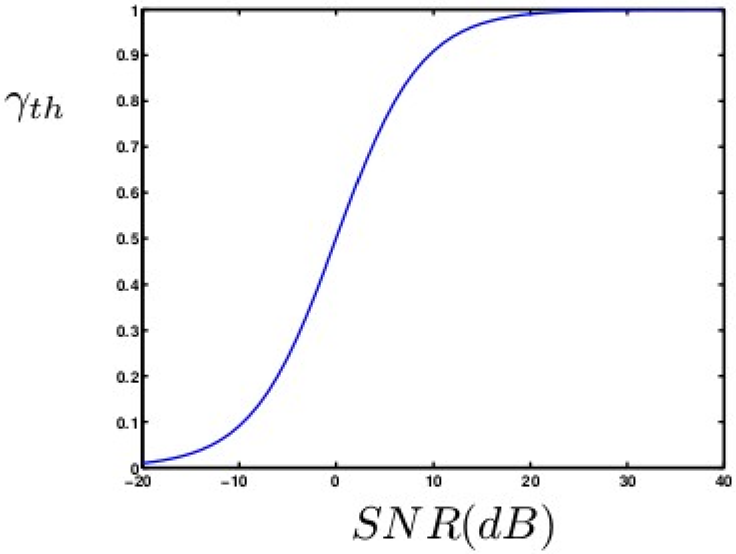

$$\gamma_{th} = \frac{1}{1 + SNR^{-1}} = \frac{SNR}{1 + SNR} \quad \text{with} \quad SNR = \frac{\mathrm{E}(|s_i|^2)}{\mathrm{E}(|n_i|^2}$$

Low reflectivity media (with low SNR): more affected by thermal decorrelation

Multiplicative structure $(\gamma = \gamma_{th}\gamma_{rem})$: thermal decorrelation cannot be compensated

Thermal (SNR) decorrelation

Intensity image

Coherence image

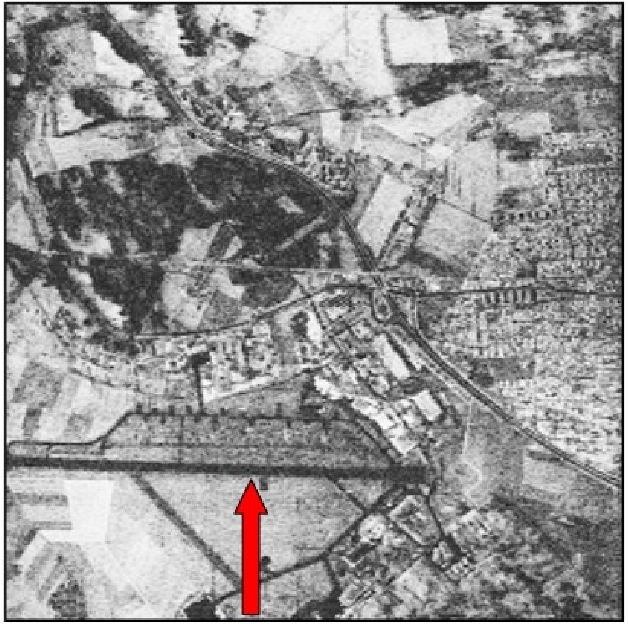

Temporal decorrelation

1 hour, 20m baseline

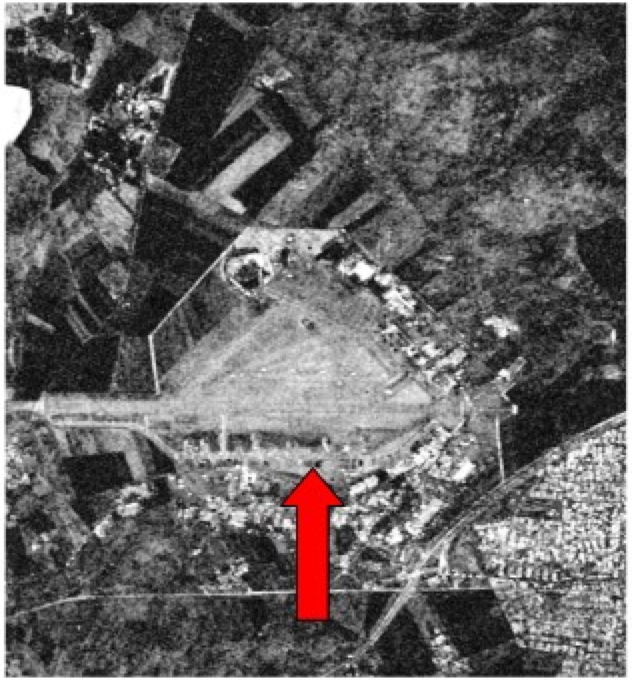

3 months, 0m baseline

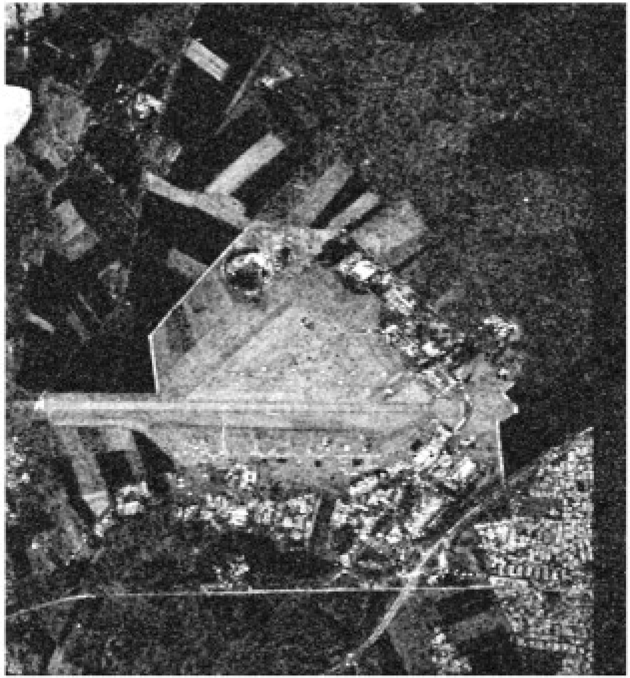

1 year, 0m baseline

Temporal decorrelation

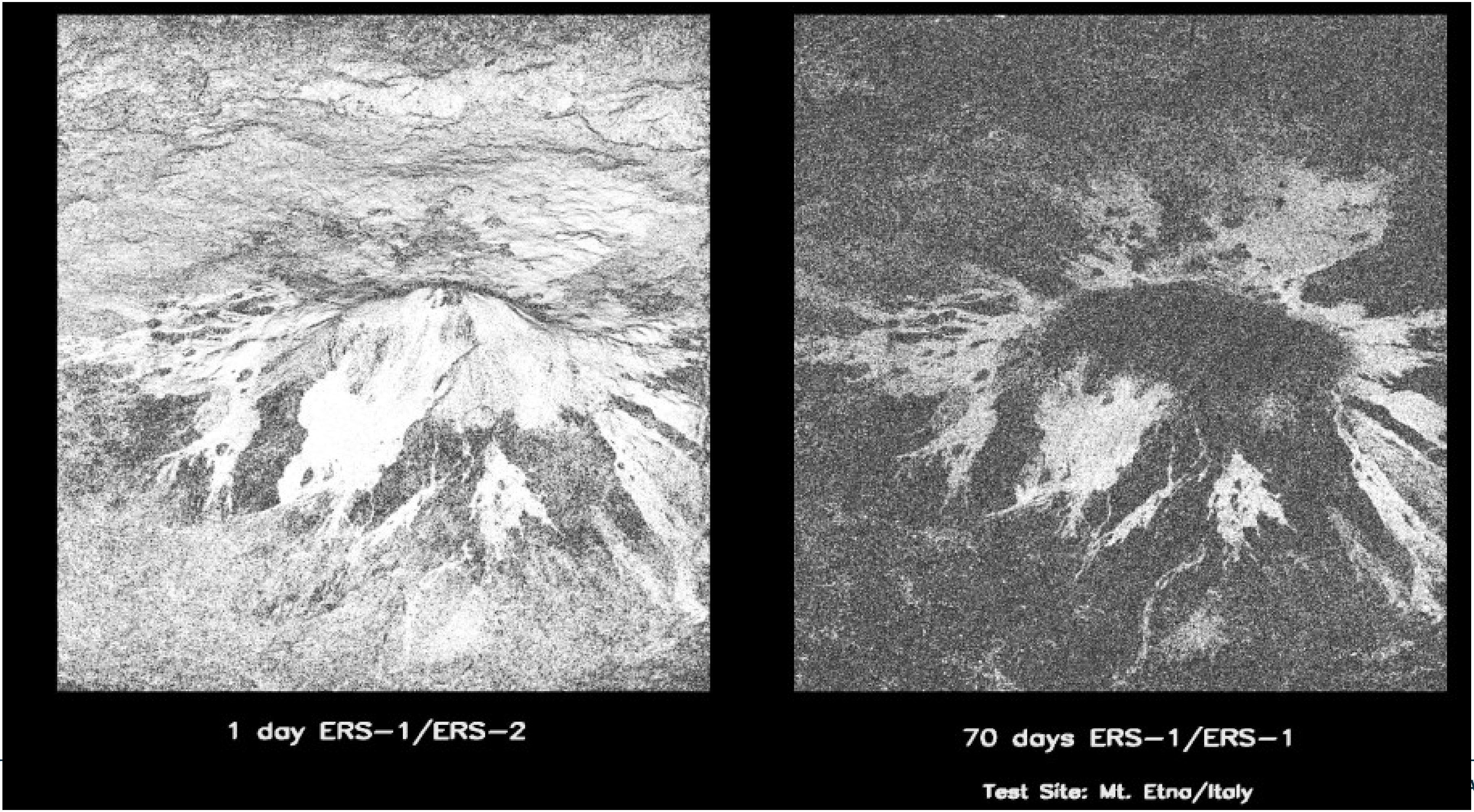

1 day ERS–1/ERS–2

70 days ERS–1/ERS–1

Test Site: Mt. Etna/Italy

Range decorrelation (spectral shift)

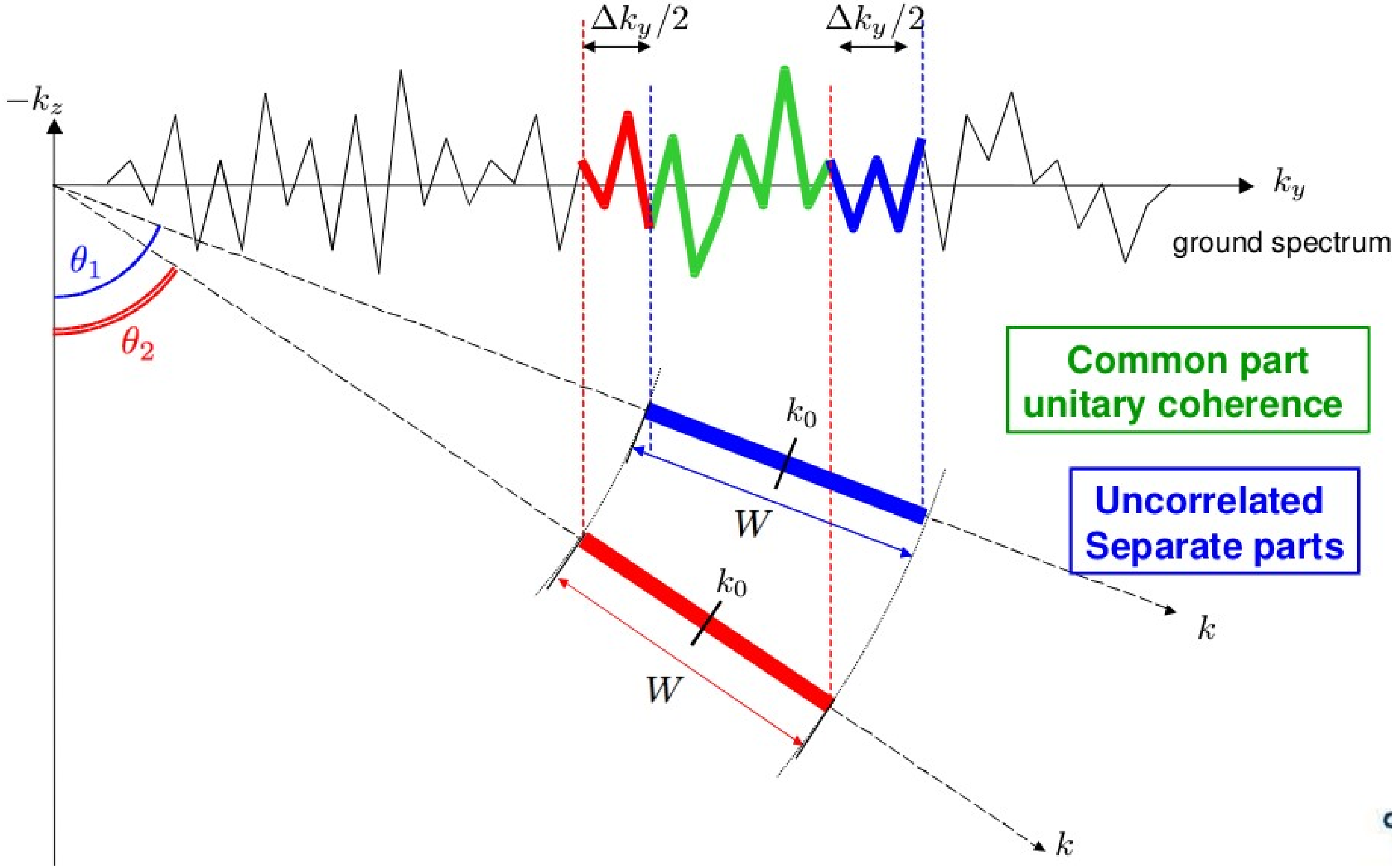

Common part unitary coherence

Uncorrelated Separate parts

$$\gamma_{ss} = 1 - \frac{B_\perp}{B_\perp^{crit}}$$

$$B_\perp^{crit} = \frac{W}{k_0} r_1 \tan(\theta - \alpha)$$

α, ground slope

Range decorrelation (spectral shift)

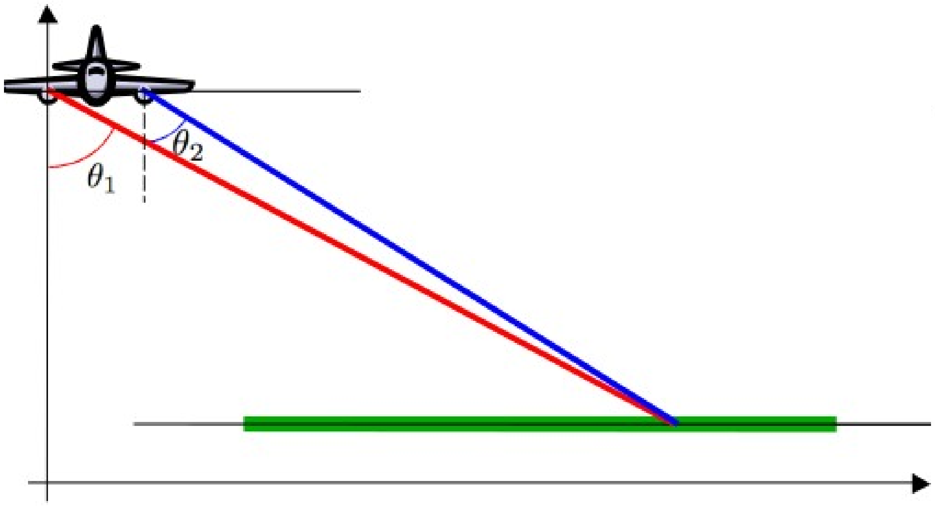

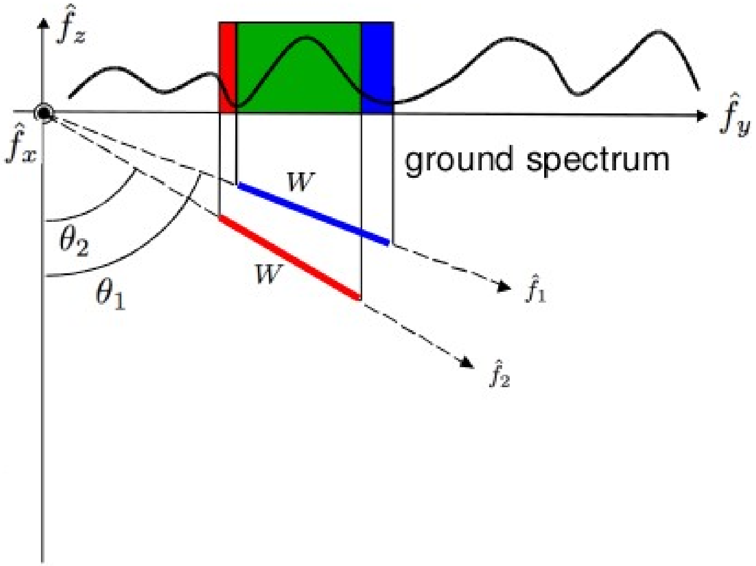

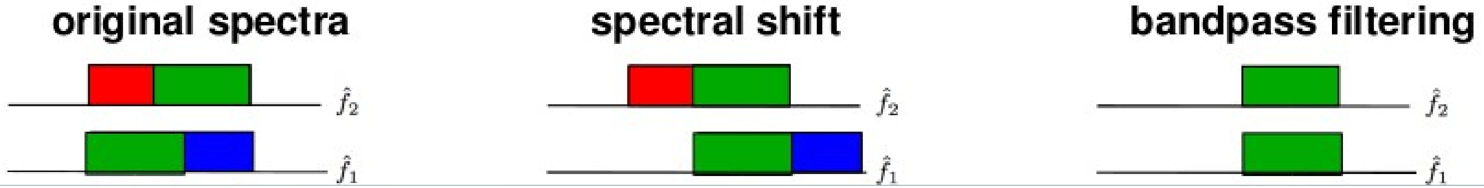
original spectra

spectral shift

bandpass filtering

Range decorrelation (spectral shift)

DLR E-SAR images, L band

with flat earth phase

without flat earth phase

after range filtering

Range decorrelation (spectral shift)

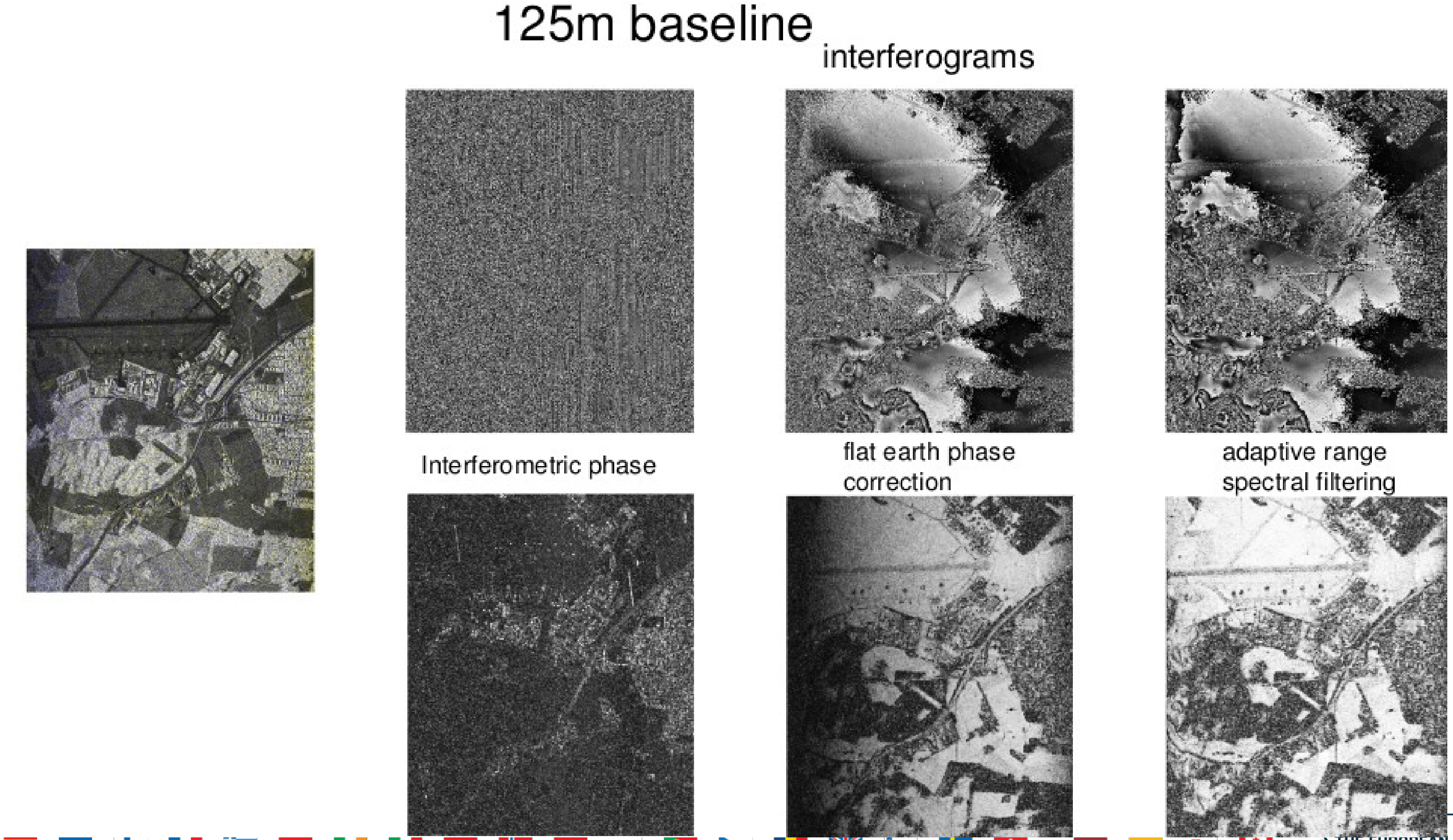

Range decorrelation: critical baseline

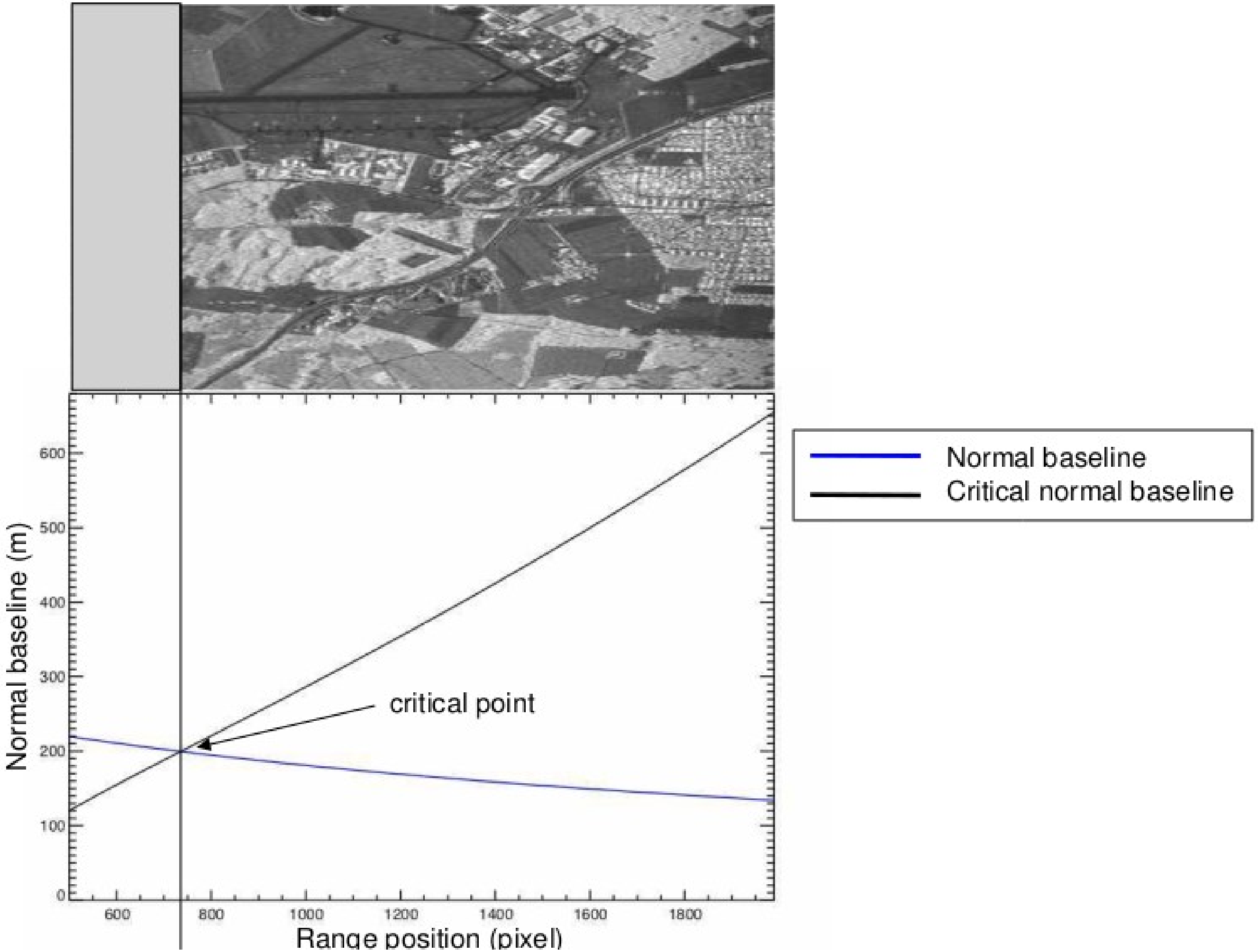

Range decorrelation: critical baseline

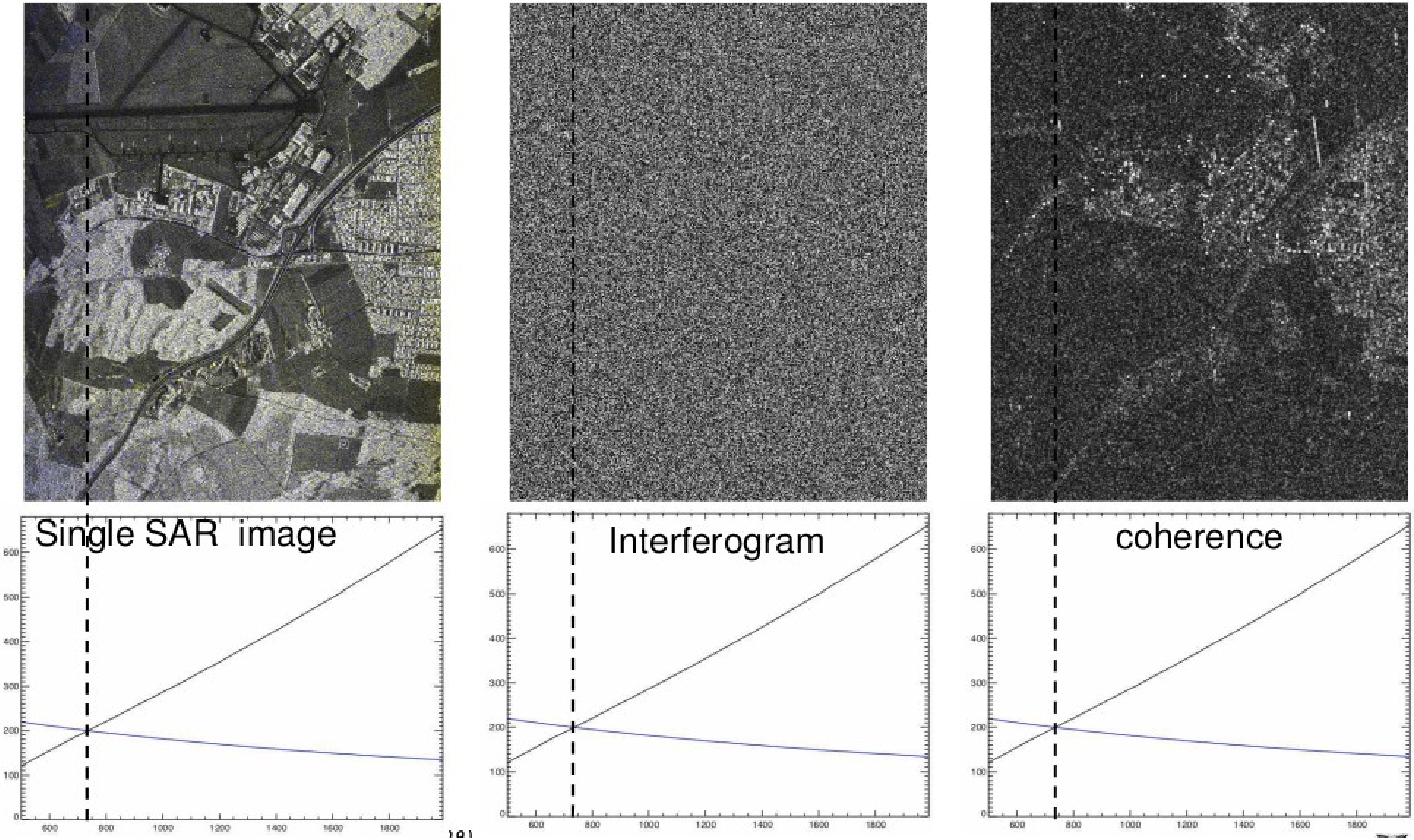

Range decorrelation: critical baseline

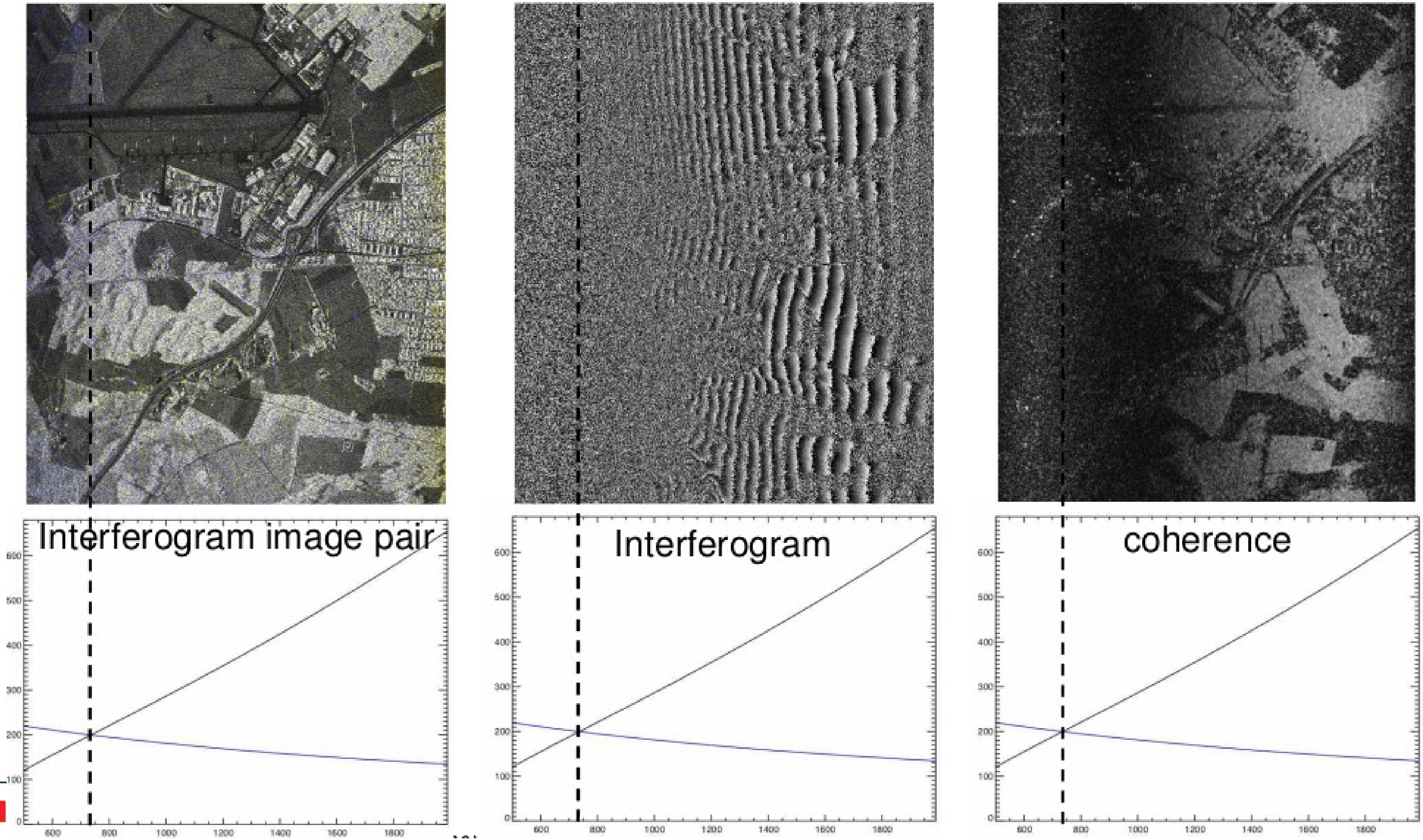

Range decorrelation: critical baseline

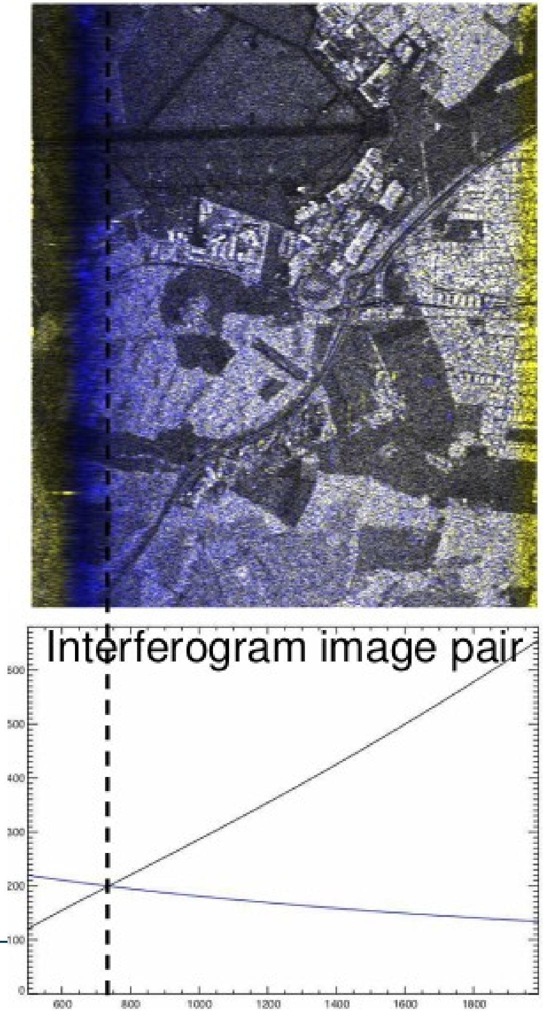

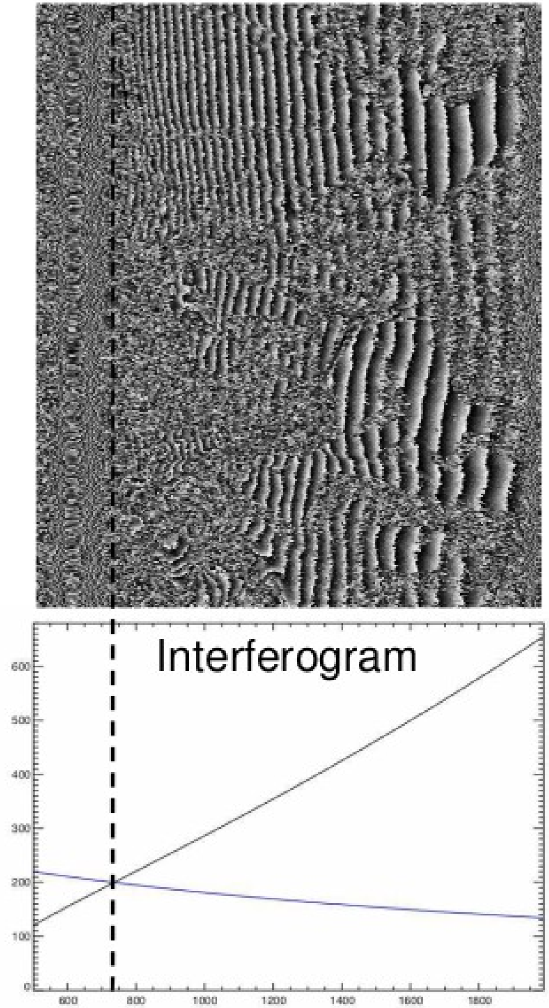

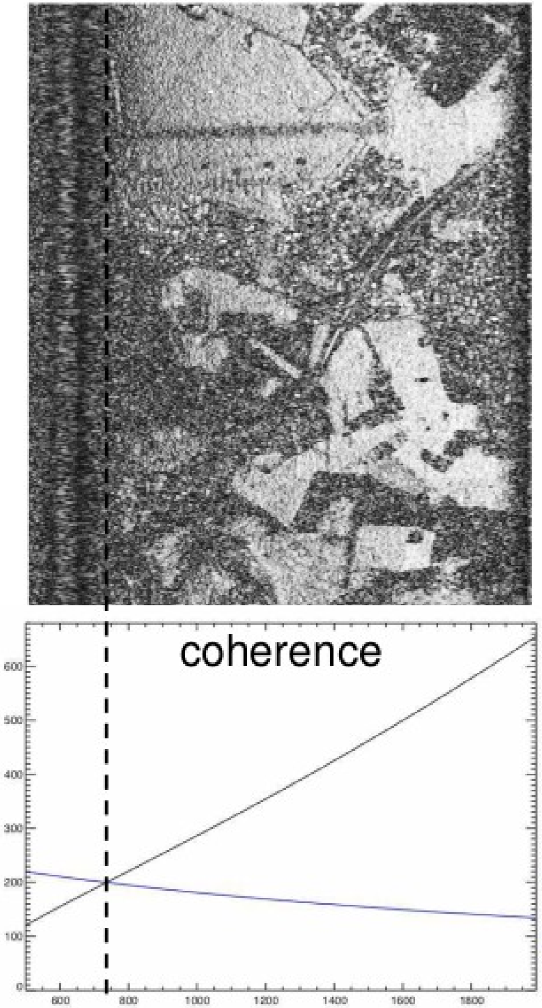

Volume decorrelation

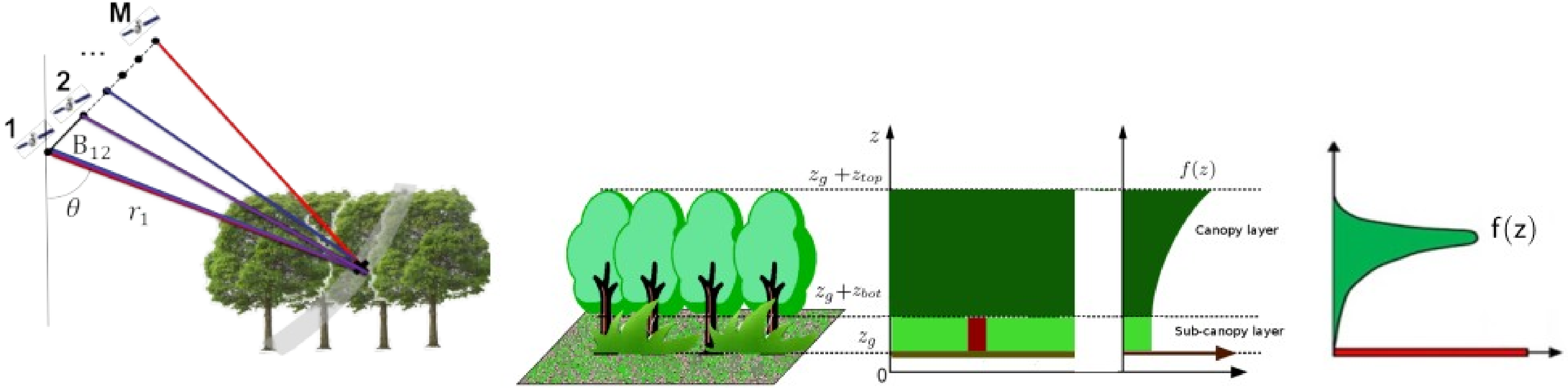

Born approx. at order 1

$$s_i \approx \int_{C(x_0,r_0)} a_c(z)e^{-jk_{z_i}z}dz,$$

Uncorrelated random reflectivity →

$$I_i = \mathrm{E}(|s_i|^2) = \int_{C(x_0,r_0)} f(z)dz, \quad f(z) = \mathrm{E}(|a_c(z)|^2)$$

Volumetric decorrelation

$$\boxed{\gamma_z = \frac{\int f(z)e^{-jk_z z}dz}{\int f(z)dz}}$$

Single SAR image statistics

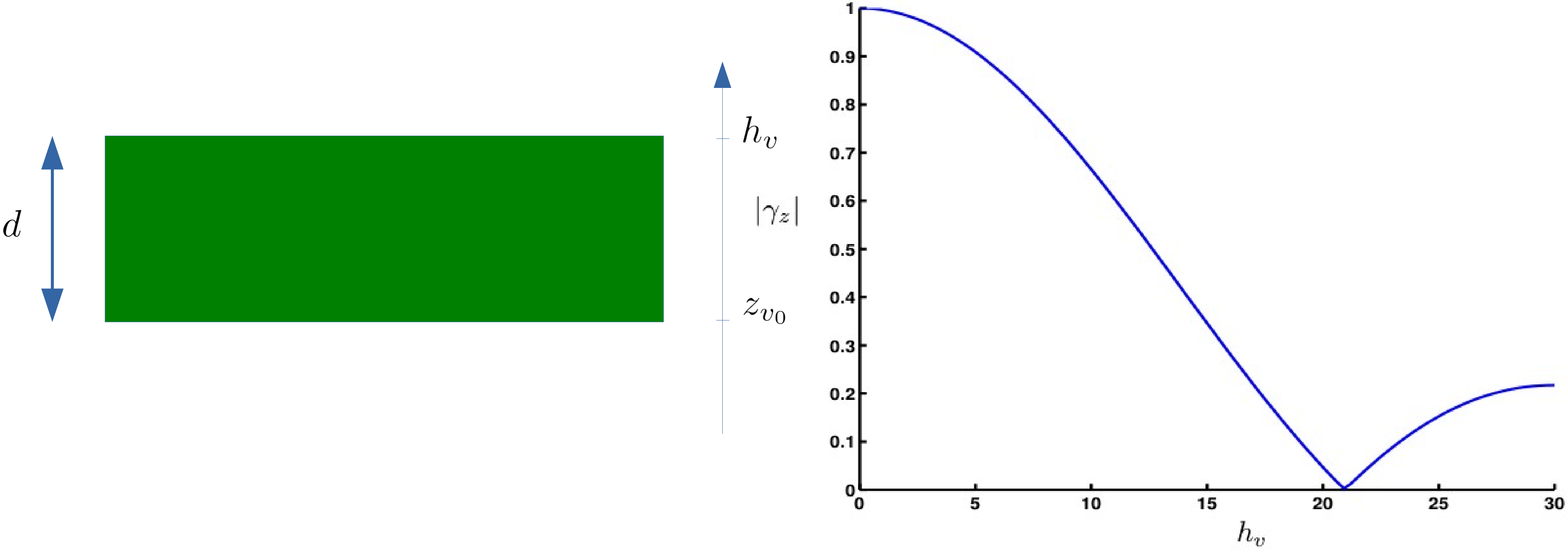

Baseline-dependent feature

Volume decorrelation

1 hour, 20m baseline, L band

Volume decorrelation & frequency